ADDIS ABABA UNIVERSITY

ADDIS ABABA INSTITUTE OF TECHNOLOGY

SCHOOL OF CIVIL AND ENVIRONMENTAL ENGINEERING

Experimental Investigation on Bond Strength Behavior of Reinforced Concrete Members Using Waste Marble as Coarse Aggregate

---

A Thesis in Structural Engineering

By Dereje Hirpa

December,2023

Addis Ababa

A Thesis

Submitted in Partial Fulfillment of the Requirements for the Degree of Master of Science

The undersigned have examined the thesis entitled '**Experimental Investigation on Bond Strength Behavior of Reinforced concrete members using Waste Marble as Coarse Aggregate**' presented by **Dereje Hirpa**, a candidate for the degree of **Master of Science** and hereby certify that it is worthy of acceptance.

Dr.-Ing. Adil Zekaria		18/12/2023
Advisor	Signature	Date
Dr. Esayas Gebreyouhannes		18/12/2023.
Internal Examiner	Signature	Date
Dr. Edom Adane		18/12/2023
External Examiner	Signature	Date
	Abrham Gebre (Dr.) Dean, School of Civil & Environmental Engineering	
Chair person	Signature	Date

Director of Postgraduate Program
Addis Ababa University
Addis Ababa Institute of Technology

UNDERTAKING

I, the undersigned, certify that research work titled "**Experimental Investigation on Bond Strength Behavior of Reinforced concrete members using Waste Marble as Coarse Aggregate**" is my own work. The work has not been presented elsewhere for assessment. Where material has been used from other sources it has been properly referred.

Dereje Hirpa

Signature: 

Date: December,2023

ABSTRACT

The expansion of the construction industry increased the demand for concrete. This results in the depletion of natural resources due to continuous quarrying. In another way, the waste generated from the marble industry will affect the environment. The use of waste in construction saves natural aggregate, energy and preserves the environment. Previous studies focused on the strength and durability properties of marble aggregate concrete and there is no sufficient literature that investigates the bond strength behavior marble aggregate concrete as it enables the use of marble aggregate in structural members.

Therefore, in this research the bond strength behavior of reinforced concrete using waste marble as coarse aggregate was investigated via Pull-out test. Deformed bars of diameters 12 mm, 14 mm, and 16 mm and length 1000mm were centrally placed in the cylindrical molds of dimensions 150 mm ×300 mm with an embedment length of five times the diameter of the bar. The bars were embedded in five different concrete mixes varying the quantity of marble replacing coarse aggregate at a ratio of 25% in C-30 concrete mixed using constant water-cement ratio. At the test date, each specimen was initially setup carefully and then an axial load was imposed on the bar at the loaded end and the slip was measured at free end. In this way pull-out test was conducted on a total of 45 specimens at the age of 28 days.

Test result indicates that compressive and splitting tensile strength of the concrete increases as the quantity of marble replacing natural coarse aggregate increases up to 50% and then decreases. Bond strength is consistent with the result of compressive and tensile strength of the concrete. For all diameter 12mm,14mm and 16mm bars the average bond strength of marble aggregate concrete is comparable with the control concrete as the percentage of marble in the mix increases up to 75%. However, the average ultimate bond strength significantly decreased in 100% marble coarse aggregate concrete because of low tensile strength of marble compared to natural aggregates. Furthermore, bond strength decreases as the diameter size of the bar increased due to nonlinear stress distribution along the embedment length of larger diameter size bars. The experimental result exceeds the bond strength calculated using equations proposed by nine different researchers. Both ES EN 1992-1-1:2015 and ACI 318-08 codes underestimated the average bond strength values of all steel bars embedded in all concrete mixes.

Keywords: Waste Marble, Coarse Aggregate, Concrete, Bond Strength, Pull-out test, Slip

ACKNOWLEDGMENTS

Above all, I would like to thank the almighty God for giving me the strength, patience, and persistence to accomplish this thesis.

I would like to express my deepest gratitude and respect to my advisor, Dr.-Ing. Adil Zekaria, for his precious support, motivation, and productive comments that greatly helped me in advancing my thesis.

I would really like to thank Dr. Abraham Assefa and Ing. Eyoel for helping me get the Center-hole jack and hydraulic pulling machine used for conducting the pull-out test. This experimental study would not have been a reality without their support and encouragement. I also extend my acknowledgement to Ing. Natnael Beksissa, Weyneshet Getachew, and all others who have directly and indirectly helped me throughout this thesis work.

I would love to forward my esteemed appreciation to my family and friends for their uncountable support and motivation throughout this study. Specially Mom I would like to thank you for your support and inspiration.

Last but not least, my sincere appreciation also goes to AAiT construction materials testing laboratory management and technicians for their positive support and guidance of laboratory work from the first day of acceptance to the end.

TABLE OF CONTENTS

LIST OF TABLES

LIST OF FIGURES

LIST OF ABBREVIATIONS

AAiT	Addis Ababa Institute of Technology
ACI	American Concrete Institute
ASTM	American Society for Testing and Materials
BS EN	British Standard European Norm
DS	Danish standard
ES EN	Ethiopian Standard European Norm
LVDT	Linear Variable Displacement Transducer
MA	Marble Aggregate
OPC	Ordinary Portland Cement
PA	Primary Aggregate
PVC	Polyvinyl Chloride
RC	Reinforced Concrete
USB	Universal Serial Bus
RILEM	Réunion Internationale des Laboratoires et Experts des Matériaux
CEB-FIP	Comite Euro-International du Beton and Federation Internationale de la Precontraine

LIST OF SYMBOLS

f'_c	Compressive strength
τ_n	Normalized bond strength
τ_u	Ultimate bond strength
$\emptyset$	Diameter of rebar
A_s	Area of steel
c	Cover
c_{max}	Maximum concrete cover
c_{min}	Minimun concrete cover
d_b	Diameter of bar
f_{bd}	Design value of the ultimate bond stress
f_{ct}	Tensile strength
f_{ctd}	Design concrete tensile strength
f_y	Yield Strength
k_{tr}	Transverse reinforcement index
l_e	Embedment Length
P	Maximum load
s	Slip
ε_s	Strain of the bar
λ	Modification factor for the weight of concrete
τ	Bond strength
ψs	Modification factor for size of the bar
ψe	Modification factor for epoxy coating of bar
ψt	Modification factor for the location of bar

1. INTRODUCTION

1.1 Background

Concrete is the most widely used building material made by mixing cement, sand, crushed rock, and water. About 60% to 75% volume of the concrete is made from aggregates. Thus, overall performance of concrete depends on the properties of its constituent materials. These properties are porosity, nominal size, moisture absorption, gradation, shape, surface texture, unit weight, crushing strength and type of deleterious substances present. These features of aggregates come from the mineral composition of the parent rock, the environmental conditions the rock was exposed to prior to mining, and the type of equipment used to manufacture the aggregate. Due to ongoing development the need for aggregate has grown as a result of the rising global demand for concrete throughout time. Thus, aggregates from industrial by-products, municipal waste, and recycled can used in concrete [1].

Marble is metamorphic rocks primarily made of limestone by heat and pressure formed in the earth. It is mainly composed of calcite ($CaCO_3$) and dolomite ($CaMg(CO_3)_2$). Marble is commonly known in its white color. But due to the presence of impurities during the recrystallization phase its color can alter. There are different types of marble based on their color, chromatic uniformity of its base, grain type, and thickness, as well as drawing of its veins. Marble is widely used in buildings, monuments and sculptures due to its strength, fire and erosion resistance and also its aesthetics. It is applicable in wall cladding, countertops, table tops, firebox facing and hearth, as a whiting in toothpaste and paint, as a soil stabilizer in agriculture. Generally, marble is utilized in metallurgical, chemical, environmental, construction, refractory and agriculture sectors [2]. In Ethiopia deposit of marble is available in different locations.

Different studies have been conducted on the use of crushed waste marble in concrete production. Hebhoub et al [3] in their study utilized marble waste as a fine, coarse and combination of both coarse and fine aggregates substitute in normal strength concrete. In their study they found that as the quantity of marble substituting gravel coarse aggregate increase up to 75%, compressive and tensile strength of the concrete increase. In the study

by Kore [4] the compressive strength of concrete produced from 75% marble coarse aggregate and 40% steel slag fine aggregate was almost as high as the control concrete mix. Andre et al [5] also added that there is no significant variation in durability performance of concrete specimens fabricated using natural and marble coarse aggregates. The findings indicate that the use of waste generated from marble industry in concrete production improves the mechanical performance which in turn reduces the need for limited natural aggregates. There is no sufficient study that examines the bond strength behavior of marble aggregate in structural concrete.

Bond is a shear stress developed at a steel-concrete interface to measure the degree of their interaction. When members of reinforced concrete structures are subjected to load the bond strength at the interface enables longitudinal forces to be transferred among the surrounding concrete and reinforcement bar. The way steel and concrete interact is a major factor in how RC structures behave as it is assumed that there is an effective bond among the steel and concrete. Thus, a suitable bond between the reinforcement bar and the concrete is necessary to guarantee safety. The slippage of a bar that results in a sudden failure of Reinforced concrete members happens if the interface bond resistance is insufficient [6].

Several factors affect bond between reinforcement bar and concrete. They are grouped under structural characteristics, concrete and bar properties. Among them Aggregate type and quantity is a specific factor categorized under concrete property that mainly affects the bond behavior of a reinforced concrete structures. Hence studying the bond behavior of marble aggregate concrete is essential to utilize it more in structural concrete.

1.2 Statement of the Problem

Due to the rapid growth of the construction industry, especially in developing countries, the demand for concrete is huge. This extensive and endless need for concrete causes depletion of natural aggregates and ecological problems which is a critical issue in the future. To minimize this, researchers have given attention for utilization of industrial waste products in construction. One of the industrial by-products used as recycled aggregate is marble. A significant amount of waste will be generated by the marble processing industry as 70% of marble is wasted during the production such as quarrying, cutting, polishing and

other processing stages [3]. It is disposed as landfills or dumps in which its accumulation will cause environmental and landscaping problems.

In Ethiopia waste generated form marble processing industry has a wider range of applicability. Crushed marble chips are used as a decorative element in gardens, pathways and driveways. They add elegance and beauty to outdoor spaces. The chips are also be utilized in the production of terrazzo flooring as it is durable and aesthetically appealing. In addition, waste marble in its powdered form is also used as a filler in the production of paint, paper, and plastic products in various industries. Waste marble is also beneficial in agricultural sector of Ethiopia to treat acidic soils and improve soil fertility.

According to previous studies the use of waste marble as a coarse aggregate improves mechanical strength of the concrete. However, to the researcher's knowledge, the effect of utilizing waste marble aggregate on the bond strength of rebars embedded in normal strength concrete has not been sufficiently studied. Furthermore, aggregate type and quantity has a significant effect on the bond strength of reinforced concrete structures. Thus, the effect of waste marble as a natural coarse aggregate on the bond strength behavior of reinforced concrete structure needs further investigation. Therefore, the objective of this study is to fill the gap by studying the bond strength behavior between waste marble aggregate concrete and reinforcement bar in normal strength concrete.

1.3 Objectives of the Study

1.3.1 Main Objective

The general objective of this study is to experimentally investigate the bond strength behavior of reinforced concrete using waste marble as coarse aggregate.

1.3.2 Specific Objective

- To examine bond strength behavior of marble coarse aggregate concrete and compare results with code provisions (ES EN 1992-1-1:2015 and ACI 318-80) and equations proposed by different researchers.
- To study the effect of reinforcement bar diameter size on the bond strength of marble coarse aggregate concrete.
- To determine the compressive and tensile strength property of marble aggregate concrete.

1.4 Scope of the Study

In this research the pull-out test was conducted to examine the bond strength performance of reinforcement bars embedded in a normal strength concrete incorporating crushed waste marble as a natural coarse aggregate in a ratio of 25%, 50%, 75% and 100% by weight. Three Turkiye imported deformed reinforcement bars of a nominal diameter 12mm ,14mm and 16mm were used. Only pull-out method of bond test was done due to ease of specimen fabrication and testing. However, due to laboratory equipment limitations and difficulty in specimen preparation and testing this study was unable to conduct bond strength test using beam specimens. In addition to pull-out bond test, mechanical test specifically compressive strength and splitting tensile strength tests were also conducted for both natural and marble coarse aggregate concrete.

1.5 Significance of the Study

In Ethiopia the deposit of marble is found in various places such as Mora, Bulen, Mankush, Baruda, Daleti, Gojam and around Mekelle. As construction increases the need for marble as a finishing material also increases. This forces more marble processing industries to emerge that in turn increase the accumulation of marble waste. More waste requires more land fill area and affects the environment. Environmentally waste marble decreases the permeability and porosity of the top soil thereby reducing its fertility. In addition, when it is dumped around a catchment area it contaminates groundwater. The dust on the surface of waste marble also spreads to air and lower the quality resulting heath problem. Previous studies state that the use of waste marble as coarse aggregate in construction improves the mechanical performance of concrete. To the best of the author's knowledge sufficient study on the bond behavior of marble aggregate concrete is not available. Thus, this research explores more properties of marble in reinforced concrete which helps to strengthen previous related works and enhance the acceptance of marble aggregate to be used in reinforced concrete. The utilization of marble as coarse aggregate saves natural aggregate, energy consumption and landfill area required and preserves the environment.

1.6 Organization of the Thesis

The thesis comprises five main chapters and organized as follows. The first chapter provides a general introduction to the thesis with a brief content of the background information associated with the concrete, marble aggregate, and bond strength, along with the objective, scope, and significance of the study. The second chapter includes in depth review of previous literatures relevant and related to the study area with proper citation. The third chapter presents the materials and their characteristics, methods employed and testing procedures used for the accomplishment of the research. Chapter four provides the experimental test results in table and graphical ways along with detail discussion of the findings. Finally, chapter five states conclusions of the study and forwarded recommendations for further investigation.

2. LITERATURE REVIEW

2.1 Introduction

This chapter covers literatures related to marble geological formation, its physical and chemical properties, availability in Ethiopia and its use in concrete production. In addition, literatures related to bond transfer mechanism, bond strength test methods, bond stress-slip models, factors affecting bond and bond stress equations in code provision and various empirical equations was also reviewed and presented.

2.2 Marble

Marble is crystalline metamorphic rocks primarily made of calcite, dolomite, or serpentine. In ancient Rome, the Italians used the word “marmor” to specifically refer to marble.

2.2.1 Mechanism of the geological formation of marble

Marble is recrystallized from the original limestone by pressure and heat in the earth crust. It is a process of changing existing rocks by the chemical reactions of fluids. The minerals that make up the rock may undergo chemical change or a structural modification as a result of this alteration. The mineral makeup of marble is affected by the impurities that exists in limestone during the re-crystallization phase. These impurities change the color appearance of marble. Hence a marble made of pure calcite mineral is white whereas marble with iron and magnesium impurities is green, generally marble is colored dark by graphite (algae), greenish grey by pyrite, and pink by finely dispersed hematite [7].

The pressure and heat of the metamorphism have mobilized and recrystallized different impurities. Quartz crystals are formed when silica impurities in carbonate minerals are exposed to relatively low temperatures. Diopside and forsterite are produced when silica and carbonates interact at higher temperatures. Calcium minerals such as brucite (Magnesium Hydroxide), monticellite (Calcium Magnesium Silicate), and rankinite (Calcium Silicate) develop in marble at very high temperatures. When there is silica, alumina, and iron in the marble, hematite and magnetite can develop [7].

The distinction between marble and limestone is made via re-crystallization. Small calcite crystals can be found in marble that has undergone minimal metamorphism. As the level of metamorphism progresses, the clay mineral within the marble will change to mica and more complex structures with large crystals will be formed. Marble is stronger and denser than the original limestone as a result of pressure and heat [7].

2.2.2 Physical and Chemical properties of Marble

2.2.2.1 Physical Properties of Marble

Marble is a hard re-crystallized rock that has fine to very fine-grained particles. It has a smooth surface texture when polished with a variable color [7]. Table 2.1 summarizes the physical properties of marble.

Table 2.1 Physical Properties of Marble [7]

No.	Physical Properties	Marble
1	Hardness	3-4 moh's scale
2	Density	2.55-2.7 kg/cm^3
3	Compressive Strength	70-140 MPa
4	Water Absorption	< 0.5%
5	Porosity	Very low
6	Weather impacts	Resistant

2.2.2.2 Chemical Properties of Marble

Marble is mainly made of calcite, dolomite or minerals having a fine to coarse grained crystalline texture. The chemicals in marble are Silica, Pyrite, limonite, iron oxides manganese etc. In addition, mineral impurities such as actinolite, micro line, quartz, muscovite, chert etc. are also available in marble. The mineral constituents in marble differ according to their origins [7]. Chemical constituents of marble are presented in Table 2.2.

Table 2.2 Chemical Composition of Marble [7]

No.	Chemical Composition	Marble
1	Lime (CaO)	28-32 %
2	Silica (SiO_2)	3-30 %
3	Magnesia (MgO)	20-25 %
4	Alumina (Al_2O_3)	-
5	$FeO+Fe_2O_3$	1-3 %
6	Alkalis	-
7	LOI	20-45 %

2.2.3 Uses of Marble

Marble is used to produce around 75% of the world's calcium carbonate. It is utilized in a wide range of industries. Due to its ability to impart stiffness, impact strength, dimensional stability and thermal conductivity marble is used in plastic industries. Marble is also applicable in painting industries because it is a good extender and filler, has a high brightness, and can withstand weathering. It is an essential component in the construction industry to produce dimensional and non-dimensional stone, cement and aggregates for the construction of roads and concrete [7].

2.2.4 Mining and Processing of Marble

There are three segments in the marble industry: mining, processing, and marketing. Mining includes the production of blocks. It is affected by various factors such as: Geologic, hydrologic and Spatial characteristics of the deposit, Hydrologic and geologic conditions, Geotechnical factors, Economic, Technological and Environmental concerns. The other stage in the marble industry is processing. It involves sizing, slabbing and polishing activities. The end products of processing stages are a polished or unpolished slabs or tiles of various thickness, monuments, articles, chips and waste. The final stage in marble industry involves providing the end products to consumers [8].

Marble is extracted and processed in an entirely different manner then any conventional mining and processing techniques (see Figure 2.1). In the previous marble quarrying process, huge blocks are dug up manually with the help of jack hammer and jib crane. But now days extraction methods are quite advanced, utilizing both water-jet technology and diamond wire cutting. The block is cut vertical and horizontally with jet belt or chain perforation and diamond wire then jacked, partitioned and loaded for further processing. The block is pulled out using winch and loaded by forklift loader [8].

The block is then vertically and horizontally cut using a stone cutter that moves on rails and then prepared for further processing. In the majority of marble quarries, wire sawing is by far the most crucial extraction method. Marbles are riskier and more challenging to blast than granites because it is soft and can easily break. In marble quarries, chain saws and diamond belt saws are being used in addition to wire saws to dig holes and "blind cuts" during underground activities. Stationary wire saws or disc saws are widely used for the final squaring of commercial blocks [8].

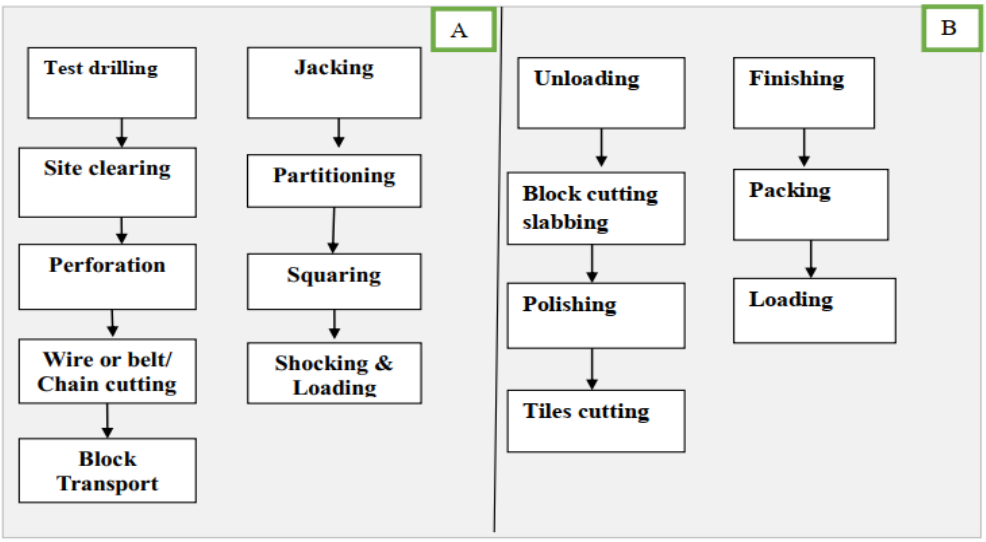

Figure 2.1 Extraction of marble (A)Mining (B)Processing [8]

2.2.5 Marble Deposit in Ethiopia

Previous studies state that marble deposits are found in north, western and southern parts of Ethiopia. It occurs in the Precambrian basement rocks at all geologic periods.

The existence of sedimentary rocks is related to marine transgression and regression cycles that occurred throughout the Mesozoic epoch. Transgression produced the Hamanele, Abay or Goha Tsion, and Antalo formations, which are mostly composed of limestone, dolomite, gypsum, and shale. Regression of the sea towards the end of the Jurassic deposited the lagoonal facies of the Agula formation in the Mekale area of Tigray region, which is composed of marl, black shale and claystone with layers of limestone, gypsum, and dolomite [8].

The deposits of marble are located in the western districts of Wellega (Daleti) and Gojam (Mora, Bulen, Mankush, and Baruda). The estimated amounts of the marble reserves in Mora are about 46.54 million tonnes where as in Baruda (Metekel) it is over 13.58 million tonnes. The marble in Mora is white grey while the marble in Baruda and Bulen is grey to dark grey [8].

In addition, the marble deposits are also found in northern Ethiopia. These deposits are older, have larger grains, and different tints than those in the West. It is estimated that over 10 million tonnes of marble are thought to exist in Tigray in five different sites [8].

2.2.6 Previous Studies on the Use of Waste Marble in Concrete Production

As reported by Jeengar [9] in the experimental investigation, waste marble was partially utilized as a natural coarse aggregate by weight up to 50% in a range of 10%. From the test result, it was seen that workability of freshly mixed concrete decreases as the quantity of marble aggregate increases. Compressive strength at the age of 28 increases up to a 40% coarse marble replacement ratio and starts to fall beyond that.

Sunil and Varghese [10] studied on the use of marble waste as coarse aggregate in concrete production. The study was aimed to determine suitability of utilizing marble waste as a partial substitute for natural coarse aggregate and set ideal percentage. The ratio of replacements is 0%, 25%, 50%,75% and 100% by weight of natural coarse aggregate with a constant water cement ratio of 0.45. The test result revealed that compressive, splitting tensile and flexural strength increases with increase in marble content up to 50%, and then starts to decrease. Concrete mix with 50% waste marble as a coarse aggregate had compressive strength that was 0.42% higher than control mix.

In the study made by Chang et al., [11] waste marble was utilized as coarse aggregate in a ratio of 20% by weight at a water-cement ratio of 0.4. In their study Chang et al investigated compressive strength, ultrasonic pulse velocity and chloride penetration depth of the concrete. The test result on fresh concrete revealed that as the replacement level of waste marble increases workability slightly increased. The compressive strength of concrete increased as the quantity of marble increased and it was observed a 5% increment when compared to control concrete at 60% replacement. In addition, resistance to chloride penetration was increased by 19% and ultrasonic pulse velocity was around 5% greater for 60% waste marble aggregate concrete when compared to the control mix.

Adham et al., [12] studied the effects of replacing coarse aggregate with crushed waste marble on properties of concrete. The aim of the study was to investigate the viability of using crushed marble waste as coarse aggregate in the concrete mix. A C25 grade concrete was casted varying marble waste in a range of 0%,25%,50%,75% and 100%. From the result, the workability of concrete increases as the quantity of marble in the mix increases. The compressive strength of the concrete also increased as marble content in the mix increased. According to this study a 10% increase in compressive strength was observed for a concrete made with 50% marble aggregate.

Kore et al.,[13] conducted an experimental investigation using marble waste as coarse aggregate in a ratio of 20%, 40%, 60%, 80% and 100% by weight using water cement ratio of 0.6. In their study, workability, compressive strength, permeability and acid resistance was evaluated. According to the test result, a 35% increment in 28^{th} day compressive strength of the concrete was noticed when 80% of crushed waste marble replaced natural coarse aggregate. In addition, the compressive strength of 100% marble coarse aggregate concrete was increased by 26.5%. Workability and permeability of the concrete also increased as marble content in the concrete increased. When compared to control concrete, there is no adverse impact of acids on concrete with marble aggregate.

Ali et al.,[14] experimentally investigated the strength property of concrete using waste marble as coarse aggregate to examine the viability using waste marble as partial natural coarse aggregate in concrete production. Five different concrete mixes were prepared varying quantities of marble in a range of 25% including control specimen. The overall test result showed decrease in compressive strength of the concrete for all replacement ratios of marble. According to this study, a 1.85%,2.97%,4.8% and 7% decrease in compressive strength was observed for marble replacement ratios of 25%, 50%, 75% and 100% respectively. It is due to weak bond resulted from smooth surface of marble aggregate. The workability of the concrete increases as the quantity of marble in the mix increases.

Chotaliya et al.,[15] performed an experimental study using waste marble chips as concrete aggregate. The objective of the study was to look into the potential of utilizing waste marble as concrete aggregate. In their study, natural coarse aggregate was fully (100%) replaced with water cement ratio of 0.45 and hardened concrete property was analyzed. The result from this study showed an increase in compressive strength of 81.32 % when compared with plain concrete at 28^{th} days. Similarly, a 46.2% and 43.42% increase in splitting tensile and flexural strength respectively was observed when compared to plain concrete.

According to Martins et al.,[16] waste from marble industry was used as a natural coarse aggregate in a ratio of 20%, 50% and 100% to study the mechanical performance of concrete. The mix was conducted at a constant water-cement ratio of 0.55. Compared to control concrete the 28^{th} day compressive strength was decreased by 4.3% and 8.7% for

50% and 100% replacement ratios respectively. However, a 6.1% increase in 28^{th} day splitting tensile strength was observed for 50% marble coarse aggregate replacement. Furthermore, tensile strength of 100% marble coarse aggregate concrete was decreased by about 1.3% compared to control concrete. In addition, a decrease in density and elastic modulus of the concrete was observed as the quantity of coarse marble in the concrete increases.

In a study conducted by Binici et al [17] waste marble and granite were fully (100%) utilized as a coarse aggregate by weight in concrete production using a water-cement ratio of 0.4. In their study river sand and ground blast furnace slag were utilized as fine aggregate to examine strength and durability property of the concrete. According to the test result, the concrete made of marble and granite coarse aggregate has 3%-6% higher compressive, flexural, splitting tensile strength and modulus of elasticity than the control respectively. The concrete's chloride penetration depths are reduced by about 70% when marble and granite are added to the mix. In addition, marble concrete demonstrated the highest Sulfate resistance than any of the samples.

2.3 Bond Strength

In reinforced concrete, the term "bond" refers to the resistance provided by the surrounding concrete against the movement of embedded reinforcement bars. It is a fundamental requirement for concrete and steel to function as a composite material. The majority of structural concrete design processes presume an adequate bond between concrete and reinforcing steel interface. If the bond resistance is insufficient, the reinforcing bar slips, eliminating the composite action. Hence brittle failure in RC members is caused by an abrupt breakdown of bond between the rebars and the concrete at the embedded zones [18]. In addition to being a requirement for any reinforced concrete structural element to function as a composite material, bond among the reinforcement bar and concrete also affects the reinforced concrete ductility, deflection, crack formation and distribution. Bond also has an impact on the seismic response of the structure and members. Under repeated loading such as earthquakes, the interface bond deteriorates quickly, resulting in a significant increase in the slip of the bar. Therefore, the bond between reinforcement bar and concrete plays a major role on the hysteretic performance of RC structures.

2.3.1 Bond Transfer Mechanism

In reinforced concrete structures the degree of interaction among reinforcement bar and concrete is measured by bond stress. Transfer of stresses between them is very important for the overall response of reinforced concrete structures. If there is insufficient bond between the reinforcement and concrete, strain compatibility between the two materials would be lost, causing excessive slip which results in ultimate structural failure.

There are three different mechanisms used to transfer load between concrete and reinforcements. These are the adhesion between the rebar and concrete, frictional forces brought on by the interface's roughness, forces parallel to the surface of the bar and relative movement of the bar with reference to concrete and ribs' mechanical anchorage or bearing against the concrete surface [19],[20]. As the reinforcement bar starts to slip under loading, the surface chemical adhesion initially lost and then a decrease in the frictional forces acting on the rebar's barrel and ribs. At the end, as a result of higher slippage and a loss of adhesion and frictional forces of the bar, the only main mechanism of bond force transfer left is the bearing of the ribs against surrounding concrete (i.e., mechanical anchorage) as shown in Figure 2.2

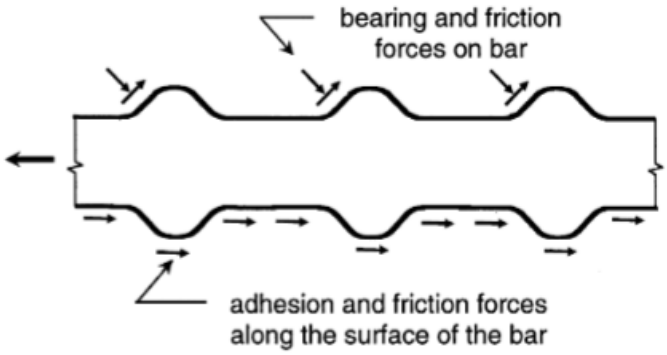

Figure 2.2 Mechanism of bond force transfer [19]

Tepfers [21] asserts that the ring tensile stresses in the surrounding concrete, as shown in Figure 2.3, balances the inclined forces on the bar. The bearing or inclined loads imposed by the ribs on the nearby concrete is divided into horizontal and vertical components. This vertical bearing force causes a splitting mode of bond failure when it exceeds the tensile capacity of the concrete. When the shear resistance of the concrete between subsequent ribs is exceeded, pull-out mode failure takes place in more tightly confined concrete.

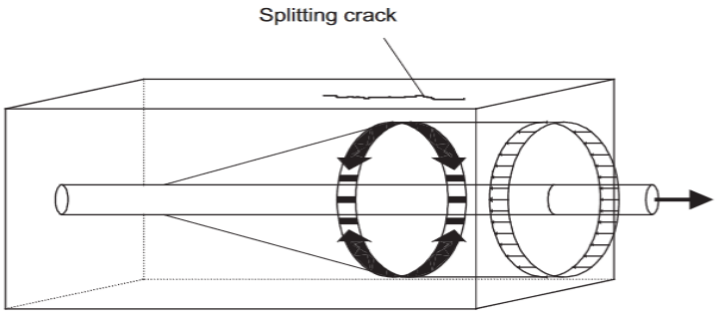

Figure 2.3 Tensile stress distribution around the bar embedded in the concrete [21]

According to Xing et al [22], the mechanical interlocking of the bar in the concrete accounts for around 80% of the bond, and adhesion and friction take the remaining 20%.

2.3.2 Bond Stress-Slip Relationship

The key to maintain the performance of Reinforced Concrete structures is adequate bonding. The majority of research on bond behavior focus on creating the constitutive relation of bond stress-slip under monotonic loading [23]. The bond-slip relation expresses the local bond stress as a function of the local slip at any point along a bar. The relationship among bond stress and slip of the bar is different according to various bond test setup arrangements [24]. Figure 2.4 shows pullout bond setup.

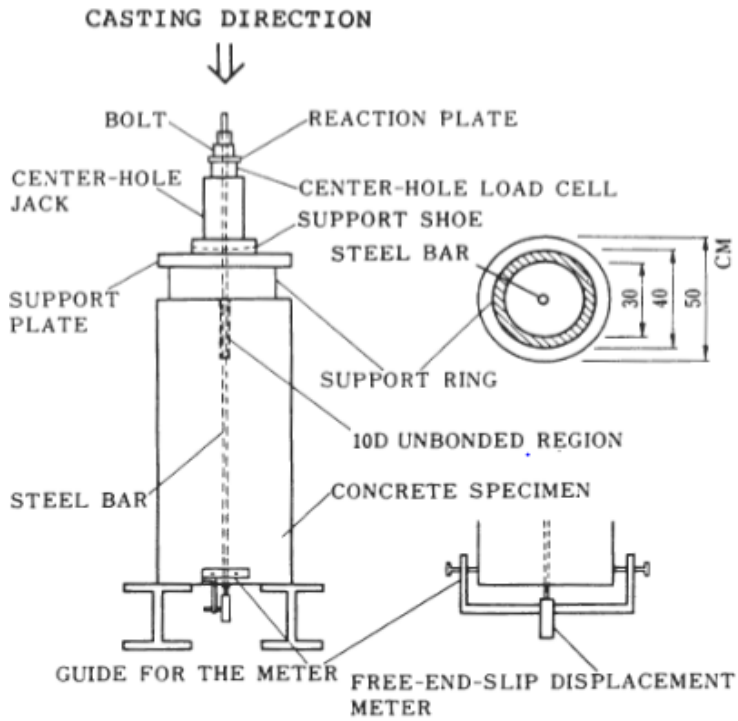

Figure 2.4 Pull-out bond test specimen and apparatus [24]

At every place on an embedded bar, the slope of the steel bar stress distribution curve is proportional to the local bond stress. Bond stress τ at any point in the embedded zone is given in equation 2.1.

$$\tau = \frac{\emptyset d\sigma}{4dx} \tag{2.1}$$

where;

$\emptyset$=diameter of rebar

$\frac{d\sigma}{dx}$ = Slope of bond stress- slip curve.

Bond stress- slip is a typical way to characterize the bond behavior of reinforced concrete members. Figure 2.5 illustrates the bond-slip relationship for both pull-out and splitting failure.

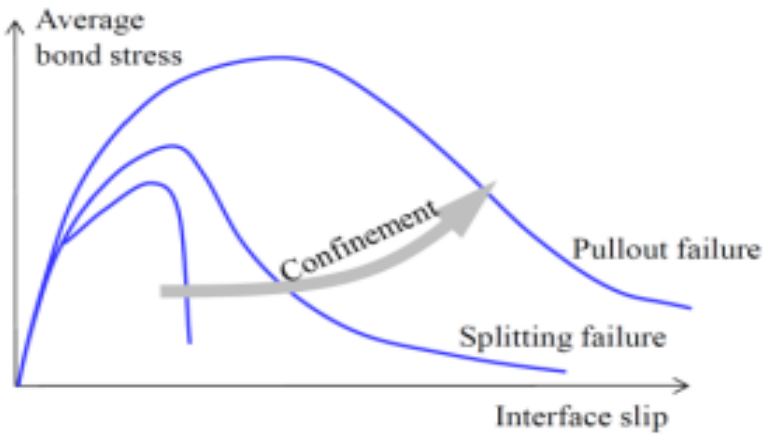

Figure 2.5 Bond stress-slip behavior [23]

2.3.3 Bond-Slip Model

The relationship between the local bond stress and the relevant local slip of the bar is considered the best description of the bond characteristic of bars. Slip is characterized as the bar's relative displacement with regard to the concrete. These bond stress slip relations are required for analytical models to accurately anticipate the bond property of anchored bars. A shorter embedment length of (5*d) is chosen to minimize the impact of an unequal bond stress distribution along the steel bar's embedded length [25].

According to Filippou et al.,[26] the bond stress was evenly distributed along the anchoring length, and the following differential equations (equation 2.2 and 2.3) was derived based on the equilibrium of forces acting on a bar embedded in concrete as shown in Figure 2.6.

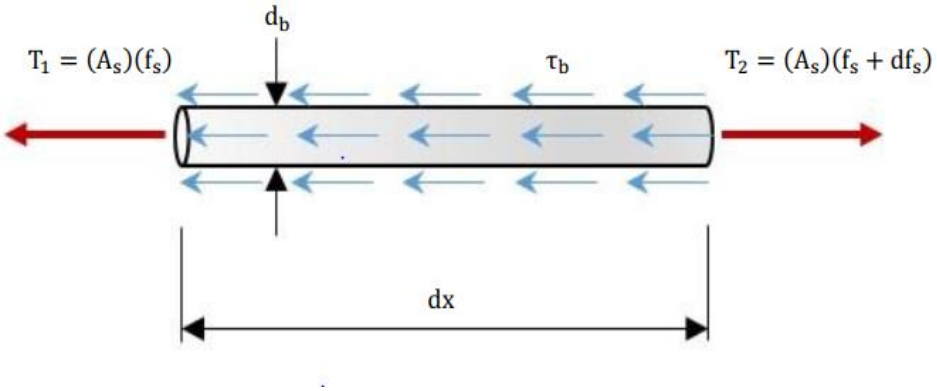

Figure 2.6 Equilibrium of forces acting on bar element in pull-out test [26]

$$\Delta T = T_2 - T_1 = A_s\, df_s = \tau(x)\pi d_b dx \quad (2.2)$$

The bond stress on the bar element $\tau(x)$ is thus found as shown in equation 2.3

$$\tau(x) = \frac{\Delta T}{\pi d_b dx} = \frac{d_b}{4}\frac{df_s}{dx} \quad (2.3)$$

Where;

T is the force acting on bar element

d_b is the diameter of bar

A_s is the area of steel bar

f_s is the tensile stress on bar element and

dx is the length of infinitesimal bar element

As stated by Tang et al [27] the bond stress slip model has four distinct regions as shown in Figure 2.7. The first region is a curvilinear ascending region ranging from 0-s_1 in which bond stress increases with slip. In this region the concrete mortar matrix is penetrated by the reinforcement ribs and results in microcracking and localized crushing. The second region is a constant maximum bond stress region from s_1-s_2 in which constant peak stress is reached for a well confined concrete as slip increases. A linearly descending region is the third zone in bond stress slip model in which bond stress linearly decreases from s_2 to s_3 due a gradual loss of bond at concrete-rebar interface resulting concrete specimen crack and rebar slip and finally, the fourth region of constant bond stress beyond s_3 is the minimum residual bond stress resulted from the remaining friction in the concrete.

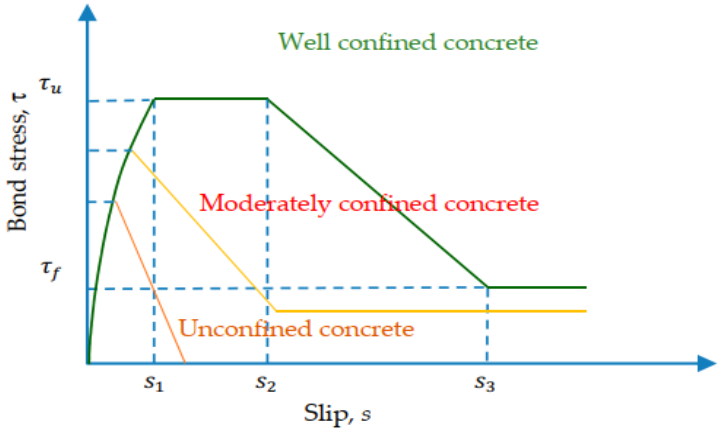

Figure 2.7 Bond stress –slip curve for various concrete confinement conditions [27]

A similar bond slip model was stated on the CEB FIP model code 2010 [28] showing analytical equations of bond stress for both pullout and splitting failure in various concrete confinement condition. For monotonic loading the bond stress (τ) as a function of relative slip (s) of the bar is calculated according to equations 2.4 to 2.7 as shown in Figure 2.8.

$$\tau = \tau_u (s/s_1)^{\alpha} \quad \text{for} \quad 0 \le s \le s_1 \tag{2.4}$$

$$\tau = \tau_u \quad \text{for} \quad s_1 \le s \le s_2 \tag{2.5}$$

$$\tau = \tau_u - (\tau_u - \tau_f) \left(\frac{s-s_2}{s_3-s_2}\right) \quad \text{for} \quad s_2 \le s \le s_3 \tag{2.6}$$

$$\tau = \tau_f \quad \text{for} \quad s > s_3 \tag{2.7}$$

where;

τ_u is the ultimate bond stress

τ_f is the residual bond stress

α is a constant coefficient indicating bond characteristics ($0 \le \alpha \le 1$)

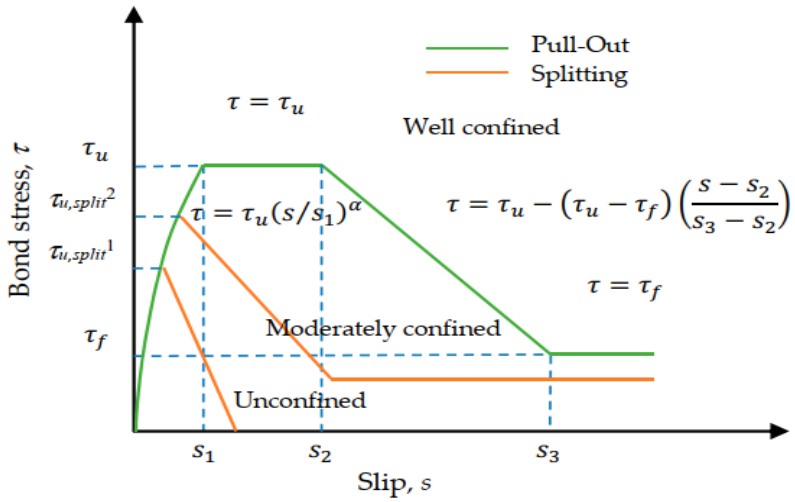

Figure 2.8 Bond stress–slip curve with analytical equations [28]

2.4 Bond Strength Test Methods

Experimental bond tests are used to investigate the strength, behavior and failure modes of reinforcement bars embedded in concrete. Various test configurations are used to explore the behavior of bonds.

There are two widely utilized test procedures to experimentally investigate the bond strength of reinforced concrete. One of the methods is the pull-out test and the other is beam test [29]. This bond test methods are schematically shown in Figure 2.9 as a) Pull-out specimens b) beam-end specimen c) beam anchorage specimens and d) Splice specimen.

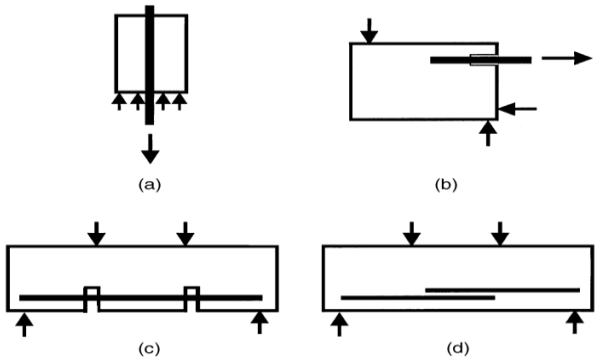

Figure 2.9 Arrangements for bond tests a) pull-out specimens b) beam-end specimen c) beam anchorage specimens d) Splice specimen [19]

Pull-out test is the most popular, preferred and simplest method for evaluating the bond strength of bars. Therefore, most of the data on bond is available from this bond test method. In this test method the concrete specimens were under compression while the bars were under tension (pull-out) hence it is the least accurate and realistic [30],[31]. Figure 2.10 presents stress distribution on the bar subjected to pullout load.

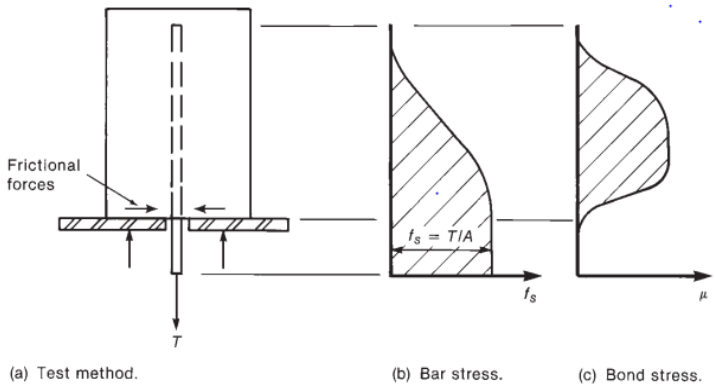

Figure 2.10 Pull-out test setup and stress distribution on the bar [30]

Beam-end specimens for bond tests are prepared as per ASTM A944-95 [32] guidelines. This bond test technique is used as a more accurate and realistic measure of bond strength than pull-out test [33]. In the other way Wassouf [34] generalized that the beam test is more costly, time consuming and gives a contradicting result than pull-out test.

2.5 Bond Strength Failure Mode

Investigating the mode of failure of each specimen is important to define the effect of different factors on the bond behavior of the concrete structures. The bond failure mode can be determined from the shape of bond stress -slip curve.

The confining action, which is brought about by the circumferential tensile forces in the concrete, as well as extra confinement such transverse reinforcement and external forces controls the mode of bond failure. It will work against the bond force's radial components, which radiate from the bar into the concrete, in an effort to create an equilibrium state [35].

CEB FIP model code 2010 categorize bond failure modes as pull-out and Splitting failure. However, Lundgren [36] divided bond strength failure modes into four. They are concrete cover splitting, pull-out (bond) failure, pull-out failure after yielding of reinforcement bar and rapture of the reinforcement bar.

Pull-out bond failure occurs when the tensile force represented by the concrete cover, stirrups or external confinement is greater than the radial component of bond force that is transferred from the bar into concrete. As the load imposed increased the chemical adhesion of concrete initially lost and microcracks developed and when the shear strength of the concrete under the ribs is exceeded then the bar starts to slip is known as pullout failure. This failure mode happens when the reinforcement bar embedded is well confined by the surrounding concrete [36],[37].

The other bond failure type is splitting of specimens. It occurs when the force generated by bond action is greater than the tensile capacity of the ring along with less concrete cover than diameter of the bar. In the other way when the bar confinement is insufficient the vertical component of the bond force induces the radial and tangential stresses in the concrete and which then results in splitting of concrete [37]. Splitting failure mode is

regarded as critical and governing in design since it yields lower bond stress values than pull-out failure [38].

2.6 Factors Affecting Bond Strength

The bond between reinforced bar and concrete is influenced by numerous factors. They are categorized under three main groups as shown in Figure 2.11. They are concrete properties, bar properties and structural characteristics [19]. The detail discussion of each factor is included in the next sections.

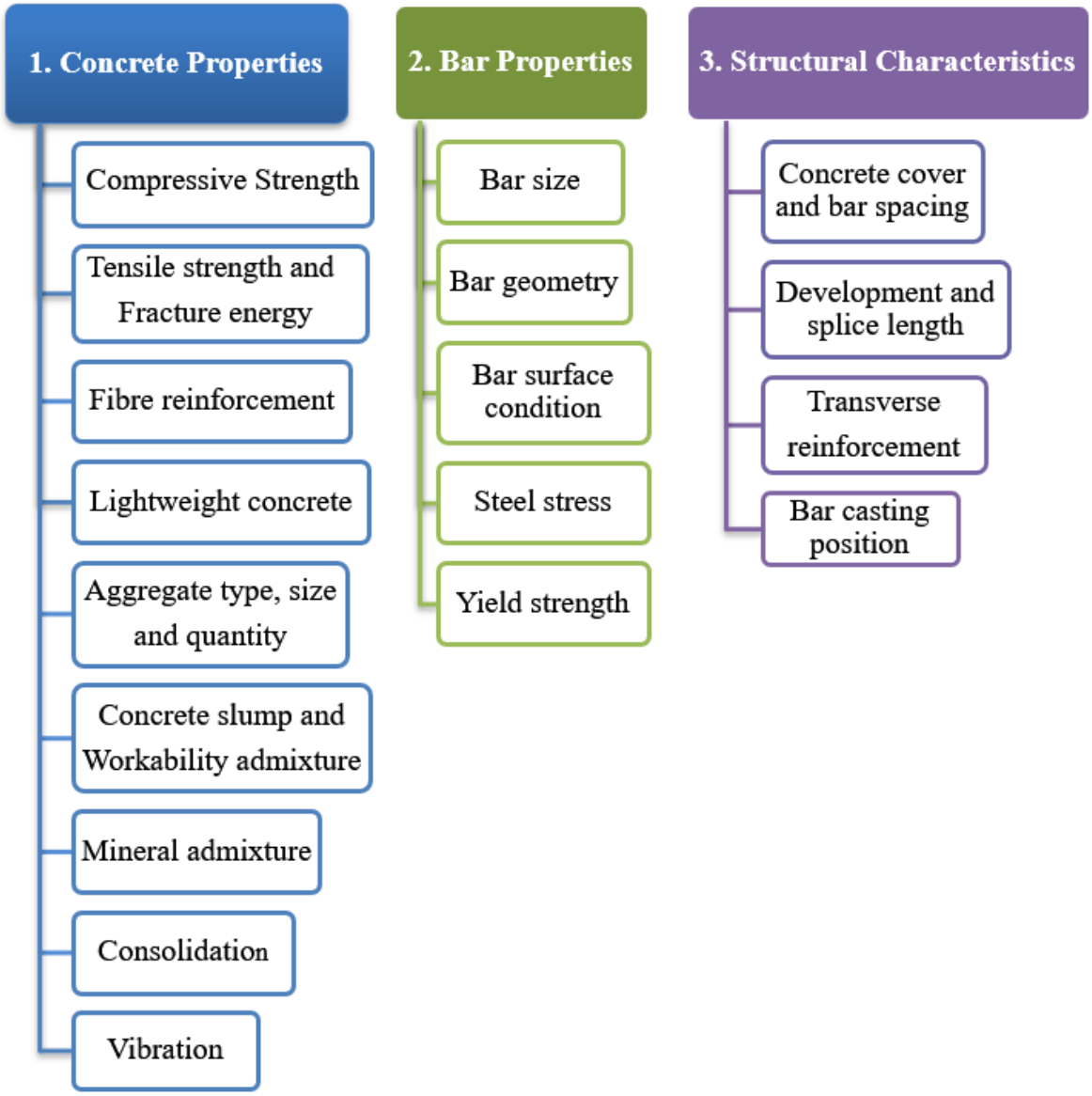

Figure 2.11 Categorization of factors that affect bond strength [19]

2.6.1 Structural Characteristics

a. Concrete cover and bar spacing

Bond strength at the interface of concrete and bar increases with increase in cover and bar spacing. Concrete cover and rebar spacing affect the bond failure modes. Pullout failure occurs for specimens with large concrete cover and rebar spacing. Smaller concrete cover and bar spacing results in small bond strength and splitting mode of bond failure [19].

b. Development and splice length

A reinforcing bar's bond capacity will increase if its development or splice length is increased. Due to the non-uniform nature of bond forces, this increase is nearly linear but not proportionate to the length [19]. Wang [39] also added that bond strength is not linear along the length of development, as a result of voids formed at the interface. Highest bond stresses are developed around the area close to the loaded end.

c. Transverse reinforcement

Transverse reinforcement confines the bar by preventing splitting cracks from spreading and increase the bond force needed to cause failure. Thus, an increase in lateral reinforcement (stirrup) causes the bond force to grow, which ultimately causes pullout failure. However, if more lateral reinforcement is provided, the increase in bond strength will be less effective [19],[40].

2.6.2 Bar Properties

a. Bar size

It is not often understood how bar size and bond strength relate to one another. It is for two reasons. The first one is that as the bar size increases, a longer development length is required to fully develop a given bar stress. Thus, it is preferable to utilize a greater number of small bars than a smaller number of large bars. The second reason is that for the same level of confinement, bars with a larger size achieve a higher bond force that causes either splitting or pull-out failure than smaller bars. Furthermore, for bars not confined by transverse reinforcement, large size bars require larger forces to cause bond failures. This shows that in addition to other parameters bar size also affects the bond force developed

at bond failure [19]. Burdzi´nski et al [37] also stated that the diameter of the bar plays a key role in determining the bond embedment length and overall dimension of the concrete specimen. It also affects bond stress-slip relationship and pullout force.

b. Bar geometry

According to a study by Abrams [41] deformed steel bars produce higher bond resistance than smooth plain bars. By directly bearing on the nearby concrete, the ribs on the deformed bars boosted the bond resistance. A study by Skorobogatov and Edwards [42] concludes that the rib face angle has no effect on the bond strength because the ribs will crush the concrete as they travel, flattening the high face angle of the rib. Hamad [43] also added that bar ribs contribute significantly to the development of bond strength by preventing the concrete between the bar ribs from sliding. The friction developed among the surrounding concrete and reinforcing bars depends on the geometry of ribs.

c. Bar surface condition

The cleanliness of the reinforcement, the amount of rust present on the bar's surface, and the use of epoxy coatings to prevent corrosion of the reinforcement are all factors that affect the surface of reinforcement bar. The reinforcement bar surface affects the force transfer mechanism ability of ribs at the interface. Therefore, the bar surface plays a key role in maintaining proper bond at the concrete-steel interface which also contributed to an overall safety of structures [19].

d. Steel stress and yield strength

Steel bars that yielded before bond failure exhibited a lower average bond stress when compared to high strength bars embedded in the same test specimens that did not yield. Because of this, test specimens were frequently set up specifically to make sure the reinforcement bars did not yield or split before the bond failure. In addition, bond strength is also affected by the presence of confining transverse reinforcement bars. When compared with identical bars with similar bonded length, the bond strength of the bars that yield is about 2% less when not confined by transverse reinforcement and 10% higher when confined by transverse reinforcement than the high strength steel bar that does not yield [19].

2.6.3 Concrete Properties

a. Compressive strength

Concrete strength is the most important property of concrete that determines the durability and performance of concrete structures. Codes and most of the previous studies represent the effect of concrete properties on bond strength using the square root of the compressive strength ($\sqrt{f'_c}$). This representation has shown to be adequate as long as concrete cylindrical strengths are maintained below 55 MPa. For high strength concrete the bearing capacity of concrete (related to f_c) grow quickly with an increase in compressive strength. Thus, the effect of concrete strength on bond is exaggerated when using $\sqrt{fc'}$ resulting an overestimated bond strength result for high strength concrete. Researchers on bond provide $fc^{1/4}$ as a more accurate representation of the effect of concrete strength on bond [19], [44].

b. Aggregate type and quantity

According to studies made by Zuo and Darwin for bars not confined by transverse reinforcement, high strength coarse aggregate(basalt) can increase the bond strength by 13% in comparison with weaker coarse aggregate (limestone).This study was also strengthened by others that concrete with basaltic coarse aggregate had only a slightly higher flexural strengths, but significantly higher fracture energy than concrete of similar compressive strength containing limestone for compressive strengths between 20 and 96 MPa.Higher fracture energy of basaltic coarse aggregate concrete increases the resistance to crack propagation which in turn increase bond strength by delaying splitting failure. It has also been noted that coarse aggregate strength and quantity increased the bond strength of confined concrete by 45% [19], [45].

In the study made by Lemlem [46] and Iqbal et al [47] the reinforcement bar was embedded in different nominal size natural coarse aggregate concrete to investigate the effect of coarse aggregate size on bond strength. The nominal size of aggregates used in their study were 37.5mm,25mm,19mm,12.5mm and 9. 5mm.According to the findings of their study the bond strength increases with increase in size of coarse aggregate and it due to a reduction in locking provided by small sized aggregates. Thus, it can be generalized that in addition to aggregate type and quantity, the size of aggregate used has also an impact on bond strength.

c. Tensile strength and fracture energy

The effect of aggregate type and quantity, as well as concrete compressive strength, can provide insight into the significance of tensile strength in relation to bond strength. The concrete contribution tensile strength Tc increases approximately with $f'c^{1/4}$. On the other hand, it is commonly accepted that the tensile strength of normal strength concrete rises approximately with $f'c^{1/2}$. The relationship between compressive strength and bond strength should be well represented by $f'c^{1/2}$ if tensile strength alone were the primary determining factor in bond strength. The relationships among compressive and tensile strength of concrete appear to be directly related to the fracture energy of concrete. According to study by Braham and Darwin, stronger bonds are a result of increased fracture energy provided by high strength fibers [19].

d. Concrete slump and workability admixtures

Slump of the concrete mix has an effect on bond strength between concrete and reinforcing steel. The tendency for concrete to settle and bleed increases with increasing concrete slump. The time it takes for settlement and bleeding to begin is prolonged by water reducers and high range water-reducing admixtures and decrease the bond. Generally, for normal strength concrete properly consolidated low slump concrete provides the best bond with reinforcement bars whereas concrete with high slump results in a decreased bond because of no or little consolidation effort is desirable [19].

2.7 Bond strength in Various Code Provisions and Empirical Equations

Bond strength is used to facilitate the development of design guidelines for the anchorage of reinforcement in concrete structures. As stated by Sadeghi et al [48] there are three references that are frequently used as a guideline for the pull-out test. These are RILEM technical recommendation, ASTM 234 and Danish standard DS 2082.

According to RILEM [49] pull-out bond test method for normal strength concrete, the bond length of the sample is limited to five times diameter of the bar to limit stress variation at the interface with increase in embedment. In this test method during loading the concrete specimen is in compression while the reinforcement bar is in tension and it doesn’t correctly simulate real-life situations. The average bond stress is determined by

dividing the pullout tensile load by the contact surface area of the bar, as shown in equation 2.8.

$$\tau = \frac{P}{\pi d_b l_e} \quad (2.8)$$

Where;

P is the maximum pull-out load (N)

d_b is diameter of the reinforcement bar (mm)

l_e is the embedment length (mm)

2.7.1 Bond Stress Equation in Code Provisions

For determining the bond strength between surrounding concrete and reinforcement bar, different codes have proposed various bond stress formula taking into account the key factors such as bar diameter, compressive strength, concrete cover and embedment length. In this study European norm Ethiopian building code ES EN 1992-1-1:2015, American Concrete institute ACI 318 and Comite Euro-International du Beton and federation Internationale de la Precontraine (CEB-FIP 2010) model codes are considered.

Ethiopian Code

According to the Ethiopian building code ES EN 1992-1-1:2015 [50] section 8.4.2(2) the design value of the ultimate bond stress, f_{bd}, for ribbed bars is given in equation 2.9.

$$f_{bd} = 2.25\ \eta_1\eta_2 f_{ctd} \quad (2.9)$$

Where;

`

f_{ctd} is design concrete tensile strength, $f_{ctd} = \frac{\alpha_{ct} f_{ctk,0.05}}{\gamma_c}$

η_1 is a coefficient related to the quality of the bond condition and the position of the bar during concreting. $\eta_1 = 1.0$ when 'good' conditions are obtained and 0.7 for all other

η_2 is related to the bar diameter (∅)

$\eta_2 = 1.0$ for $\emptyset \leq 32$ mm and

$\eta_2 = \frac{(132-\emptyset)}{100}$ for $\emptyset > 32$ mm

American Concrete Institute

According to ACI 408R-03 [19] the bond stress (τ) is determined as shown in equation 2.10.

$$\tau = \frac{f_y\, d_b}{4\, l_d} \tag{2.10}$$

Where;

f_y is the yield strength of steel bars (MPa)

d_b is diameter of bars (mm)

l_d is development or embedment length of bars (mm)

The development length, l_d for deformed bars in tension is calculated by equation 2.11 as stated on ACI 318-08 [51] under section 12.2.3

$$l_d = \left(\frac{f_y\, \psi_t \psi_e \psi_s}{1.1\, \lambda \sqrt{f'_c}\, (\frac{c_b + k_{tr}}{d_b})} \right) d_b \tag{2.11}$$

Where;

f_y is yield strength of rebar (MPa)

ψ_t is the modification factor for the location of bar

ψ_e is the modification factor for epoxy coating of bar

ψ_s is the modification factor for size of the bar

λ is the modification factor for the weight of concrete

f'_c is the mean value of cylindrical compressive strength (MPa)

c_b is cover over the bar (mm)

d_b is diameter of bar (mm)

k_{tr} is transverse reinforcement index

CEB-FIP Model Code

According to Comite Euro-International du Beton and federation Internationale de la Precontraine (CEB-FIP Model Code 2010**)** [28] the maximum bond strength (τ_u) at steel concrete interface for the specimens with good confinement is presented in equation 2.12.

$$\tau_u = 2.5\sqrt{f_c'} \tag{2.12}$$

where;

f_c' is the mean value of cylindrical compressive strength (MPa)

2.7.2 Bond Stress Empirical Equations

A number of experimental studies have been conducted by various researchers to investigate bond strength of reinforcement bar embedded in concrete. Different test methods and parameters were taken by various researchers. In this study experimental layout, parameters considered, proposed bond stress equations and the limitations of equations of nine different researchers were assessed.

Orangun et al [40]

Orangun et al conducted an experimental test to investigate the bond strength of anchored bars using beam specimen. To perform the bond test longitudinal deformed bars were placed at the opposite top and bottom corners in the beam and tied using stirrups as show in Figure 2.12. The test was done using reinforcement bars of diameter 10mm,18mm and 26mm embedded in varying dimensions of the beam specimen.

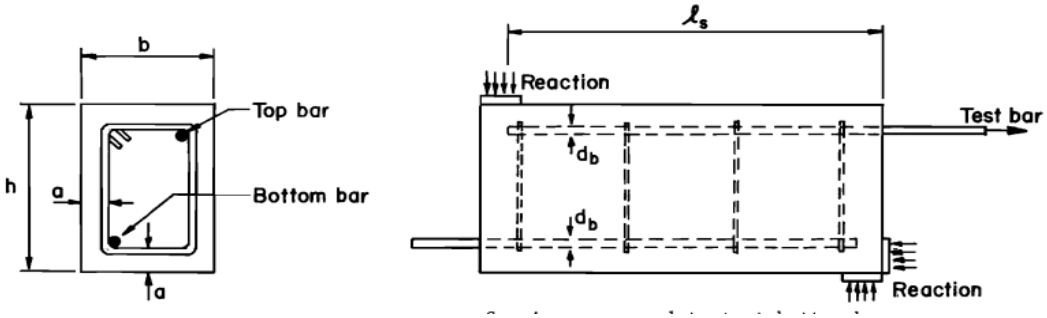

Figure 2.12 Details of Orangun et al's beam specimens [40]

Based on nonlinear regression analysis of test result, Orangun et al. developed an empirical bond stress equation as shown in equation 2.13. The equation reflects the effects of

concrete strength, diameter of the bar, concrete cover and development length of the bar on bond strength. The formula can also be used to calculate the basic development lengths.

$$\tau_u = 0.083045\sqrt{f_c'}\,[1.2 + 3\left(\frac{c}{d_b}\right) + 50\,(\frac{d_b}{l_d})] \quad (2.13)$$

Where;

τ_u is the ultimate bond stress (MPa)

f_c' is the mean value of cylindrical compressive strength (MPa)

c is concrete cover (mm)

d_b is the diameter of the bar (mm)

l_d is development length of the bar (mm)

Darwin et al [52]

Darwin et al investigated the bond performance of bars not confined by transverse reinforcement and proposed an equation that predicted the ultimate bond stress. The predicted formula as shown in equation 2.14 included the effects of concrete strength, concrete cover, bar diameter size and embedment length.

$$\tau_u = 0.083045\sqrt{f_c'}[(1.06+2.12(\frac{c}{d_b})(0.92 + 0.08\frac{c_{max}}{c_{min}}) + 75\frac{d_b}{l_d})] \quad (2.14)$$

Where;

τ_u is the ultimate bond stress (MPa)

f_c' is the mean value of cylindrical compressive strength (MPa)

c is concrete cover (mm)

c_{min} is minimun concrete cover (mm)

c_{max} is maximum concrete cover (mm)

d_b is the diameter of the bar (mm)

l_d is development length of the bar (mm)

Esfahani and Rangan [53]

Esfahani et al performed an experimental test to study bond strength of steel bar embedded in both normal and high strength concrete. The test was conducted using spliced beam specimens in two stages. The first stage investigated the bond strength of steel bar in normal strength concrete while the second stage examine bond strength of steel bar in high strength concrete. Based on the test result an empirical equation was estimated to calculate

the ultimate bond strength as shown in equation 2.15. The equation incorporated tensile strength of concrete, cover thickness of the concrete and diameter size of the bar. The impact of bar embedment length on bond was disregarded in the equation.

$$\tau_u = 8.6 \left(\frac{\frac{c}{d_b} + 0.5}{\frac{c}{d_b} + 5.5} \right) f_{ct} \quad (2.15)$$

Where;

τ_u is the ultimate bond stress (MPa)

c is concrete cover (mm)

d_b is the diameter of the bar (mm)

f_{ct} is tensile strength of the concrete (MPa)

Shima et al [24]

In order to formulate the constitutive model for bond strength of reinforced concrete Shima et al conducted a pullout test using different type deformed bar. The bars are deformed reinforcement bars, steel bar and deformed aluminum bars as shown in Figure 2.13. The deformed bars have a nominal diameter 19,25 and 32mm.All bars were centrally embedded in cylindrical specimens of diameter 500mm and varying height.The bars are unbonded at loaded end with a length of ten times diameter of the bar. The overall Pullout specimen setup was presented in Figure 2.4.

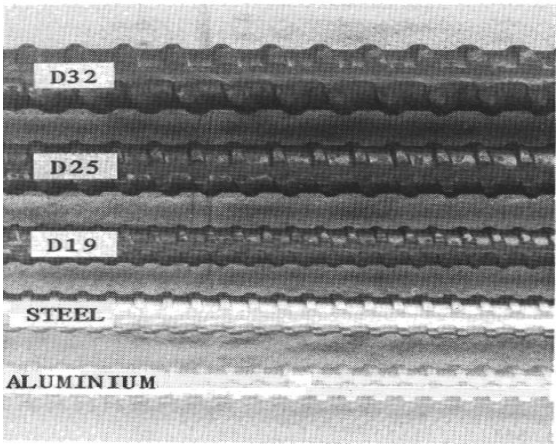

Figure 2.13 Bar types used for Shima et al's bond test [24]

The study conducted by Shima et al proposed an empirical bond stress equation as shown in equation 2.16. The equation includes parameters such as compressive strength,

reinforcement bar diameter and the relative movement of the bar (slip) for prediction of ultimate bond. The equation gives more emphasis to the effect of concrete strength. Other bond parameters such as embedment length of the bar, concrete cover was not considered.

$$\tau_u = 0.9f_c'^{2/3}[1\text{-}e^{-40\left(\frac{s}{d_b}\right)^{0.6}}] \quad (2.16)$$

Where;

τ_u is the ultimate bond stress (MPa)

f_c' is the mean value of cylindrical compressive strength (MPa)

d_b is the diameter of the bar (mm)

s is slip (mm)

Aslani and Nejadi [54]

The study conducted by Aslani and Nejadi examines the bond performance of reinforcement bar embedded in both conventional and self-compacting concrete. The bond was measured using pullout test method on a single bar embedded in prismatic specimens and the ultimate bond at interface of bar and concrete was developed as shown in equation 2.17. The equation incorporates the parameters that affect bond strength such as concrete compressive strength, concrete cover, diameter and embedded length of the bar.

$$\tau_u = f_c'^{0.55}(0.672(\frac{c}{d_b})^{0.6} + 4.8\frac{d_b}{l_e}) \quad (2.17)$$

Where;

τ_u is the ultimate bond stress (MPa)

f_c' is the mean value of cylindrical compressive strength (MPa)

c is concrete cover (mm)

d_b is the diameter of the bar (mm)

l_e is embedment length of the bar (mm)

Chapman et al [55]

Chapman et al conducted an experimental investigation to examine the early age bond strength between reinforcement bar and concrete. Pull-out method of bond test was conducted using both smooth and deformed steel bar types with different embedment length. The test was done at different ages of curing from 1 to 28 days. In their study

Chapman et al forwarded an empirical equation stated in 2.18 to predict the early age ultimate bond strength of steel bar embedded in the concrete. In their equation chapman et al included the effect of all concrete properties (i.e. compressive strength), bar properties (i.e. bar diameter and embedment length) and structural properties (i.e. cover).

$$\tau_u = 0.083035\sqrt{f_c'}\,(3.5+ 3.4\frac{c}{d_b}+ 57\frac{d_b}{l_e}) \quad (2.18)$$

Where;

τ_u is the ultimate bond stress (MPa)

f_c' is the mean value of cylindrical compressive strength (MPa)

c is concrete cover (mm)

d_b is the diameter of the bar (mm)

l_e is embedment length of the bar (mm)

Huang et al [56]

Huang et al conducted an experimental and analytical investigation to assess the bond strength behavior of deformed steel bar embedded in high strength concrete. Based on the test result Huang et al predicted an equation for ultimate bond strength shown in equation 2.19. The equation considered compressive strength of concrete as the only parameter and the effect of bar properties such as embedment length and bar diameter size were not considered. In addition, the impact of concrete cover thickness was also not included in the equation.

$$\tau_u = 0.45f_c' \quad (2.19)$$

Where;

τ_u is the ultimate bond stress (MPa)

f_c' is the mean value of cylindrical compressive strength (MPa)

Hadi [57]

Hadi et al investigated bond strength at the interface of high strength concrete and high strength bar .Seven deformed bars of nominal diameter 12,16,20,25,28,32 and 36mm were used for bond test using cylindrical specimens of height 30mm and diameters (D) 240mm and 300mm.All bars were embedded in 70MPa concrete at an embedment length of 150mm from the top as shown in Figure 2.14 and pullout test method was conducted to

measure bond strength at the interface of concrte and reinforcement bar. The configuration of pullout setup was shown in Figure 2.15.

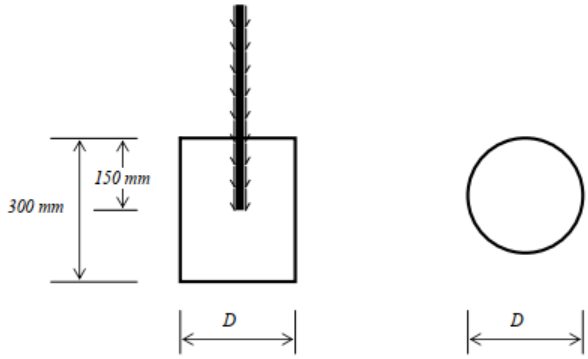

Figure 2.14 Test specimen detail of Hadi [57]

Figure 2.15 Hadi's Pullout test setup [57]

Hadi proposed an empirical bond stress equation stated in 2.20. The parameters considered were compressive strength, concrete cover, reinforcement bar diameter and embedment length of the bar. The equation includes more parameters that will affect bond between steel bar and concrete.

$$\tau_u = 0.083045\sqrt{f_c'}\ [\ 22.8 - 0.208\left(\frac{c}{d_b}\right) - 38.212\ \left(\frac{d_b}{l_d}\right)\ ] \qquad (2.20)$$

Where;

τ_u is the ultimate bond stress (MPa)

f_c' is the mean value of cylindrical compressive strength (MPa)

c is concrete cover (mm)

d_b is the diameter of the bar (mm)

Melkam [58]

Melkam conducted an experimental test to investigate effect of coarse Steel Slag aggregate on bond strength. In her study melkam applied pull-out method of bond test using reinforcement bars of diameter 12mm,14mm and 16mm.The bars were centrally anchored in cylindrical specimens of diameter 150mm and height 300mm which extended 80mm at the bottom for slip measurement. A detail specimen dimension and experimental configuration was shown in Figures 2.16 and 2.17 respectively.

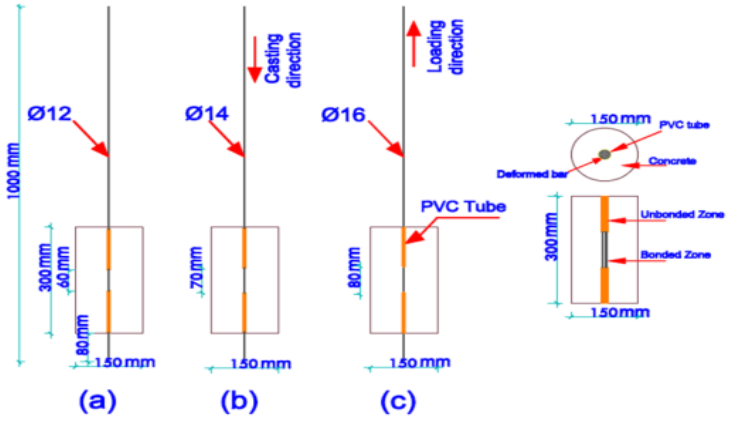

Figure 2.16 Specimen detail of Melkam [58]

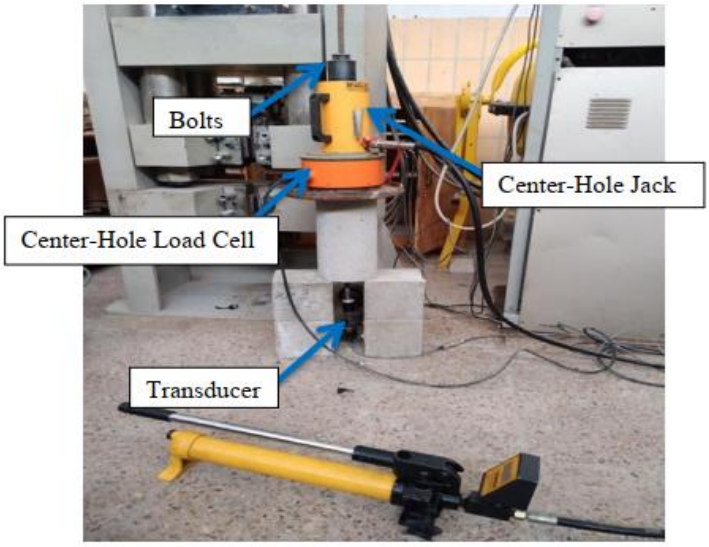

Figure 2.17 Pullout test setup of Melkam [58]

In her study Melkam proposed an empirical bond stress equation stated in 2.21. The parameters considered were concrete compressive strength, concrete cover thickness and

reinforcement bar diameter. However, the effect embedment length of bar on bond strength was ignored in this equation.

$$\tau_u = 4.31\sqrt{f_c'} + 0.95\frac{c}{d_b} - 12.85 \quad (2.21)$$

Where;

τ_u is the ultimate bond stress (MPa)

f_c' is the mean value of cylindrical compressive strength (MPa)

c is concrete cover (mm)

d_b is the diameter of the bar (mm)

Generally, the bond stress equations of codes and those proposed by various researchers considering different parameters were summarized as shown in Table 2.3.

Table 2.3 Summarized review of bond stress equations

No	Author [Ref.]	Bond Stress Equations	Eq. no.	Parameters considered	Remark
1	ES EN 1992-1-1:2015 [50]	$f_{bd} = 2.25\ \eta_1\eta_2 f_{ctd}$	(2.10)	Concrete tensile strength, bar diameter and bar casting position	Ignore effect of bar embedment condition
2	ACI 318-08 [51]	$\tau = \frac{f_y\, d_b}{4\, l_d}$	(2.11)	Compressive strength, cover, diameter, yield strength, embedment length, surface and location of the bar	Good as it includes more bond parameters
3	CEB-FIP Model Code 2010 [28]	$\tau_u = 2.5\sqrt{f_c'}$	(2.12)	Only concrete compressive strength and pull-out failure mode	The effect of other bond parameters was ignored
4	Orangun et al [40]	$\tau_u = 0.083045\sqrt{f_c'}\,[1.2 + 3\left(\frac{c}{d_b}\right) + 50\,(\frac{d_b}{l_d})]$	(2.13)	Compressive strength, cover, bar diameter and embedment length	Relatively include more bond parameters
5	Darwin et al [52]	$\tau_u = 0.083045\sqrt{f_c'}[(1.06+2.12(\frac{c}{d_b})(0.92 + 0.08\frac{c_{max}}{c_{min}}) + 75\frac{d_b}{l_d})]$	(2.14)	Compressive strength, cover, bar diameter and embedment length	Relatively include more bond parameters
6	Esfahani et al [53]	$\tau_u = 8.6\,(\frac{\frac{c}{d_b}+0.5}{\frac{c}{d_b}+5.5})\,f_{ct}$	(2.15)	Concrete tensile strength, cover and bar diameter size	Ignore the effect bar embedment length

7	Shima et al [24]	$\tau_u = 0.9f_c'^{2/3}[1\text{-}e^{-40\left(\frac{s}{d_b}\right)^{0.6}}]$	(2.16)	Compressive strength, bar diameter and slip	Only for long embedment length
8	Aslani et al [54]	$\tau_u = f_c'^{0.55}(0.672(\frac{c}{d_b})^{0.6} + 4.8\frac{d_b}{l_e})$	(2.17)	Compressive strength, cover, bar diameter and embedment length	Included more parameters
9	Chapman et al [55]	$\tau_u = 0.083035\sqrt{f_c'}(3.5+ 3.4\frac{c}{d_b}+ 57\frac{d_b}{l_e})$	(2.18)	Compressive strength, cover, bar diameter and embedment length	Relatively include more parameters
10	Huang et al [56]	$\tau_u = 0.45f_c'$	(2.19)	Only compressive strength	The effect of other bond parameters was not considered
11	Hadi [57]	$\tau_u = 0.083045\sqrt{f_c'}[22.8 - 0.208(\frac{c}{d_b})- 38.212(\frac{d_b}{l_d})]$	(2.20)	Compressive strength, cover, bar diameter and embedment length	Relatively include more parameters
12	Melkam [58]	$\tau_u = 4.31\sqrt{f_c'} + 0.95\frac{c}{d_b}$ -12.85	(2.21)	Compressive strength, cover and bar diameter	The embedment length of bar was not considered

3. MATERIAL AND METHODS

3.1 Introduction

In this chapter, the characterization of materials, specimen preparations, experimental work, and test setups carried out in the study are briefly described. Preparation of materials, testing, and a detailed experimental programme were conducted in the Addis Ababa Institute of Technology (AAiT) construction material testing laboratory. Materials were examined in accordance with the requirements outlined in the ASTM standards and specifications.

3.2 Materials

The materials used in this study include Cement, Fine aggregate, Coarse aggregate, Crushed marble aggregate, water, and deformed reinforcement bars.

3.2.1 Cement

The binder used in this study was Type 1 Dangote Ordinary Portland Cement (OPC), purchased from the local market. It has a grade of CEM 42.5R and conforms to the guidelines of ASTM C150 [59]. The relative density of the cement is 3.15 g/cm^3.

3.2.2 Aggregate

Aggregate is the general term which refers to a coarse to medium-grained particulate materials used in construction. It consists of geosynthetic aggregates, fine sand, gravel, crushed stone, slag, and recycled concrete. Aggregates cover 65-75 percent of the volume of concrete. In this study to eliminate any variations in the characterization of materials both fine and coarse aggregates were supplied from the same source. The aggregate has been cleaned to get rid of any dust or other contaminants like silt that could lower the quality of the concrete. All pertinent aggregate physical tests, such as bulk density, specific gravity, and moisture content of the aggregate, have been performed in Addis Ababa Institute of Technology construction material testing laboratory as per Abebe Dinku Construction Materials Laboratory Manual [60] to ensure that the material complies with the requirements for concrete work. Until mixing day, the aggregates were stored in a plastic bag to maintain the moisture content.

3.2.2.1 Fine Aggregate

ASTM C-125 [61] defines fine aggregate as an aggregate primarily retained on the 0.075mm sieve after passing the 9.5 mm sieve and nearly totally passing the 4.75 mm sieve. For this study, natural river sand from Jida was used in all test specimen preparation. Before using it in concrete mix, the fine aggregate was first properly washed, dried, and sieved through a 4.75-mm sieve. Then, to minimize moisture fluctuations in the fine aggregates, they were collected in plastic bags. The physical properties of fine aggregates were examined in the Addis Ababa Institute of Technology material testing laboratory and summarized in Table 3.1 below. Furthermore, the gradation of fine aggregate was conducted as per ASTM C-33 [62] guidelines and presented as shown in Figure 3.1. The overall laboratory physical examination of fine aggregate is provided in Appendix A-1.

Table 3.1 Physical Property Test Result of Fine Aggregate

No	Laboratory Physical Tests	Results
1	Unit Weight	1531.52 kg/m^3
2	Bulk Specific Gravity	2.45
3	Water Absorption	2.333 %
4	Moisture Content	1.71 %
5	Silt content	1.69 %
6	Fineness Modulus	2.72

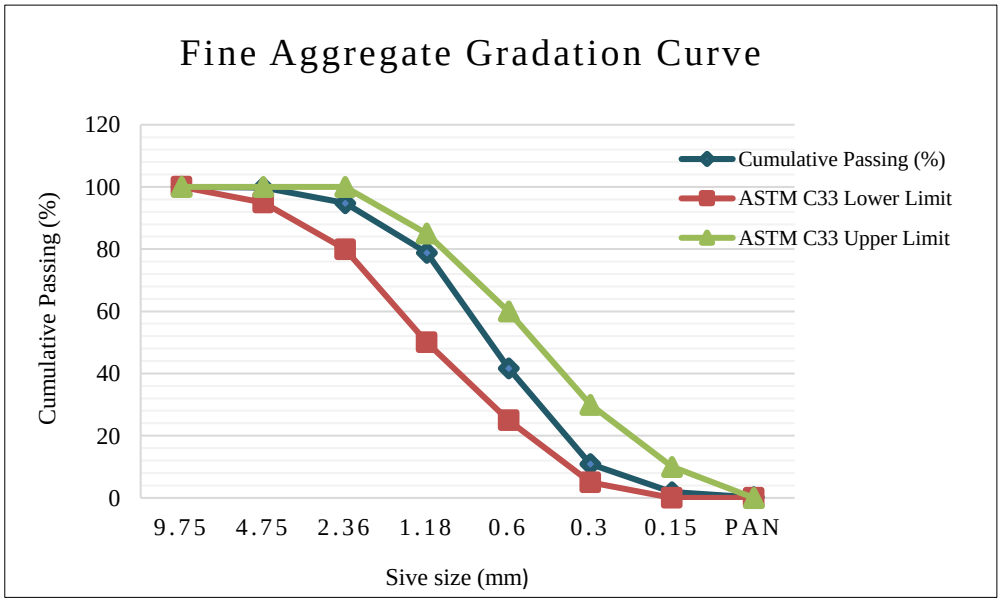

Figure 3.1 Particle Size distribution Curve of Fine Aggregate

To minimize silt and other impurities, the fine aggregate was washed using tab water at the Addis Ababa Institute of Technology (AAiT) construction material testing laboratory, as shown in Appendix H. Then the silt content was examined in laboratory as shown in Figure 3.2, and it was 1.69%.

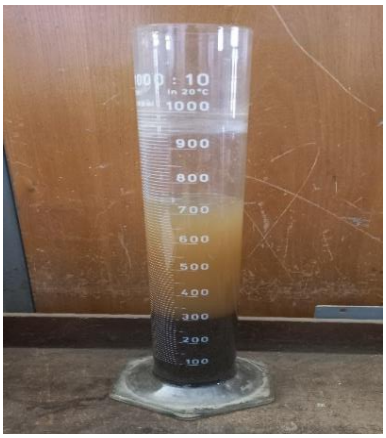

Figure 3.2 Silt Content of Fine Aggregate

3.2.2.2 Coarse Aggregate

Coarse Aggregate is a granular material that is predominantly retained on the 4.75-mm (No. 4) sieve [61]. Basaltic crushed hard rock coarse aggregate purchased from Dereje Belete Shabera hard rock crushing site located at Goro, Addis Ababa, was used. The aggregate was sieved with a nominal 25-mm sieve, as shown in Appendix H, and packed in a plastic bag. The aggregate physical properties were examined at the Addis Ababa Institute of Technology material testing laboratory, and results are summarized in Table 3.2. Particle Size distribution was done as per ASTM C33 [62] standard and the gradation was within the range shown in Figure 3.3. A detail physical tests of basaltic natural coarse aggregate were included in Appendix A-2.

Table 3.2 Physical Property Test Result of Natural Coarse Aggregate

No	Laboratory Physical Tests	Results
1	Unit Weight	1649.49 kg/m^3
2	Bulk Specific Gravity	2.72
3	Water Absorption	0.522 %
4	Moisture Content	0.376 %
5	Aggregate Impact Value	5.21 %
6	Fineness Modulus	7.22

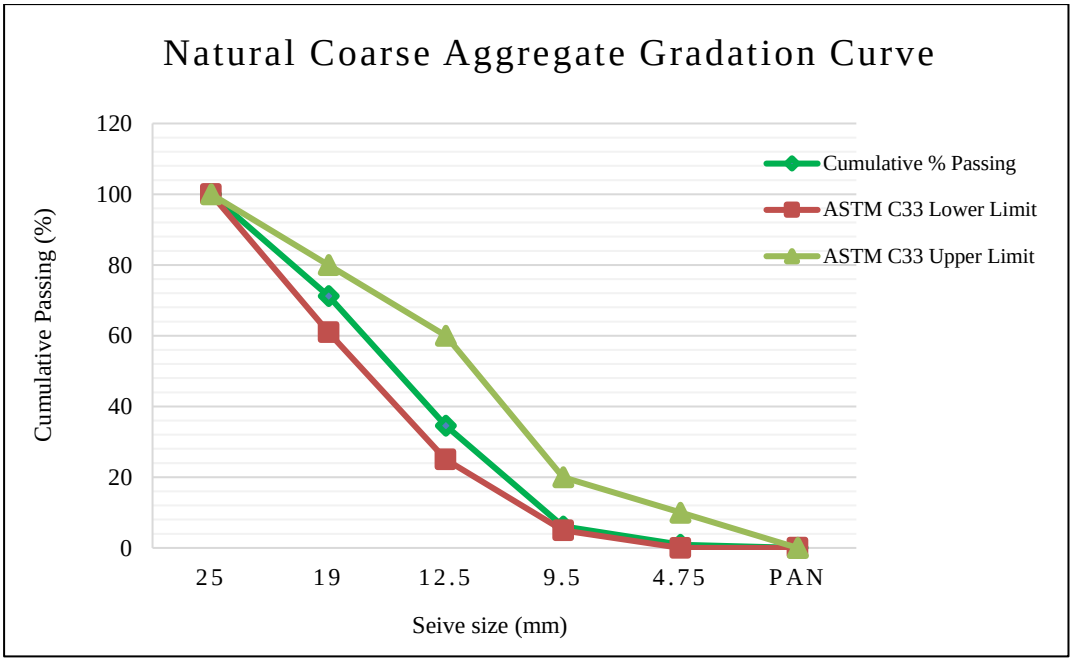

Figure 3.3 Particle Size distribution Curve of Coarse Aggregate

3.2.2.3 Marble Aggregate

Marble is a metamorphic rock consisting of carbonate minerals mainly calcite ($CaCO_3$) or dolomite ($CaMg(CO_3)_2$) that recrystallize under the influence of high temperatures and pressures. Waste Marble aggregate used for this study was collected from Rehobot marble and terrazzo processing industry located at Burayu in chips form as shown in Figure 3.4 (a). The chips were then screened, manually crushed, sieved and blended in the laboratory and finally prepared for laboratory physical examination as shown in Figure 3.4 (b). Crushed marble aggregate has a nominal aggregate size of 4.75 mm to 25 mm with an overall particle size distribution conforming to ASTM C33 [62] standards. The result of grain size distribution of crushed waste marble aggregate was graphically presented shown in Figure 3.5. The physical properties of marble aggregate were examined in Addis Ababa Institute of Technology (AAiT) construction material testing laboratory while the chemical composition test was done at the Geological Institute of Ethiopia and a summary of test results are provided in Tables 3.3 and 3.4 respectively. A complete physical property and chemical composition test results of marble aggregate was attached in Appendices A-3 and G respectively.

Figure 3.4 Marble Aggregate (a) chips at the source (b) after crushed

Table 3.3 Physical Property Test Result of Marble Aggregate

No	Laboratory Physical Tests	Results
1	Unit Weight	1562.54 kg/m^3
2	Bulk Specific Gravity	2.57
3	Water Absorption	0.42 %
4	Moisture Content	0.05 %
5	Aggregate Impact Value	27.9 %
6	Fineness Modulus	7.06

Table 3.4 Chemical Composition of Marble Aggregate

Oxides	Percentage (%)
Silica (SiO_2)	4.86
Alumina (Al_2O_3)	<0.01
Ferric oxide (Fe_2O_3)	0.12
Lime (CaO)	51.22
Magnesium oxide (MgO)	0.80
Sodium oxide (Na_2O)	0.24
Potassium oxide(K_2O)	<0.01
Manganese oxide (MnO)	<0.01
Phosphorus pentoxide (P_2O_5)	0.15
Titanium dioxide (TiO_2)	<0.01
Water (H_2O)	0.24
Loss on ignition (LOI)	41.35

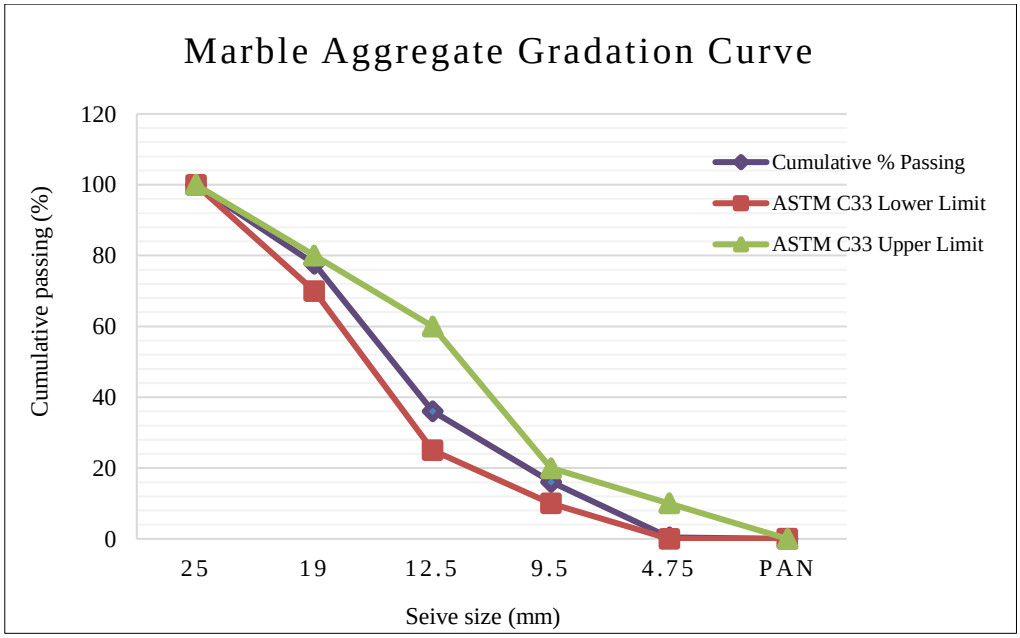

Figure 3.5 Particle size distribution of Marble Aggregate

3.2.3 Water

Water is strongly required in the production of concrete to precipitate the chemical reaction with cement. Furthermore, it is also used to lubricate concrete mixtures, wash aggregates, and cure test specimens. Hence, the water that plays key roles in the concrete production should be free from harmful ingredients such as chemicals, silt, oil, clay, and suspended solids, as they adversely affect quality. So, the water used in this study was tap water from the Addis Ababa Institute of Technology material testing laboratory supply line.

Figure 3.6 Tab water at AAiT material testing laboratory

3.2.4 Reinforcement

Turkiye imported normal strength deformed reinforcement bars purchased from the local market were used in this study. Three different bars with a nominal diameter of 12 mm, 14 mm, and 16mm were used in all test specimen preparation. In order to characterize the mechanical behavior of the reinforcement bar, a tensile strength test was done in the Addis Ababa Institute of Technology material testing laboratory, as shown in Figure 3.7 and the results are summarized in Table 3.5. A complete tensile strength test result is presented in Appendix B.

Figure 3.7 Tensile Strength test of reinforcement bars

Table 3.5 Laboratory Mechanical Property Test Results of Reinforcement Bars

Diameter of Bars	Average Diameter (mm)	Average Yield Load (kN)	Average Failure Load (kN)	Average Yield Strength (MPa)	Average Ultimate Strength (MPa)	Average Elongation (%)
Φ12	12.10	63.10	73.93	549.20	643.49	7.83
Φ14	14.14	90.20	108.73	574.67	692.73	8.70
Φ16	16.13	115.80	133.90	567.28	655.95	9.80

Methods

The techniques employed to accomplish the research's goals are described in this section.

3.3 Mix Design

The mix proportioning is carried out in accordance with ACI 211.1–91 [63] standard procedures. The desired concrete grade was C-30, in which the natural coarse aggregate was replaced by crushed waste marble in a ratio of 25% by weight. A detail description of

all mix notations was presented in Table 3.6 and the quantities of ingredients used in each concrete mix were summarized Table 3.7. The complete mix design calculation is presented in Appendix C.

Table 3.6 Detail description of the concrete mix notations

No	Mix notation	Detail Description
1	MA 0	Concrete mix with 0% marble coarse aggregate
2	MA 25	Concrete mix in which 25% of basaltic coarse aggregate was replaced by marble aggregate
3	MA 50	Concrete mix in which 50% of basaltic coarse aggregate was replaced by marble aggregate
4	MA 75	Concrete mix in which 75% of basaltic coarse aggregate was replaced by marble aggregate
5	MA 100	Concrete mix in which 100% of basaltic coarse aggregate was replaced by marble aggregate

MA-Marble Aggregate

Table 3.7 Quantity of ingredients per unit volume of concrete

Concrete mix	Quantity of ingredients (kg/m^3)				
	Water	Cement	Fine Aggregate	Coarse Aggregate	Marble Aggregate
MA 0	184.83	406.82	675.83	1118.35	0
MA 25	184.83	406.82	675.83	838.76	279.59
MA 50	184.83	406.82	675.83	559.17	559.17
MA 75	184.83	406.82	675.83	279.59	838.76
MA 100	184.83	406.82	675.83	0	1118.35

MA-Marble Aggregate

3.4 Specimen

In this study, the bond behavior of reinforcement bars embedded in marble coarse aggregate concrete was investigated using a pullout test. Five different concrete mixes (MA 0, MA 25, MA 50, MA 75, and MA 100), including control concrete, were prepared along with three different reinforcement bar diameters (12, 14, and 16 mm). The pullout test specimens were cast with a cylindrical specimen of 150mm diameter by 300mm height, placing rebar at the center. For each concrete mix, three cubical specimens of dimension 150 mm and three cylindrical specimens of dimension 150 x 300 mm were fabricated and cast for compressive strength and splitting tensile strength tests,

respectively. Hence, a total of 45 (forty-five) cylindrical pullout specimens, 30 (thirty) cubical compressive strength specimens, and 15 (fifteen) cylindrical splitting tensile strength specimens were prepared and cast. The details of the specimens, along with their respective test type and test age, are summarized in Table 3.8.

Table 3.8 Overall number of specimens fabricated in this study

Concrete mix	Bond parameters				Pullout specimen (Cylinder 150x300mm)	Compressive strength specimen (cube 150x150x150mm)		Splitting tensile strength (cylinder 150x300mm)
	Dia. of rebar (mm)	Cover (mm)	Embedment length 300 mm		28 days	7 days	28 days	28 days
			Bonded L_e=5d (mm)	Unbonded L_u=300-L_e (mm)				
MA 0	12	69	60	240	3	3	3	3
	14	68	70	230	3			
	16	67	80	220	3			
MA 25	12	69	60	240	3	3	3	3
	14	68	70	230	3			
	16	67	80	220	3			
MA 50	12	69	60	240	3	3	3	3
	14	68	70	230	3			
	16	67	80	220	3			
MA 75	12	69	60	240	3	3	3	3
	14	68	70	230	3			
	16	67	80	220	3			
MA 100	12	69	60	240	3	3	3	3
	14	68	70	230	3			
	16	67	80	220	3			
Total					45	30		15

Le-Bonded length *L_u-Unbonded length*

3.4.1 Pull-out Test Specimen Fabrication

All reinforcement bars are from the same origin; hence, they have identical rib arrangements. The bars were first cut into equal lengths, then plastic conduit was inserted, and finally they were cleaned. For all pullout specimens, the bond length was five times the bar diameter (5*d), as recommended by RILEM [49]. By using this short embedment length, a consistent bond stress distribution at the steel-concrete interface was expected to be attained. The other remaining portion of the bars in the cylindrical mold was debonded from the concrete by plastic conduits. The ends of the PVC conduits were covered with Vini plastic tape to avert any entrance of cement grout in the conduit while casting as shown in Figure 3.8 a. The bars prepared in this way were manually placed in the middle of the cylindrical mold, as shown in Figure 3.8 b, and were ready for concrete casting.

Figure 3.8 Specimen preparation a) diameter 12,14 and 16mm reinforcement bars with plastic conduit [right to left] b) cylindrical pullout mold with rebar at the center

In all pullout specimen fabrications, 1000-mm-long deformed rebars of nominal diameters 12 mm, 14 mm, and 16mm were centrally fixed. The loaded end of the bar, which is gripped out by the pullout machine, extends 630 mm, while the free end length extended through the centre hole steel plate at the bottom of the cylindrical mould for slip measurement is 70mm. A detail dimension of pull-out specimen was shown in Figure 3.9.

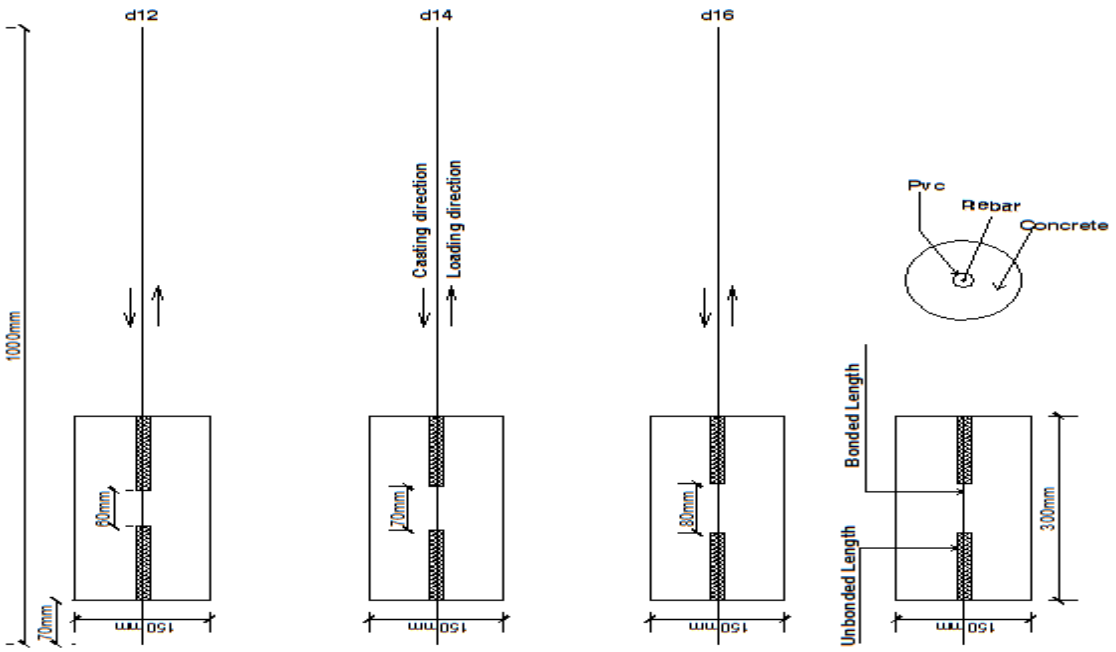

Figure 3.9 Pull out test specimen dimension

3.5 Laboratory Mix

All concrete mix was done in the Addis Ababa Institute of Technology construction material testing laboratory using Zyklos electrically rotating drum mixer with a capacity of 0.05 m^3. The concrete test specimens were made and properly cured as per ASTM C192 [64] concrete making and curing standards. During mixing, initially coarse aggregate was added, then cement, and finally fine aggregate, as shown in Figure 3.10. It was then dry blended for about half a minute with no addition of water. About two-thirds of the measured water was added, and mixing proceeded. Then the other remaining water was added to the ingredients in the mixer and mixed until a uniform consistency of concrete was attained.

Figure 3.10 Drum mixer along with materials ready for mix

Immediately after mixing was finished, a slump test was performed to examine the workability of the concrete. In this study, the slump test of every batch of fresh concrete was performed in accordance with the ASTM C-143 [65] standard test method for slump of concrete. To conduct a slump test, first equipments used for slump test such as tamping rod, cone and steel plates are washed and prepared for test. Then fresh concrete was added and compacted for each of the three consecutive layers, and finally the top surface was leveled, then the cone was lifted off, inverted and placed near the molded fresh concrete mix. Finally, the slump was measured using measuring tape as shown in Figure 3.11 and the results were recorded.

Figure 3.11 Measurement of slump for fresh concrete mix

Before casting fresh concrete into the cubical and cylindrical molds, they were properly smeared with machine oil, as shown in Figure 3.12. After oiling pullout cylindrical molds, the rebar was manually placed in the mold extending 70 mm below the bottom centre hole steel plate, and firmly held in position at the top by a mechanically prepared steel bar. The freshly mixed concrete was then filled into the molds and vibrated using an internal vibrator for pullout test specimens and a table vibrator for compressive and splitting tensile test specimens, as shown in Figure 3.13. Pouring of concrete into molds and vibrating to remove trapped air were done in layers. The concrete samples were then removed from their molds after 24 hours of setting as shown in Figure 3.14 and placed in a water tank to cure at room temperature until their respective test dates, as shown in Figure 3.15.

Figure 3.12 Oil coated molds ready for concrete casting

Figure 3.13 Casting and vibrating of concrete specimens

Figure 3.14 Removing concrete specimens from their mold

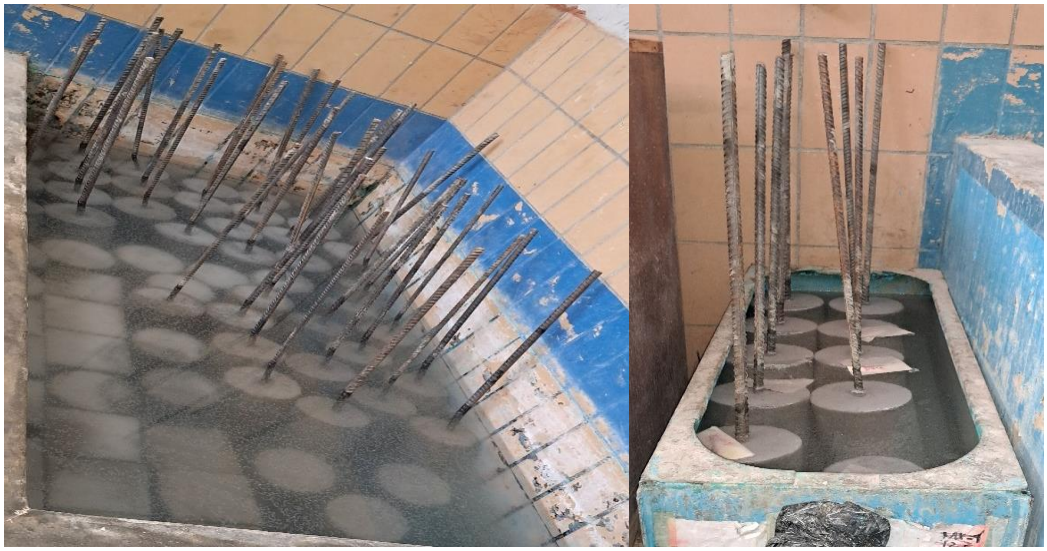

Figure 3.15 Curing of concrete specimens

3.6 Specimen Test setup and Instrumentation

3.6.1 Test specimens

After properly curing concrete specimens in a water tank under continuous inspection, they were taken out at their test dates and prepared for testing, as shown in Figure 3.16.

Figure 3.16 Concrete specimens ready for test

3.6.2 Compressive Strength Test

In this study, cubical specimens of a dimension 150mm were prepared and tested as per BS EN 12390-3 [66] guidelines for testing hardened concrete compressive strength. The specimens taken out of the tank were surface dried and prepared for testing. The marked specimens of each mix were first weighed and properly positioned under the universal testing machine shown in Figure 3.17 and assigned to start loading. The machine with a capacity of 3000 kN started to apply loads at a uniform loading rate of 0.28 MPa/s until failure. Just at failure, the machine stops loading, and it shows the results of ultimate load and compressive stress immediately on the display screen, which are to be recorded. In this way, three cube samples of each mix were tested for the compressive strength of the concrete at seven and twenty-eight days of age.

Figure 3.17 Compressive strength test specimen setup

3.6.3 Splitting Tensile Strength Test

Concrete tensile strength could be determined both directly by uniaxial testing and indirectly by techniques such as flexural and splitting strength tests. In conducting this test, a diametric compressive force along the length of the cylindrical specimen with plywood strips at loading tips, as shown in Figure 3.18, was applied at a rate of 689 to 1380 KPa/min until failure of the specimen occurred as per ASTM C-496-96 [67]. A total of fifteen cylindrical splitting tensile specimens of diameter 150mm by height 300mm from five mixes, with three samples representing each mix, were tested for twenty-eight days of curing.

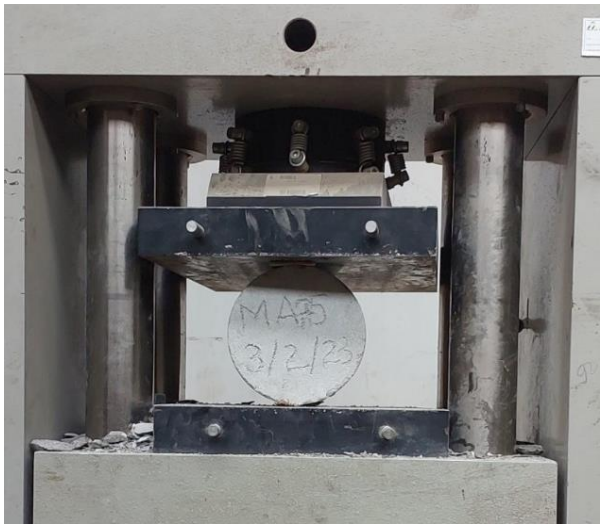

Figure 3.18 Splitting tensile strength test specimen setup

Equation 3.1 determines the tensile strength of concrete

$$f_{ct} = \frac{2P}{\pi d_b l_b} \quad (3.1)$$

where;

f_{ct} is the tensile strength of concrete (MPa)

P is failure load (N)

d_b is the diameter of the cylinder (mm)

l_b is the length of the cylinder (mm)

3.6.4 Pull-out Bond Test

The pull-out test is one of the methods of investigating bond stress between embedded bars and concrete by measuring the force needed to pull them out of the concrete. The test setup in this test was primarily to record the specimen's bond stress slip. In this test, the reinforcement at the loading end passes through the centre hole jack, which grips and pulls out, while the upward movement of the bar was measured by linear variable displacement transducers (LVDT) mounted at the free end of the specimens. A center-hole load cell was used to record the load imposed by a hydraulic center-hole jack with a capacity of 130 kN. The jack with bolts at its upper end was connected to a hydraulic pressing machine, while the load cell and transducers were connected to a high-performance TDS-630 data logger shown in Figure 3.19 (f). A load was manually applied using a hydraulic pressing machine at a uniform rate. A video was recorded while conducting the test, and the whole experimental result from the data logger was collected via USB drive. All pullout specimens were set up as shown in Figure 3.20 and tested at the age of twenty-eight days.

Figure 3.19 Test equipment a) Bolts b) Center-hole jack c) Center-hole load cell d) hydraulic pressing machine e) displacement transducer f) Data logger

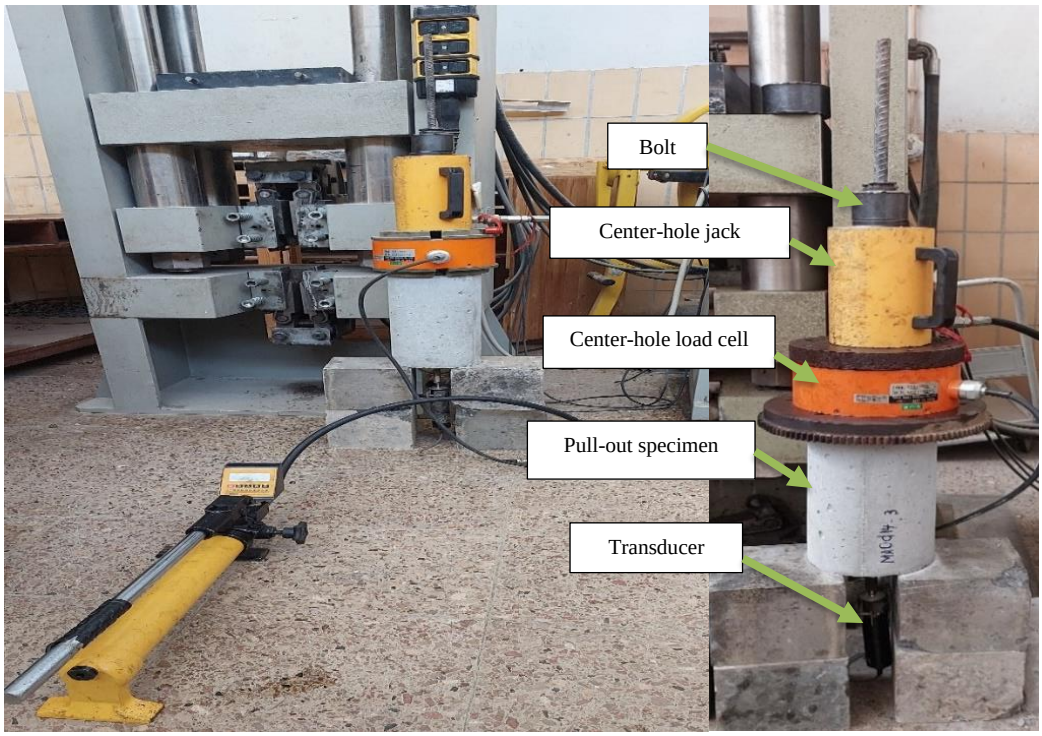

Figure 3.20 Pull-out test specimen setup

4. RESULTS AND DISCUSSION

4.1 Introduction

This section discusses the findings of experimental tests conducted in a laboratory to examine the fresh and hardened characteristics of the concrete. Slump test results have been discussed under fresh concrete properties, while compressive strength, splitting tensile strength, and pull-out bond strength test results were investigated under hardened concrete properties. The results were summarized in a table and shown graphically, followed by a detailed discussion in relation to prior studies and standards.

4.2 Fresh Concrete Properties

4.2.1 Slump

Slump test is the simplest and most widely used test conducted on fresh concrete to determine its workability. In this study a total of five concrete mixes varying percentage replacement of waste marble were prepared. A slump test was performed and measured for each mix and average results were summarized as shown in Figure 4.1.

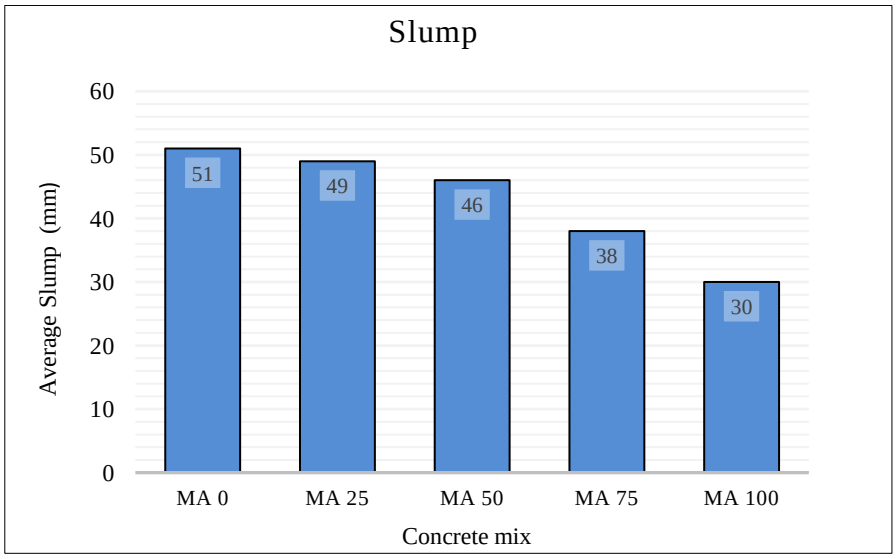

Figure 4.1 Average Slump values for all concrete mixes

As shown in Figure 4.1, the slump value decreases as the quantity of marble replacing coarse aggregate in a ratio of 25% increases with a constant water-cement ratio throughout the mix. This shows that the workability of the concrete decreases as the quantity of marble in the concrete increases. Aggregate size, gradation, shape, and surface texture are some

factors that will affect the workability of fresh concrete mix. The crushed waste marble used in this study has an irregular and angular shape, a rough surface texture, and free lime dust on it, which demands more water and hence lowers workability. It was stated in [63] that as the aggregate became more angular and harsher in texture, more water was needed. The decrease in workability of concrete as a result of the increase in percentage replacement of coarse aggregate by marble aggregate was however contradicted by [11] and [12] as they used a flat and smooth surface of marble aggregate.

4.3 Hardened Concrete Properties

In this study, compressive strength, splitting tensile strength, and bond strength tests were conducted for five different mixes varying in waste marble as coarse aggregate replacement in normal-strength concrete of grade C30.

4.3.1 Compressive Strength

A compressive strength of normal-strength concrete with waste marble as a natural coarse aggregate replacement was prepared, tested, and discussed. For each mix, three specimens were tested at seven and twenty-eight days of curing, and the average results are graphically presented as shown in Figure 4.2. Appendix D contains the full findings of the compressive strength test result.

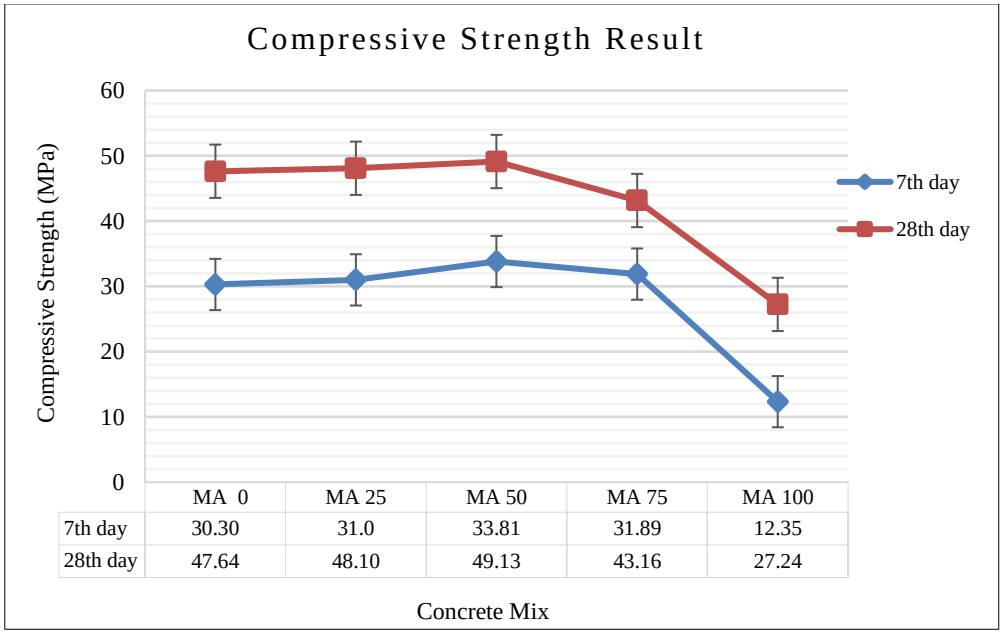

	MA 0	MA 25	MA 50	MA 75	MA 100
7th day	30.30	31.0	33.81	31.89	12.35
28th day	47.64	48.10	49.13	43.16	27.24

Figure 4.2 Average compressive strength result of the concrete mix

As shown in Figure 4.2, the compressive strength result of the concrete examined for both the 7th and 28th days was plotted graphically. The result shows that as the quantity of

marble aggregate increases up to 50% (MA 50), the compressive strength of the concrete slightly increases for both ages. However, as the percentage level of marble in concrete continues to increase, compressive strength starts to decrease, and a significant strength loss was observed at 100 marble coarse aggregate concrete (MA 100). When compared to the control specimen (MA 0), the compressive strength of MA 50 concrete increased by 3.13% at the age of 28 days, but MA 100 concrete is decreased by 42.82%. Further, the 7th-day compressive strength of the concrete incorporating 50% marble (MA 50) was increased by 11.58%, while a 59.24% decrease in strength was observed for a MA 100 concrete compared to the control specimen.

A significant decrease in compressive strength of concrete incorporating 100% marble aggregate was likely due to lack of fine fraction in the grain size distribution of marble aggregate and low strength of marble compared to basaltic coarse aggregate. In the other way the improvement in compressive strength of marble aggregate concrete was due to angular shape and rough surface texture of marble aggregate which enhances the aggregate cement paste bond of the mix. The increase in compressive strength of concrete incorporating marble up to 50% by weight of natural coarse aggregate was also supported by the findings of Sunil et al [10] and Adham et al [12].

4.3.2 Splitting Tensile Strength

The splitting tensile strength test examines the tensile strength property of the concrete. The test is performed by imposing a uniform compressive line load through the horizontal axis of the cylindrical specimen and splitting along its length, as shown in Figure 4.3. For each replacement level of waste marble, the average of three cylindrical specimens was tested at the age of twenty-eight days, and the results are plotted in Figure 4.4. A complete splitting tensile strength test result for all concrete specimens is provided in Appendix E.

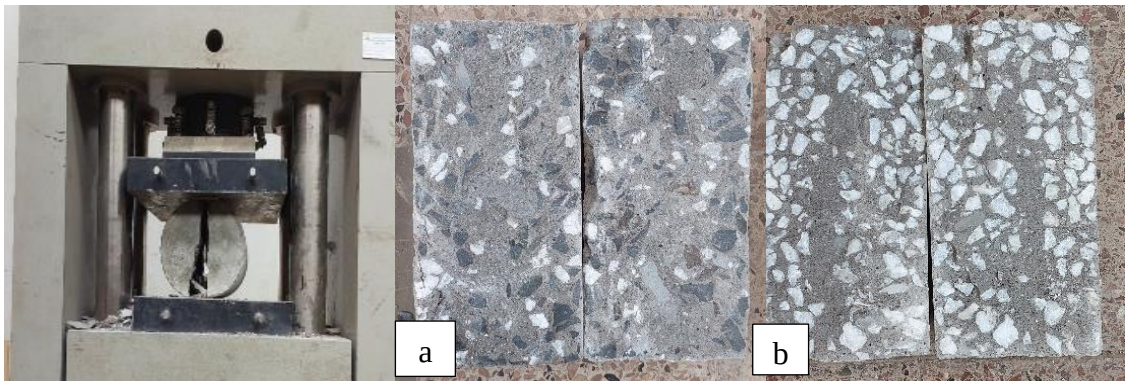

Figure 4.3 Splitting of tensile strength test specimens (a)MA 25 (b)MA 100

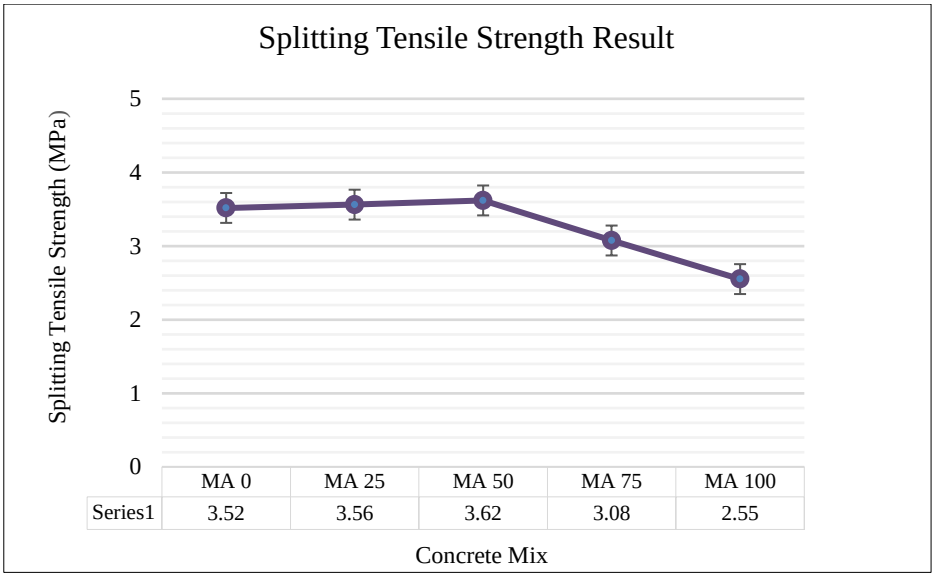

Figure 4.4 Average splitting tensile strength result of the concrete mix

From Figure 4.4, it can be observed that the 28th day splitting tensile strength of the concrete slightly increases up to MA 50 mix and decreases beyond as the quantity of marble aggregate in the concrete increases. When compared to control concrete specimens (MA 0), the concrete with 50% marble coarse aggregate (MA 50) showed a 2.84% increase in tensile strength. A concrete with full marble coarse aggregate is about 27.56% lower in tensile strength than control concrete (MA 0). According to experimental findings made by Hebhoub et al. [3], the use of marble as coarse aggregate up to 75% by weight improves the tensile strength of the concrete.

4.3.3 Pull out Bond Strength

Bond strength is a shear stress developed at the interface of embedded reinforcement bars and concrete. It is obtained by dividing the Pull-out tensile load by the reinforcement bars' effectively bonded area. For short embedment length bond stress (τ) is assumed to be uniform and calculated using equation 4.1.

$$\tau = \frac{P}{\pi d_b l_e} \tag{4.1}$$

where;

P is the maximum pull-out load (N)

d_b is the diameter of the reinforcement bar (mm)

l_e is the effectively embedded length (mm)

The idea of normalized bond strength was used to compare the bond strengths obtained by specimens having varying compressive strengths so that the impact of compressive strength differences was eliminated. It is determined by dividing the computed bond strength to the square root of cylindrical compressive strength as shown in equation 4.2.

$$\tau_n = \frac{\tau}{\sqrt{f_c'}} \tag{4.2}$$

where;

τ_n is the normalized bond stress

τ is the ultimate bond stress computed in equation 4.1

f_c' is the mean cylindrical compressive strength (MPa)

Table 4.1 Provides a quantitative summary of the outcomes of all pull-out test specimens using three different bar diameters embedded in all concrete mixes. Detail pull-out test results are presented in Appendix F.

Table 4.1 Summary of Pull-out Test Result

Mix Id	Nominal diameter of rebars (mm)	Embedment Length (mm)	Average Failure Load (kN)	Average Bond Strength (MPa)	Norm. Bond Strength	Average Slip (mm)	Mode of Failure
MA 0	12	60	48.28	21.34	3.46	0.97	Pull-out
	14	70	66.03	21.45	3.47	0.91	Pull-out
	16	80	81.11	20.17	3.27	0.69	Pull-out
MA 25	12	60	48.32	21.36	3.44	0.73	Pull-out
	14	70	64.38	20.91	3.37	0.63	Pull-out
	16	80	83.46	20.75	3.35	0.73	Splitting
MA 50	12	60	50.03	22.12	3.53	1.02	Pull-out
	14	70	65.69	21.34	3.40	0.78	Pull-out
	16	80	81.41	20.25	3.23	0.59	Splitting
MA 75	12	60	48.79	21.57	3.67	0.98	Splitting
	14	70	66.39	21.56	3.67	1.31	Pull-out
	16	80	81.75	20.33	3.46	0.43	Splitting
MA 100	12	60	34.74	15.36	3.29	0.67	Pull-out
	14	70	47.81	15.53	3.33	0.74	Pull-out
	16	80	58.82	14.63	3.13	1.18	Pull-out

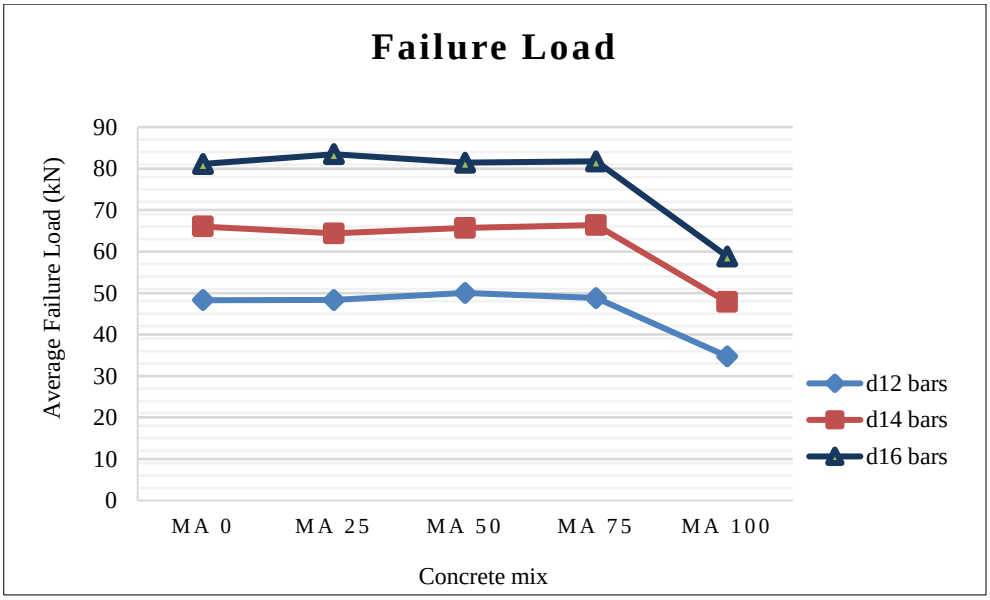

Figure 4.5 Average failure load for diameter 12,14 and 16mm reinforcement bars

Failure load is the maximum tensile force that is imposed on the specimen that, when it exceeds the material strength, causes failure. As it can be seen from Figure 4.5, the average failure load shows a slight increasing trend in the concrete incorporating marble as partial natural coarse aggregate. For diameter 12 mm reinforcement bars, it is observed from Table 4.4 that the maximum average failure load was 50.03 kN in MA 50 concrete, and it was 3.63% higher than that of control concrete (MA 0), and similarly, a maximum failure load of 66.39 kN and 83.46 kN was recorded in MA 75 and MA 25 concrete, indicating an increase of 0.55% and 2.89% over the control concrete for diameter 14mm and 16mm reinforcement bars respectively. For diameter 12, 14, and 16mm reinforcement bars embedded in concrete made of fully marble coarse aggregate (MA 100), the failure load significantly decreased by 28.04%, 27.59%, and 27.48%, respectively, when compared to control concrete (MA 0).

The failure load was also influenced by the diameter of reinforcement bars embedded in the concrete. Small-diameter bars have a small interface bond length, thus requiring less load to debond, which results in either splitting of concrete or the pull-out of bars. From Figure 4.5, it is clearly seen that the failure load of diameter 12mm bars is smaller than that of diameter 14mm and 16mm reinforcement bars in all concrete mixes.

4.3.3.1 Bond Stress

All pull-out tests were conducted at the age of 28 days on forty-five specimens using reinforcement bars of nominal diameters of 12 mm, 14 mm, and 16mm embedded in all concrete mixes (MA 0, MA 25, MA 50, MA 75, and MA 100). From the test results, three maximum tensile loads for each diameter bar embedded in concrete was recorded and averaged. Then the average bond stress is determined using equation 4.1, which assumes a uniform bond stress for short embedment lengths of bars. Based on the pull-out tests conducted in this study, the effect of marble aggregate (MA) on the overall bonding strength, the effect of the diameter size of rebar, failure mode, bond stress-slip curve of specimens and comparison of experimental result with code and predicted equations were discussed next section.

Effect of Marble Aggregate on the Bond Behavior of the Concrete

In this study, five different mixes (MA 0, MA 25, MA 50, MA 75, and MA 100) with varying percentages of marble as a natural coarse aggregate were prepared and tested. The average ultimate bond strength of 12-, 14-, and 16-mm steel bars embedded in all concrete mixes was examined and plotted.

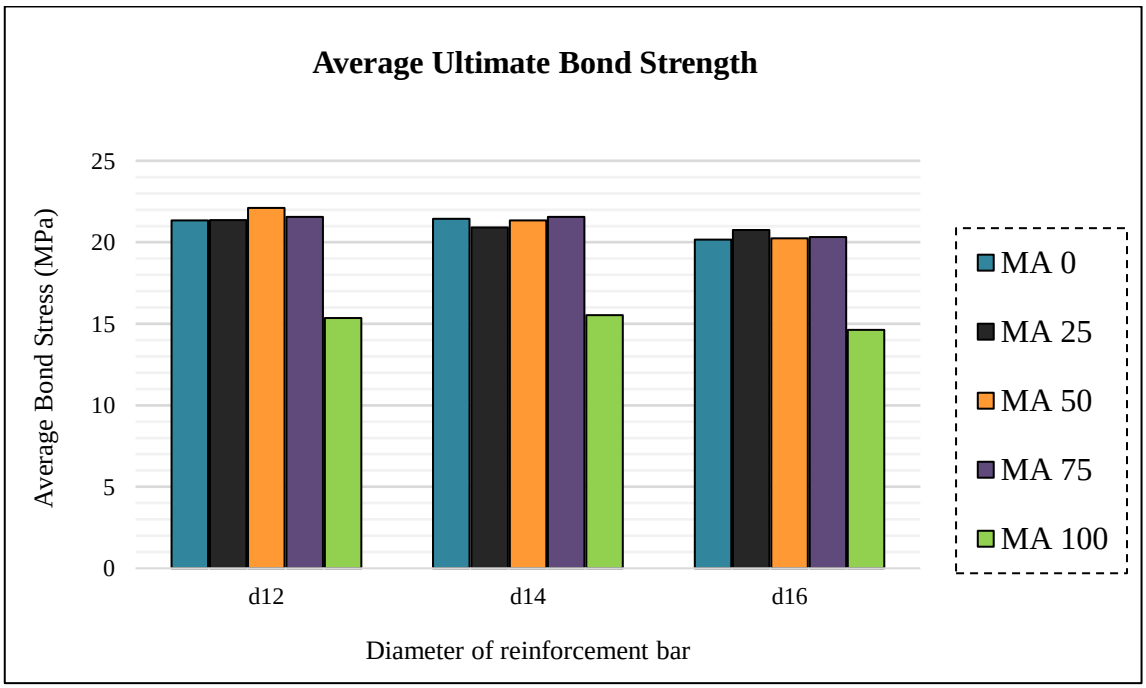

Figure 4.6 Average bond strength values for all bars embedded in all concrete mixes

From the test result shown in Figure 4.6, it is observed that as the quantity of marble replacing natural coarse aggregate increased up to 75%, the average bond strength value was comparable to the control concrete. For a diameter of 12mm bar, the average ultimate bond strength without marble aggregate (MA 0) was 21.34 MPa, and the maximum average bond strength value was 22.12 MPa in the concrete with 50% marble as coarse aggregate, showing a 3.65% increment. Similarly, for diameter 14mm and 16mm bars, the maximum average ultimate bond strength was 21.56 MPa and 20.75 MPa in MA 75 and MA 25 concrete mixes, showing a slight increase of about 0.51% and 2.88%, respectively. But in the case of 100% marble utilization (MA 100), the average bond strength was 15.36 MPa, 15.53 MPa, and 14.63 MPa and decreased by 28.02%, 27.6%, and 27.47%, respectively, for diameter 12, 14, and 16mm reinforcement bars when compared to their respective control concrete (MA 0).

The average ultimate bond strength test result was consistent with the compressive and tensile strength test results of the concrete. This experimental finding was supported by Tang et al. [27] and Wang et al. [68] that incorporation of limestone aggregate in concrete improves the cement matrix, which in turn improves compressive and splitting tensile strength, resulting in higher bond between rebar and concrete before the occurrence of failure. Based on the compressive and splitting tensile strength result, the use of marble as a natural coarse aggregate replacement by weight up to 50% is recommended as it gives a comparable value of bond strength, compressive strength, and splitting tensile strength with respect to the control concrete (MA 0).

Effect of Reinforcement Bar Diameter on Bond Strength

Deformed reinforcement bars of a nominal diameter of 12 mm, 14 mm, and 16mm with identical rib arrangements were embedded in all concrete mixes. The bonded length of the bars were five times the diameter (5d), i.e., 60 mm, 70 mm, and 80 mm respectively. The quantitative summary of the pull-out bond strength test findings was provided in Table 4.1. From the pull-out test result plotted in Figure 4.7, it can be observed that in all concrete mixes, 16-mm reinforcement bars have a lower average bond strength than others. It is related to the stress distribution along the embedment length of the bar. The 16mm diameter size bar has higher embedment length (80mm) compared to diameter 14mm and 12mm bars that has an embedment length of 70mm and 60mm respectively. Thus, with a

relatively long embedment length of diameter 16mm bar, the stress distribution along the embedment was nonlinear that leads to low bond strength values than others.

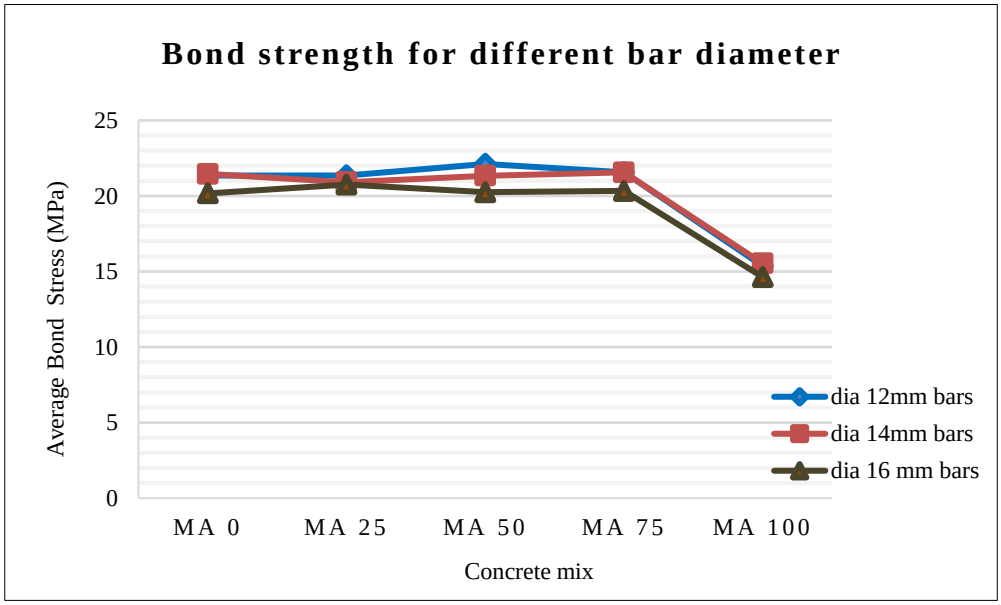

Figure 4.7 Bond strength properties for different bar diameter

In addition, the bond strength is also influenced by concrete cover thickness and rib spacing of the bar diameter. Small-diameter (12 mm) bars have a higher concrete cover when compared to larger-diameter bars, which increases the confinement of the concrete surrounding the bar and thus increases the specimen's resistance to failure by eliminating the stresses created by tensile forces acting on the concrete surface. The bond strengths of a diameter of 12 mm, 14 mm, and 16mm reinforcement bars embedded in MA 0 concrete are 21.34 MPa, 21.45 MPa, and 20.17 MPa, and those embedded in MA 50 concrete are 22.12 MPa, 21.34 MPa, and 20.25 MPa, respectively. It was noted that the bond strength of the diameter 16mm bars was decreased by 5.5% and 8.5%, respectively, in MA 0 and MA 50 concrete when compared to the diameter 12 mm bars embedded in the same mix. This result was supported by Shunmuga et al. [69] that due to the higher surface area for bonding and low spacing among the ribs of small-diameter bars, the bond strength decreases as the size (or diameter) of the bar increases.

4.3.3.2 Mode of Failure

Failure modes of all forty-five specimens were recorded and tabulated in Appendix F during the pullout test. The bond strength was studied on a short concrete-rebar interface of five times the diameter of the bars. At this interface, adhesion, mechanical interlock,

and friction were used to transfer the load among the concrete and rebar. As the load imposed gradually increases, the rib of reinforcement either splits or crushes the concrete locked in it, resulting in either overall crushing of the concrete or the slip of rebar out of the concrete.

There are two common types of bond strength failure modes: splitting and Pull-out failure. In this study, the majority of specimens were failed by pull-out, as shown in Figure 4.8 a. It occurs when the radial force developed by the loaded steel bar is less than the shear force generated by the surrounding concrete, allowing the reinforcement bar to simply pull out of the concrete specimen without any visible breaking of the concrete.

On the other side, it was observed from Table 4.1 that splitting failure occurred on specimens of 16-mm-diameter bars embedded in MA 25, MA 50, and MA 75 concrete mixes. Splitting mode of failure as shown in Figure 4.8 b is because of small concrete cover confining diameter 16mm bar results in minimum circumferential tensile strength resistance of the concrete. In this failure type, as the rebar was loaded, the surrounding concrete was unable to resist the radial pressure exerted by the rebar, and cracks developed at the interface. As these cracks propagated to the surface, it resulted in the failure of the concrete specimen due to the concrete cover splitting. In splitting failure mode, since embedment is too short (5*d), the bond strength is mainly governed by mechanical interlocking action among the ribs and the concrete.

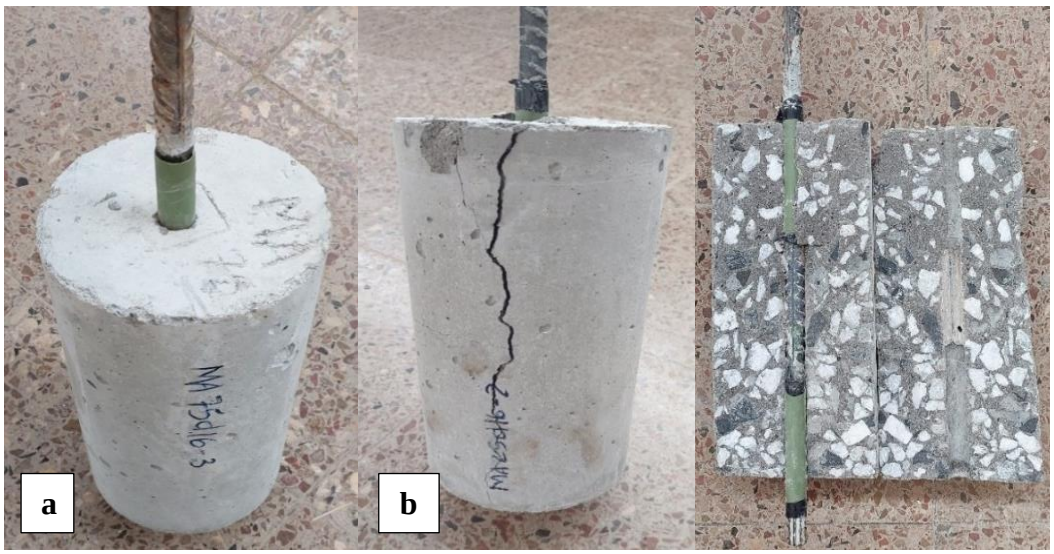

Figure 4.8 Pull-out test failure mode (a) Pull-out failure and (b) Splitting failure

For all specimens that failed in pull-out mode, the concrete under the ribs was crushed, while for those that failed in splitting mode, the mark of the ribs remained on the concrete. Generally, failure mode of Pull-out bond test was affected by several factors, such as casting and loading direction, loading rate, mechanical strength of the concrete and steel bars, concrete cover thickness, type and size of steel bars, surface condition, rib height and geometry of the steel bars.

4.3.3.2 Bond Stress-Slip Relationship

A pullout bond strength test was conducted on all specimens by applying a tensile load to the reinforcement bar at the loaded end and recording slip at the free end. The ultimate bond stress for all concrete mixes was calculated by equation 4.1 using the ultimate tensile load from the experimental results. Then bond stress as a function of the free end slip of the reinforcement bar was drawn to represent the bond strength behavior of all concrete specimens under loading. Figures 4.9, 4.10, and 4.11, respectively, present the bond strength slip curve of diameter 12mm, 14mm, and 16mm reinforcement bars embedded in all concrete mixes.

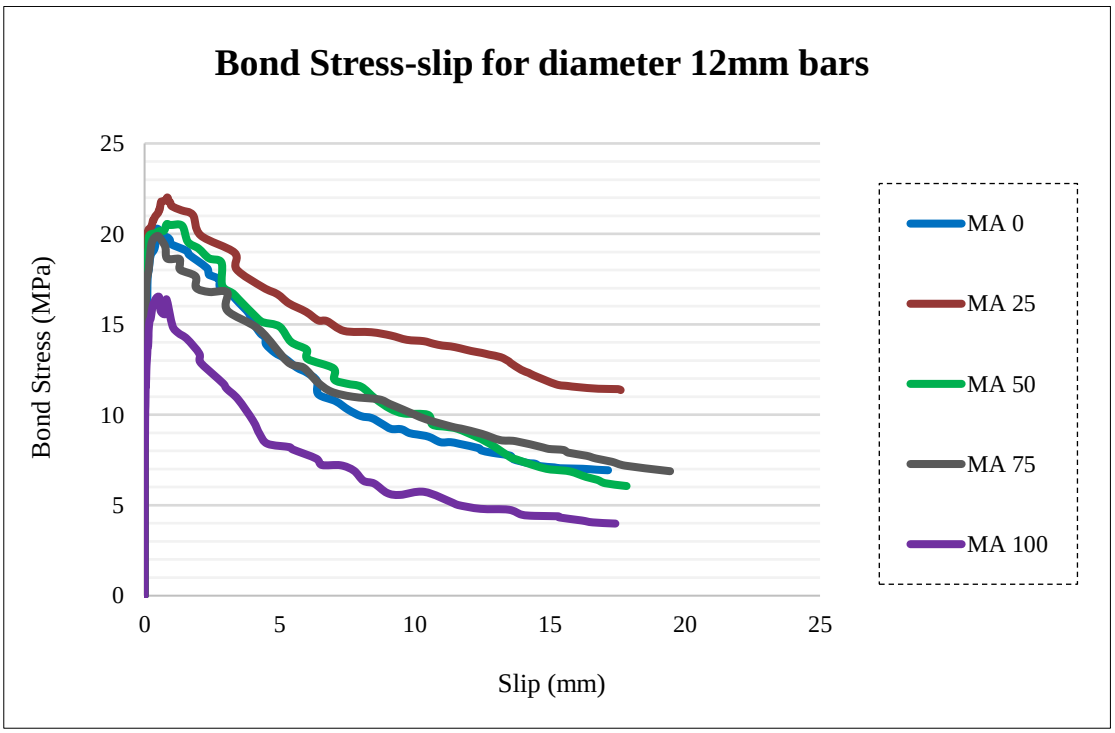

Figure 4.9 Bond Stress-slip curve for diameter 12mm reinforcement bars

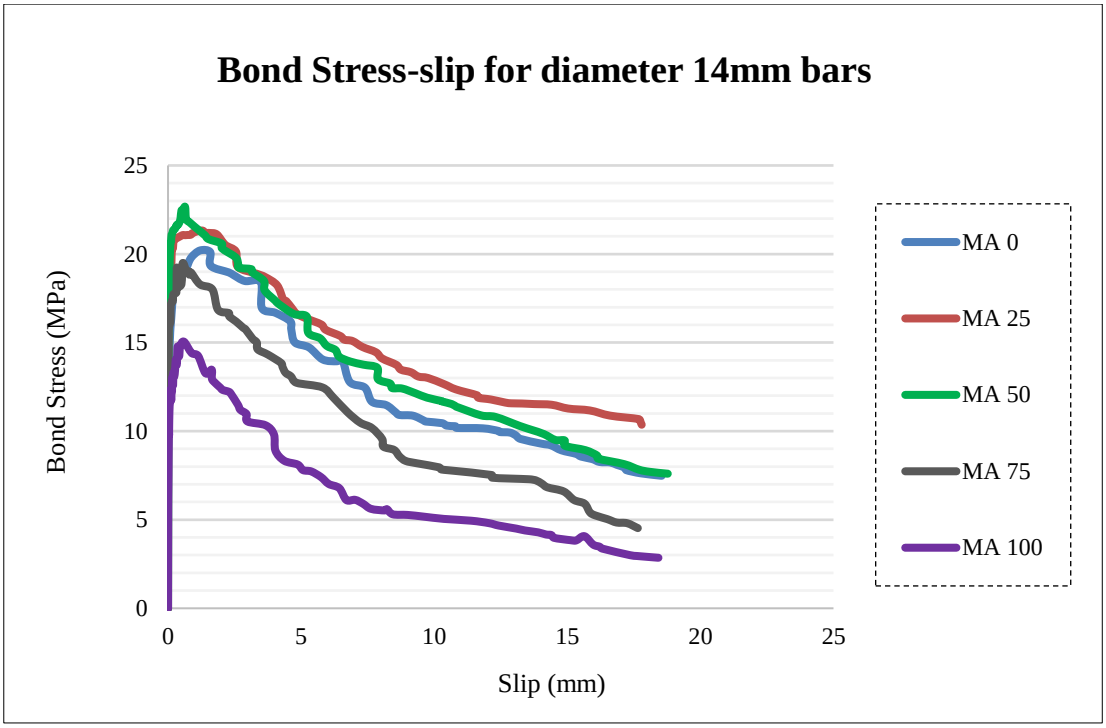

Figure 4.10 Bond Stress-slip curve for diameter 14mm reinforcement bars

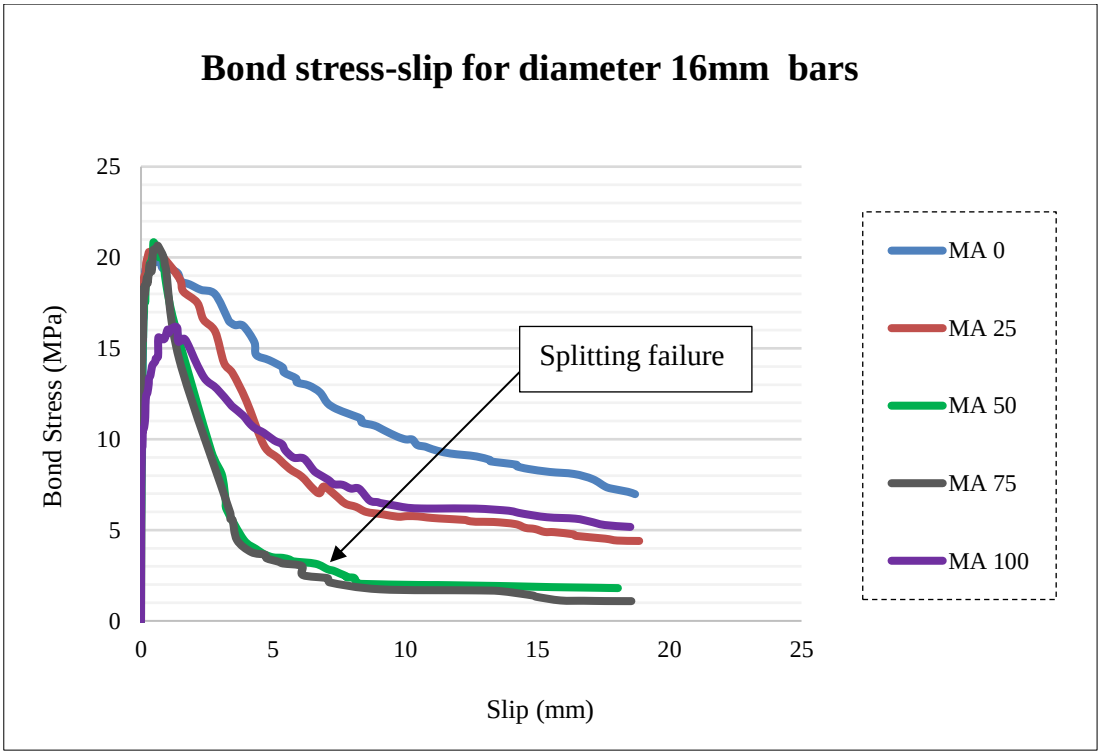

Figure 4.11 Bond Stress-slip curve for diameter 16mm reinforcement bars

The shape of the bond stress-slip curve of the three reinforcement bars (dia. 12 mm, 14 mm, and 16mm) embedded in all concrete mixes (MA 0, MA 25, MA 50, MA 75, and MA 100) was nearly the same. For all specimens, the bond stress reaches its peak at the ultimate failure load and starts to drop gradually as slip increases, though the degree of attainment of peak bond stress varies according to the specimen mode of failure.

Generally, the relationship between bond stress and slip of specimens under loading was controlled by the bond transfer mechanism at the interface. At the initial stage of loading, the bond stress was small, straight line on the curve and no slip measured due to chemical adhesion and friction between the rebar and concrete. As the load gradually increased, the chemical adhesion between the bar and concrete was exceeded, and a small relative slip was recorded. As further loading continued, splitting bond stress was attained as a result of the higher radial pressure exerted by the rebar lugs on the surrounding concrete than the resistance of the concrete (i.e., splitting failure). The bond stress slip curve of specimens failed at this stage was very steep as the maximum strength was attained within a very small slip of the bar.

In the other way, ultimate bond stress at the peak of the curve was reached when peak failure load was imposed on well confined specimens having higher concrete resistance than the radial pressure of the rebar. During this stage, the ultimate load applied to the rebar completely crushes the concrete within the ribs, and the rebar starts to move (i.e., Pull-out failure), resulting in a decrease in bond stress as the slip still increases. Finally, as the load was further imposed, residual bond stress coming from interface friction did not keep the curve decreasing but rather uniform as slip increased.

The bond strength was consistent with the compressive and tensile strengths of the concrete mix. As the percentage of marble in the mix increases until 75% (MA 75), it can be observed from the graph that the average ultimate bond strength was nearly comparable to the control concrete specimen (MA 0) and starts to fall with additional marble in the mix. Similar to compressive and tensile strength test results, a significant decrease in bond strength was also observed at MA 100 concrete. It was observed from Figures 4.9 and 4.10 that the bond stress-slip curve was almost similar for the specimens with rebar of 12 mm and 14 mm diameter that failed in pullout modes. However, for a diameter 16mm bars

embedded in MA 75 and MA 100 concrete mixes, as shown in Figure 4.11, the curve was steep, indicating splitting failure.

4.4 Bond Strength in Various Code Provisions and Empirical Equations

Bond between concrete and rebar is a crucial factor in the design and performance of reinforced concrete structures. It refers to the ability of the concrete to grip and transfer the load to the reinforcement ensuring the structural integrity and load-carrying capacity of the structure. Study on bond strength have been conducted by several researchers and they have proposed bond stress equations considering different parameters. The parameters include strength of concrete, diameter of the bar, embedment length, transverse reinforcement, the thickness of the concrete cover and etc.

In this study the result of bond strength obtained from experimental test were compared with the calculated bond strength based on code provision and predicted equations. Nine different equations proposed by various researchers were considered for comparison and the calculated bond strength results are presented in Table 4.3.

Table 4.2 Parameters used in this study for the comparison of bond strength

Concrete Mix	Parameters				
	Compressive strength f_c' (MPa)	Splitting tensile strength f_{ct} (MPa)	Diameter of bars d_b (mm)	Embedment length l_e (mm)	Concrete cover c (mm)
MA 0	38.11	3.52	12	60	69
			14	70	68
			16	80	67
MA 25	38.48	3.56	12	60	69
			14	70	68
			16	80	67
MA 50	39.30	3.62	12	60	69
			14	70	68
			16	80	67
MA 75	34.53	3.08	12	60	69
			14	70	68
			16	80	67
MA 100	21.79	2.55	12	60	69
			14	70	68
			16	80	67

Table 4.3 Average Bond strength values calculated using codes and proposed equations

Concrete Mix	dia. (mm)	Bond Strength (MPa)												
		Exper. Result	ES EN 1992	ACI 318	CEB-FIB	Orangun et al.	Darwin et al.	Chapman et al	Aslani et al	Esfahani et al	Shima et al	Huang et al	Melkam G.	Hadi
MA 0	12	21.34	4.49	5.31	15.43	14.59	14.48	17.66	21.32	16.82	10.20	17.15	19.21	6.95
	14	21.45	4.49	5.31	15.43	13.21	13.51	16.10	19.96	15.66	10.19	17.15	18.36	7.07
	16	20.17	4.49	5.31	15.43	12.18	12.78	14.94	18.86	14.65	10.18	17.15	17.72	7.17
MA 25	12	21.36	4.54	5.33	15.51	14.66	14.55	17.74	21.44	17.01	10.26	17.31	19.34	6.98
	14	20.91	4.54	5.33	15.51	13.28	13.58	16.18	20.06	15.84	10.27	17.31	18.49	7.11
	16	20.75	4.54	5.33	15.51	12.24	12.85	15.01	18.96	14.81	10.25	17.31	17.85	7.20
MA 50	12	22.12	4.62	5.39	15.67	14.81	14.71	17.93	21.69	17.30	10.41	17.69	19.62	7.05
	14	21.34	4.62	5.39	15.67	13.42	13.72	16.35	20.30	16.10	10.40	17.69	18.77	7.18
	16	20.24	4.62	5.39	15.67	12.37	12.98	15.17	19.18	15.06	10.37	17.69	18.14	7.28
MA 75	12	21.57	3.93	5.05	14.69	13.88	13.79	16.81	20.20	14.72	9.55	15.54	17.93	6.61
	14	21.56	3.93	5.05	14.69	12.58	12.86	15.33	18.90	13.70	9.55	15.54	17.08	6.73
	16	20.33	3.93	5.05	14.69	11.60	12.17	14.22	17.86	12.82	9.49	15.54	16.44	6.82
MA 100	12	15.36	3.25	4.01	11.67	11.03	10.95	13.35	15.68	12.18	7.01	9.81	12.72	5.25
	14	15.53	3.25	4.01	11.67	9.99	10.22	12.18	14.68	11.34	7.02	9.81	11.88	5.35
	16	14.63	3.25	4.01	11.67	9.21	9.67	11.30	13.87	10.61	7.03	9.81	11.24	5.42

As it can be seen from Table 4.6, the ultimate bond strength obtained from the experimental test was nearly comparable with the bond strength calculated using some of proposed equations. But there is a significant variation with most of the predicted value due variation in bond parameters. Codes, however, recommend a minimum bond strength for design purposes based on the design concrete strength values. In this study the experimental mean value of cylindrical compressive strength was used in calculating the predicted bond strength. Generally, it was observed that the code-recommended values were always on the lower side for all concrete mixes.

ES EN 1992-1-1:2015 and ACI 318-08

The bond strength calculated based on equations of the ES EN 1992-1- [50] and ACI 318-08 [51] codes was significantly lower than the experimental results. Equation 2.9 of the ES EN 1992-1-1:2015 is exclusively suggested for conventional concrete and focuses solely on the tensile strength of the concrete. Though it includes the factor that considers quality of bond with the position and diameter of the bar, it does not consider the effect of embedment length and concrete cover thickness in the computation of bond strength.

The ACI code gives more emphasis on the computing development length of steel bars embedded in concrete. In doing so, factors related to location, epoxy coating, bar size, weight of coarse aggregate used in concrete, and compressive strength of concrete were included. This code used the yield strength, embedment length and diameter of the steel bar as a key parameter to estimate bond strength.

According to results from both codes, there was no variation in bond strength between the specimens with different diameters of bars embedded in the same compressive strengths of concrete. But as the compressive strength of the concrete mix varied, a small amount of variation in the calculated bond strength was observed. Generally, both the ES EN 1992-1-1:2015 and ACI 318-08 codes recommend a minimum design value. Hence, they underestimate the bond strength of the specimens with natural and waste marble coarse aggregates.

CEB-FIP Model Code

The CEB-FIP model code [28] estimates a relatively higher bond strength than those predicted by ES EN 1992-1-1:2015 and ACI 318-08. It considers the compressive strength of the concrete as the only parameter to estimate bond strength. The main limitation of CEB-FIP models is that it did not include the effect of other bond parameters such as concrete cover, diameter and embedment length of the bar. The experimental bond strength value of specimens that failed in pull-out was also higher than the bond strength estimated by this mode code in all concrete mixes. CEB-FIP model underestimated the bond strength value of specimens with both natural and waste marble coarse aggregate.

Orangun et al and Darwin et al

They are famous for predicting bond strength. As stated in equation 2.13 and 2.14 Concrete compressive strength, cover, rebar diameter, and embedment length were the main parameters included in their bond strength prediction equation. As shown from Table 4.6, the bond strength calculated by using the proposed equations of Orangun et al. [40] and Darwin et al. [52] is lower than the experimental result for both conventional and marble coarse aggregate concrete.

Esfahani & Rangan's, Huang et al. and Hadi

All of them predicted the bond strength equation for a deformed steel bar embedded in high-strength concrete. The bond parameters considered in the equation 2.15 of Esfahani & Rangan's [53] were concrete cover, diameter of bar, and concrete tensile strength whereas that included in equation 2.20 of Hadi [57] were compressive strength, cover, bar diameter, and embedment length. Huang et al. [56], however, considered the compressive strength of the concrete as the only parameter to predict the ultimate bond stress and ignored the effects of the other factors. It can be noted from Table 4.6 that the bond strength

of both conventional and marble coarse aggregate concrete was underestimated by equations proposed by Esfahani & Rangan's and Hadi. But compared to that of Esfahani et al and Hadi the bond strength calculated using equation of Huang et al (equation 2.19) is relatively close to the experimental result.

Chapman et al, Aslani et al, Shima et al and Melkam

All researchers predicted the bond strength equation of a deformed steel bar embedded in normal-strength concrete. The bond parameters considered in the equations of Chapman et al. [55] and Aslani et al. [54] were cover, diameter of bar, and embedment length. Melkam [58], however, considered the first two parameters only, while Shima et al. [24] as stated in equation 2.16 take into account slip and bar diameter as parameters. All of them in common included concrete compressive strength as a parameter. It can be noted from Table 4.6 that for all bars embedded in all concrete mixes the bond strength predicted by all of them was lower than the experimental value. However, the calculated bond strength of Aslani et al. showed good agreement with the experimental result.

Generally, the experimental and calculated bond strength results of all reinforcement bars (diameter 12mm,14mm and 16mm) embedded in all concrete mixes were summarized and graphically presented as shown in Figures 4.12, 4.13 and 4.14.

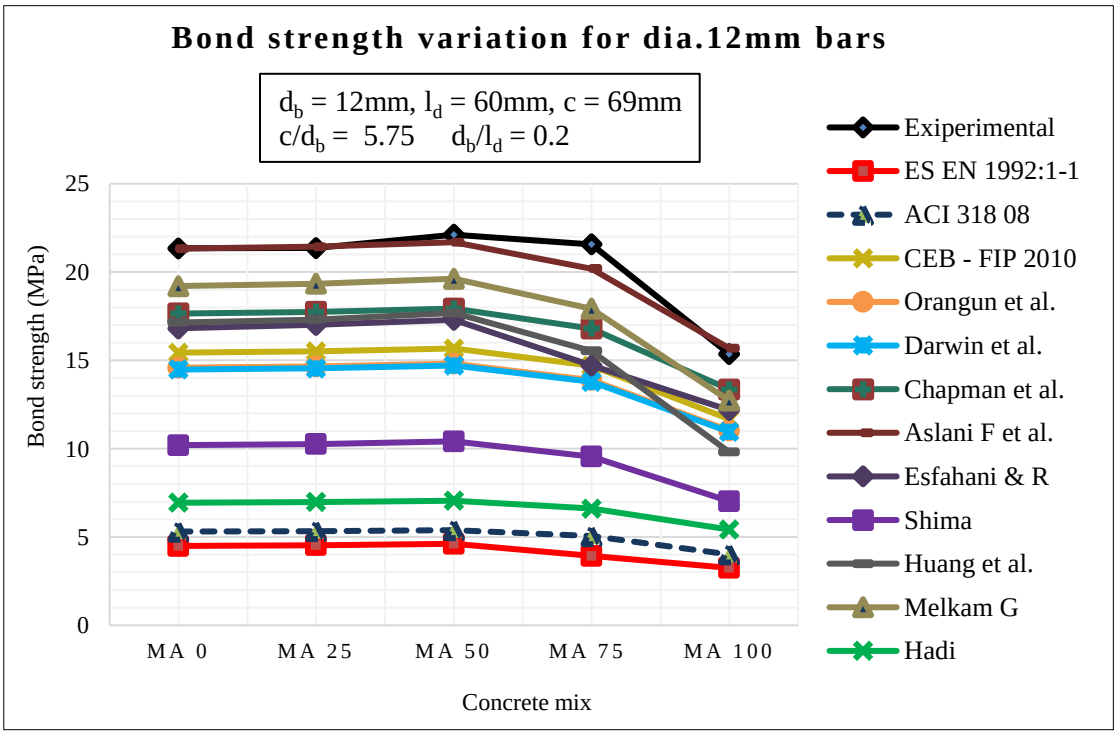

Figure 4.12 Bond strength variation for diameter 12mm bar

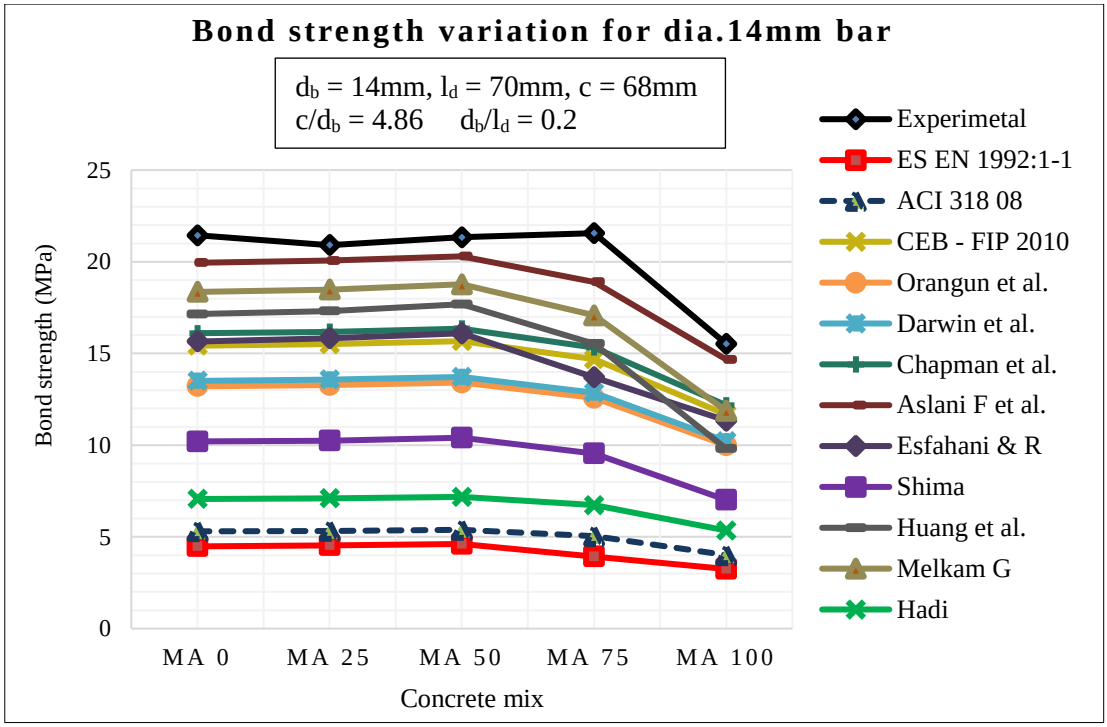

Figure 4.13 Bond strength variation for diameter 14mm bar

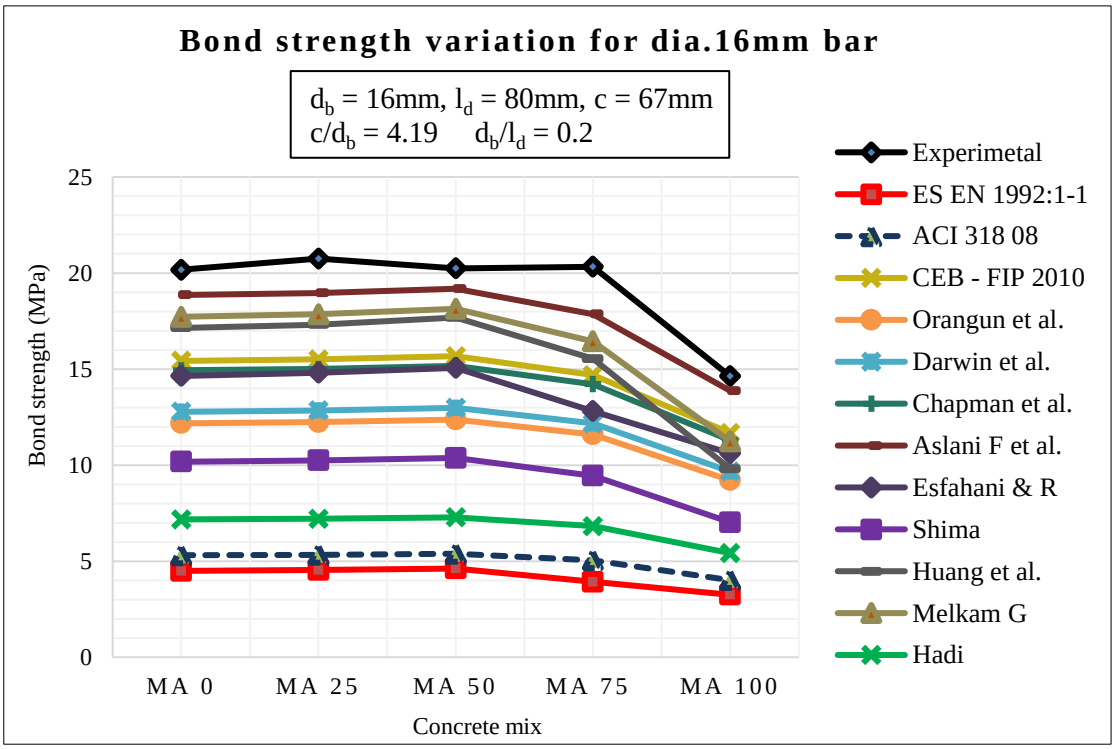

Figure 4.14 Bond strength variation for diameter 16mm bar

As it can be observed from Figures 4.12, 4.13, and 4.14, the experimental result is relatively close to the bond strength calculated using equations proposed by Aslani et al.

However, there is a variation in bond strength with other researchers for all reinforcement bars embedded in all concrete mixes. It is because the bond strength equations proposed by researchers are only limited to a specific bond parameter. The effect of coarse aggregate type on bond strength was underestimated in their equations. The angular shape and rough texture of marble coarse aggregate improved the aggregate cement paste of the mix, which in turn enhanced the strength of the concrete. There is a linear relationship between the bond strength and the compressive strength of the concrete as shown in Figure 4.15.

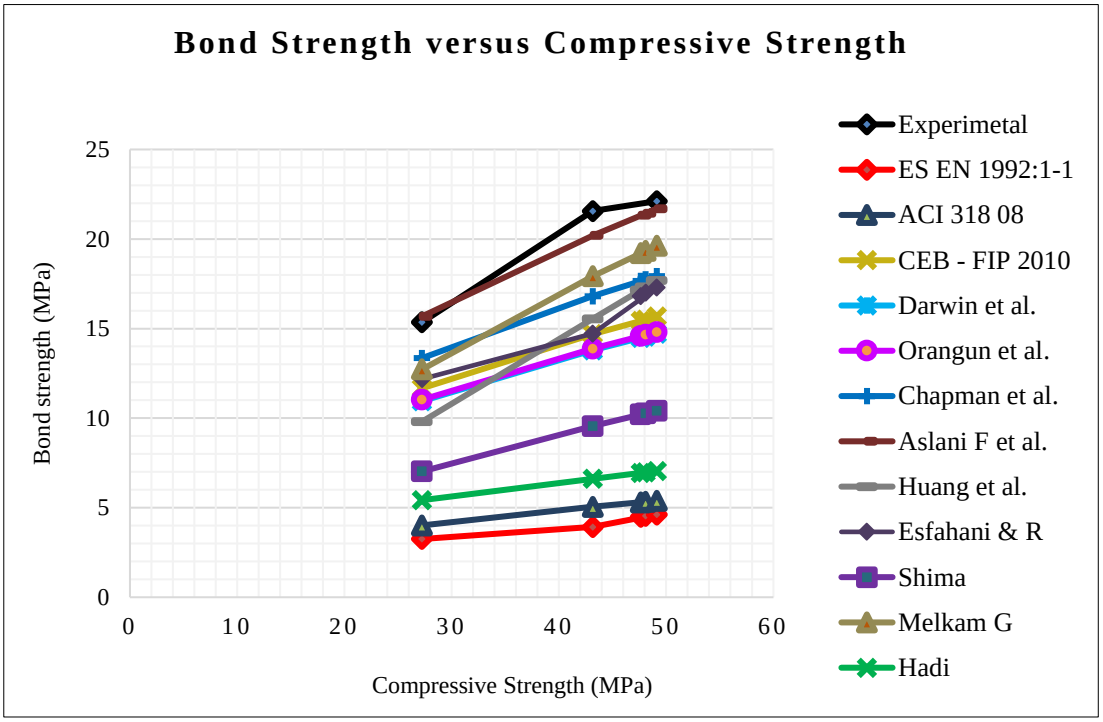

Figure 4.15 Relation between Bond Strength and Compressive Strength

5. CONCLUSIONS AND RECOMMENDATIONS

5.1 Conclusions

In this study, the bond strength behavior of reinforcement bar embedded in marble aggregate concrete was experimentally investigated using a pull-out test. Based on the test results, the following conclusions are drawn:

1. The workability of the concrete decreases as the quantity of marble in the mix increases.
2. The compressive and splitting tensile strengths of the concrete slightly increase as the percentage of marble increases up to 50% and a significant decrease in strength was observed at 100% marble coarse aggregate.
3. The average bond strength of marble aggregate concrete is comparable with the control concrete as the percentage of marble in the concrete mix increases up to 75% and then decreases.
4. According to the experimental results, the average bond strength decreases as the diameter size of the bar increases. It is due to nonlinear stress distribution along the higher embedment length of large diameter bars.
5. It is noticed that most of the specimens of diameter 12 mm and 14 mm bars have dominantly failed in Pull-out mode while splitting of concrete was mostly observed on diameter 16mm bar specimens.
6. The bond stress-slip curves of all specimens are similar to the curve proposed by CEB-FIB 2010 model code. The curve initially increased linearly and attained its peak at the ultimate loading then gradually drop. The shape of curve for both conventional and marble aggregate concrete specimens are also the same. However, the bond stress-slip curve of specimens that failed in splitting mode was different from those that failed in pull-out.
7. The experimental bond strength was higher than the calculated value for all steel bars embedded in all concrete mixes. Both the ES EN 1992-1-1:2015 and ACI 318-08 codes are conservative in predicting the bond strength of the concrete. In the other way, the bond strength calculated using the equation of Aslani and Nejadi was relatively close to the experimental result.

5.2 Recommendations

Based on the findings of the experimental investigation of the bond strength behaviour of marble coarse aggregate concrete, the following list of recommendations are forwarded:

- Due to laboratory equipment limitations, this study solely conducted the Pull-out test using cylindrical specimens with a centrally embedded deformed bar. However, additional research can be carried out using more bond strength test techniques, such as beam end specimens, beam anchorage specimens, or splice specimens.

- The bond strength of large-scale pullout specimens with a large cover, embedment length, and sample size might be studied in the future.

- The effect of the age of marble aggregate concrete on the bond strength behaviour of reinforcement bars needs investigation for future studies.

- The impact of steel bar corrosion on the bond strength of marble aggregate concrete could be studied.

REFERENCES

[1] Mehta, P.K. and Monteiro, P.J., 2014. *Concrete: Microstructure, Properties, and Materials*. McGraw-Hill Education.

[2] Marble, http://.en.wikipedia.org/wiki/marble , accessed May 12, 2023.

[3] Hebhoub, H., Aoun, H., Belachia, M., Houari, H. and Ghorbel, E., 2011. Use of waste marble aggregates in concrete. *Construction and Building Materials*, vol. 25, no. 3, pp.1167-1171.

[4] Kore, S.D.,2020. Performance of Concrete Mixes Using Marble Waste and ISF Slag, *Journal of Waste Management and Xenobiotics,* vol. 3, no.1, pp. 2640-2718.

[5] Andre, A., de Brito, J., Rosa, A. and Pedro, D., 2014. Durability Performance of Concrete Incorporating Coarse Aggregates from Marble Industry Waste. *Journal of Cleaner Production*, vol. 65, pp.389-396.

[6] Tastani, S.P. and Pantazopoulou, S.J., 2010. Direct Tension Pullout Bond Test: Experimental Results. *Journal of Structural Engineering*, vol. 136 no.6, pp.731-743

[7] Awol,A., 2011, Using Marble Waste Powder in Cement and Concrete Production, M.Sc. Thesis, Addis Ababa University School of Graduate Studies.

[8] Mohammednur, H., 2019.Quality and Quantity Assessments of Marble Deposit in Benishangul Gumuz Reginal State around Daleti area, M.Sc Thesis, Addis Ababa University School of Graduate Studies.

[9] Jeengar, R., 2022.Experimental Study on Partial Replacement of Natural Coarse Aggregate with Marble Waste Aggregate in Concrete. *International Journal for Research in Applied Science & Engineering Technology,* vol. 10, pp.1155-1160.

[10] Sunil,S.and Varghese,N.,2020. Study on Waste Marble as Partial Replacement of Coarse Aggregate in Concrete. *International Journal of Scientific and Engineering Research*, vol. 11, no. 10, pp.117-123.

[11] Chang, K.Y., Kwan, W.H. and Kua, H.B., 2018. The Application of Waste Marble as Coarse Aggregate in Concrete Production. *Scientific Research Journal*, vol. 15, no.1, pp.75-84.

[12] Adham, T.I., Abd Elrahman, A.M., Akasha, N.M., Khalifa, M.M., Abd Elgader, Y., Mohammed, E.H., Suliman, A.M. and Ahmed, M.E., 2017. Effects of Replacing Coarse Aggregate with Crushed Marble Tile Waste on Concrete Properties. *Red Sea University Journal of Basic and Applied Science*, vol. 2, no.3, pp.78-85.

[13] Kore, S.D. and Vyas, A.K., 2016. Impact of Marble Waste as Coarse Aggregate on Properties of Lean Cement Concrete. *Case Studies in Construction Materials*, vol. 4, pp.85-92.

[14] Ali, T., Ajwad, A., Abbas, A., Khan, M.A., Kashif, M. and Usman, M., 2016. Used Marble Waste Aggregate: Opportunities for Production of Eco-friendly Concrete. *Science International (Lahore)*, vol. 28, no. 2, pp.1333-1337.

[15] Chotaliya, J.P., Makwana, K.B. and Tank, P.D., 2016. Waste Marble Chips as Concrete Aggregate. *International Journal of Engineering Development and Research*, vol. 4, no. 3, pp.78-81.

[16] Martins, P., Brito, J.D., Rosa, A. and Pedro, D., 2014. Mechanical Performance of Concrete with Incorporation of Coarse Waste from the Marble Industry. *Materials Research*, vol. 17, no. 5 pp.1093-1101.

[17] Binici, H., Shah, T., Aksogan, O. and Kaplan, H., 2008. Durability of Concrete Made with Granite and Marble as Recycle Aggregates. *Journal of Materials Processing Technology*, vol. 208, no.1-3, pp.299-308.

[18] Annapoorna, G.V. and Suresh, S., 2017. Experimental Study on Bond Behavior of Reinforcing Bars in Plain and Fiber Reinforced Concrete. *International Journal of Advanced. Mechanical and Civil Engineering*, vol. 2394, no.4, pp.83-86.

[19] ACI 408 Committee, 2003. Bond and Development of Straight Reinforcing Bars in Tension (ACI 408R-03). *American Concrete Institute, Detroit, Michigan, US.*

[20] Lutz, L.A. and Gergely, P., 1967. Mechanics of bond and slip of deformed bars in concrete. *ACI Journal Proceedings*, vol. 64, no. 11, pp. 711-721.

[21] Tepfers, R., 1973. A Theory of Bond Applied to Overlapped Tensile Reinforcement Splices for Deformed Bars. Division of Concrete Structures, Chalmers University of Technology. vol. 73, no.2, p.328.

[22] Xing, G., Zhou, C., Wu, T. and Liu, B., 2015. Experimental Study on Bond Behavior Between Plain Reinforcing Bars and Concrete. *Advances in Materials Science and Engineering*, vol. 2015, no.6, pp.1-9.

[23] Soraghi, A. and Huang, Q., 2022. Probabilistic Modeling of Reinforced Concrete Bond Behavior Considering Failure Mode and Corrosion. *Structure and Infrastructure Engineering*, vol. 18, no.5, pp. 1573-2479.

[24] Shima, H., Chou, L.L. and Okamura, H., 1987. Micro and Macro Models for Bond in Reinforced Concrete. *Journal of the Faculty of Engineering*, vol. 39, no. 2, pp.133-194.

[25] Eligehausen, R., Popov, E.P. and Bertero, V.V., 1982. Local Bond Stress-Slip Relationships of Deformed Bars under Generalized Excitations. *In proceeding of the 7th European Conference on Earthquake Engineering*, vol. 4, pp. 69–80.

[26] Filippou, F.C., Popov, E.P. and Bertero, V.V., 1983. Modeling of Reinforced Concrete Joints under Cyclic Excitations. *Journal of Structural Engineering*, vol. 109, no. 11, pp.2666-2684.

[27] Tang, C.W. and Cheng, C.K., 2020. Modeling Local Bond Stress–Slip Relationships of Reinforcing Bars Embedded in Concrete with Different Strengths. *Construction and Building Materials*, vol. 13, no.17, pp.1-22.

[28] Code, M., 2010. FIB model Code for Concrete Structures. Committee Euro-International du Beton, Lausanne, Switzerland.

[29] Hong, S. and Park, S.K., 2012. Uniaxial Bond Stress-Slip Relationship of Reinforcing Bars in Concrete. *Advances in Materials Science and Engineering*, vol.2012, pp.328-570.

[30] Wight, J. and MacGregor, J.G., 2009. *Reinforced Concrete. Mechanics and Design*. 6th edition, Pearson Education, Upper Saddle River, New Jersey.

[31] Tsiotsias, K. and Pantazopoulou, S.J., 2021. Analytical Investigation on the Effect of Test Setup on Bond Strength. *Civil Engineering*, vol. 2, no.1, pp.14-34.

[32] ASTM A944 – 95,2010. Standard Test Method for Comparing Bond Strength of Steel Reinforcing Bars to Concrete Using Beam-End Specimens, *in Annual Book of ASTM Standards, ASTM International*, West Conshohocken, pp. 1–4.

[33] Ali, A., 2017. Bond behavior of lightweight steel fibre-reinforced concrete. Doctoral Dissertation, Technical University Bergakademie, Freiberg.

[34] Wassouf, M., 2015. Bond and Ductility of Concrete Reinforced with Various Steel Bars Surface and Ductility Conditions. Doctoral Dissertation, University of Birmingham.

[35] Den Uijl, J.A. and Bigaj, A.J., 1996. A Bond model for Ribbed Bars Based on Concrete Confinement. *Heron*, vol. 41, no. 3, pp.201-226.

[36] Lundgren, K., 2005. Bond between Ribbed Bars and Concrete. Part 1: Modified Model. *Magazine of concrete research*, vol. 57, no.7, pp.371-382.

[37] Burdziński, M. and Niedostatkiewicz, M., 2022. Experimental-Numerical Analysis of the Effect of Bar Diameter on Bond in Pull-Out Test. *Buildings*, vol. 12, no.9, pp.1209-1392.

[38] DeVilliers, J.P., 2015. Bond behavior of deformed steel reinforcement in lightweight foamed concrete. Doctoral dissertation, Stellenbosch University, Stellenbosch.

[39] Wang, H., 2009. An Analytical Study of Bond Strength Associated with Splitting of Concrete Cover. *Engineering Structures*, vol. 31, no.4, pp.968-975.

[40] Orangun, C. O. Jirsa, J. O. and Breen, J. E.,1977. Reevaluation of Test Data on Development Length and Splices. *ACI Journal*, vol. 74, no.3, pp.114-122.

[41] Abrams, D.A., 1913. Tests of Bond Between Concrete and Steel. *Bulletin No 71. Engineering Experiment station*, University of Illinios, urbana, p.105.

[42] Skorobogatov, S. M. and Edwards, A. D., 1979.The Influence of the Geometry of Deformed Steel Bars on Their Bond Strength in Concrete. *Proceedings of the Institution of Civil Engineers*, vol. 67, no. 2, pp. 327-339.

[43] Hamad,B.S. ,1995. Bond Strength Improvement of Reinforcing Bars with Specially Designed Rib Geometries. *ACI Structural Journal*, vol. 92, pp. 3-13.

[44] Azizinamini, A.Starck,M.Roller,J.Jand Ghosh,S.K.,1993.Bond Performance of Reinforcing Bars Embedded in High strength concrete, *ACI Structural Journal* ,vol. 90,no.5,pp.554-561.

[45] Zuo, J., and Darwin, D., 2000.Splice Strength of Conventional and High Relative Rib Area Bars in Normal and High-Strength Concrete, *ACI Structural Journal*, vol. 97, no. 4, pp. 630-641.

[46] Abebaw, L.,2021. Experimental Investigation of the Role of Coarse Aggregate for Bond Strength of Reinforced Concrete, M.Sc. Thesis, Addis Ababa University School of Graduate Studies.

[47] Iqbal, S., Ullah, N. and Ali, A., 2018. Effect of Maximum Aggregate Size on the Bond Strength of Reinforcements in Concrete. *Engineering, Technology and Applied Science Research*, vol. 8, no.3, pp.2892-2896.

[48] Sadeghi, M. and Sharma, A., 2019. Pull-out Test for Studying Bond Strength in Corrosion Affected Reinforced Concrete Structures-A review. *Otto-Graf-Journal*, vol. 18, pp.259-272.

[49] RILEM TC. RC6, 1994.Bond Test for Reinforcement Steel.2. Pull-out test, *In RILEM Recommendations for the Testing and Use of Constructions Materials*, E & FN SPON, pp. 218–220.

[50] Ministry of Urban Development and Construction, 2015. Design of Concrete Structures, ES EN 1992-1-1:2015, Ethiopian Standards Agency, pp. 133–136.

[51] ACI Committee, 2008. Building Code Requirements for Structural Concrete (ACI 318- 08) and Commentary. American Concrete Institute.

[52] Darwin, D., McCabe, S.L., Idun, E.K. and Schoenekase, S.P., 1992. Development Length Criteria: Bars not Confined by Transverse Reinforcement. *ACI structural Journal*, vol. 89, no. 6, pp.709–720.

[53] Esfahani, M.R. and Rangan, B.V., 1998. Bond Between Normal Strength and High-Strength Concrete (HSC) and Reinforcing Bars in Splices in Beams. *ACI Structural Journal*, vol. 95, no.3, pp.272-280.

[54] Aslani, F. and Nejadi, S., 2012. Bond Behavior of Reinforcement in Conventional and Self-Compacting Concrete. *Advances in Structural Engineering*, vol. 15, no. 12, pp.2033-2051.

[55] Chapman, R.A. and Shah, S.P., 1987. Early-Age Bond Strength in Reinforced Concrete. *Materials Journal*, vol. 84, no.6, pp.501-510.

[56] Huang, Z., Engström, B. and Magnusson, J., 1996. Experimental and Analytical Studies of the Bond Behaviour of Deformed Bars in High Strength Concrete. *In Proceedings of the 4th International Symposium on the Utilization of High Strength/High Performance Concrete*, vol. 3, pp. 1115–1124.

[57] Hadi, M.N., 2008. Bond of High Strength Concrete with High Strength Reinforcing Steel. *The Open Civil Engineering Journal*, vol. 2, pp.143-147.

[58] Gubay,M., 2022, Experimental Investigation of the Effect of Steel Slag Aggregate on the Bond Strength of Reinforced Concrete Member, M.Sc. Thesis, Addis Ababa University School of Graduate Studies.

[59] ASTM, C150-07, 2007. Standard Specification for Portland Cement. *ASTM International*, Conshohocken.

[60] Dinku, A., 2002. Construction Materials Laboratory Manual. Department of Civil Engineering, Addis Ababa University, Addis Ababa.

[61] ASTM, C-125, 2003. Standard Terminology Relating to Concrete and Concrete Aggregates, 1-4 S. *ASTM International*, Conshohocken.

[62] ASTM, C-33, 2003. Standard Specification for Concrete Aggregates. *American Society for Testing and Materials*, Philadelphia.

[63] Dixon, D.E., Prestrera, J.R., Burg, G.R., Chairman, S.A., Abdun-Nur, E.A., Barton, S.G., Bell, L.W., Blas Jr, S.J., Carrasquillo, R.L., Carrasquillo, P.M. and Carter, A.C., 1991. Standard practice for selecting proportions for normal, heavyweight, and mass concrete (ACI 211.1-91), *American Concrete Institute*, *Farmington Hills.*

[64] ASTM, C-192, 2002. Standard Practice for Making and Curing Concrete Test Specimens in the Laboratory, *Annual Book of ASTM Standards*, vol. 04. pp. 1–8.

[65] ASTM, C-143, 2008. Standard Test Method for Slump of Hydraulic-Cement Concrete, *Annual Book of ASTM Standards*, vol.4, no.2. pp.1–3.

[66] BS EN 12390-3,2009. Testing Hardened Concrete. Compressive Strength of Test Specimens, British Standard Institution.

[67] ASTM, C-496., 2011. Standard Test Method for Splitting Tensile Strength of Cylindrical Concrete Specimens. *ASTM international*, West Conshohocken.

[68] Wang, F., Wu, X., Guo, C. and Song, W., 2018. Experimental Study on Bond Strength of Deformed Steel Bars in Recycled Glass Aggregate Concrete. *Journal of Korean Society of Civil Engineering*, vol. 22, no.9, pp.3409-3418.

[69] Shunmuga Vembu, P.R. and Ammasi, A.K., 2023. A Comprehensive Review on the Factors Affecting Bond Strength in Concrete. *Journal of Buildings*, vol. 13, no.3, pp.577-604.

APPENDIX

Appendix A- Aggregate Physical Property Test Result

A-1 Tests for Fine Aggregate

- **Silt Content**

A=Amount of silt deposited= 0.5ml

B=Amount of clean Sand = 29.5ml

Silt Content (%) = $\frac{A}{B}$ *100 = $\frac{0.5}{29.5}$ *100 = 1.69%

- **Sieve Analysis of Fine Aggregate**

Sieve size (mm)	Weight of sieve (g)	Weight of sieve and retained (g)	Weight retained (g)	Percentage retained (%)	Cumulative percent retained (%)	Cumulative passing (%)	ASTM C33 standard passing range (%)
9.75							100
4.75	432.1	433.2	1.1	0.22	0.22	99.78	95-100
2.36	396.8	421.6	24.8	4.94	5.16	94.84	80-100
1.18	372.6	452.8	80.2	15.98	21.14	78.86	50-85
0.6	312.5	498.9	186.4	37.13	58.27	41.73	25-60
0.3	308.7	463.5	154.8	30.84	89.10	10.90	5-30
0.15	277.9	323.2	45.3	9.02	98.13	1.87	0-10
Pan	347.2	355.8	8.6	1.71	99.84	0.16	0

Fineness Modulus (FM) = $\frac{\sum(\text{Cumulative Percent retained})}{100}$ = $\frac{272.02}{100}$ = 2.72

- **Moisture Content of Fine Aggregate**

Weight of original Sample = 500g

Weight of Oven-dry sample = 491.6 g

Moisture Content = $\frac{\text{weight of Original Sample} - \text{Weight of Oven-dry Sample}}{\text{Weight of Oven-dry Sample}}$ *100

Moisture Content = $\frac{500-491.6}{491.6}$ *100 = 1.71 %

- **Unit Weight of Fine Aggregate**

Weight of measure = 4.85 kg

Weight of measure and Aggregate = 25.985 kg

Net weight of Fine Aggregate = (Weight of measure and Aggregate) – Weight of measure

Net weight of Aggregate = 25.985kg – 4.85kg = 21.135 kg

Volume of measure (v) = $\frac{\pi d^2}{4}$ * h d = 0.255m h = 0.27 m

Volume of measure (v) = $\frac{\pi(0.255)^2}{4}$ * 0.27 = 0.0138 m^3

Unit weight of fine Aggregate = $\frac{\text{Net Weight of Aggregate}}{\text{Volume of measure}}$ = $\frac{21.135\ \text{kg}}{0.0138\ \text{m3}}$ = 1531.52 kg/m^3

- **Specific gravity and Absorption of fine Aggregate**

Weight of Original Sample = 500 g

B = Weight of Pycnometer + water, = 706.8 g

C = Weight of Pycnometer + water + sample = 1007.2 g

A = Weight of oven-dry sample = 488.6 g

Bulk Specific Gravity = $\frac{\text{A}}{\text{B+500−C}}$ = $\frac{488.6}{706.8 + 500 - 1007.2}$ = 2.45

Bulk Specific Gravity (SSD basis) = $\frac{500}{\text{B+500−C}}$ = $\frac{500}{706.8 + 500 - 1007.2}$ = 2.51

Apparent Specific Gravity = $\frac{\text{A}}{\text{B+A−C}}$ = $\frac{488.6}{706.8 + 488.6 - 1007.2}$ = 2.6

Absorption (%) = $\frac{500-\text{A}}{\text{A}} * 100$ = $\frac{500-488.6}{488.6}$ * 100 = 2.33 %

A-2: Tests for Coarse Aggregate

- **Sieve Analysis of Coarse Aggregate**

Seive Size (mm)	Weight of Seive (g)	Weight of sieve and retained (g)	Weight retained (g)	Percentage retained (%)	Cumulative Percent retained (%)	Cumulative passing (%)	ASTM C33 passing range (%)
25	1198.8	1198.8	0	0	0	100	95-100
19	1380.2	1955.7	575.5	28.78	28.78	71.23	-
12.5	1155.6	1889	733.4	36.67	65.45	34.56	25-60
9.5	1157.7	1726.6	568.9	28.45	93.89	6.11	-
4.75	1177.5	1281.2	103.7	5.19	99.08	0.92	0-10
Pan	1059.4	1074.1	14.7	0.73	99.81	0.19	0

Fineness modulus of Coarse aggregate is the total cumulative percent retained values of sieves (38.1,19,9.5,4.75,2.36,1.18,0.6,0.3 and 0.15mm) divided by 100

Sieve size (mm)	Cumulative percent retained (mm)
38.1	0
19	28.78
9.5	93.89
4.75	99.07
2.36	100
1.18	100
0.6	100
0.3	100
0.15	100
Total $\sum$	721.74

Fineness Modulus (FM) = $\frac{\sum(\text{Cumulative percent Retained})}{100} = \frac{721.74}{100} \approx 7.22$

- **Moisture Content of Coarse Aggregate**

Weight of Original Sample = 2000 g

Weight of Oven dry Sample = 1992.5 g

Moisture Content = $\frac{\text{weight of Original Sample} - \text{Weight of Oven dry Sample}}{\text{Weight of Oven dry Sample}} * 100$

Moisture Content = $\frac{2000-1992.5}{1992.5} * 100 = 0.376\ \%$

- **Unit Weight of Coarse Aggregate**

Weight of measure = 4.85 kg

Weight of measure and Aggregate = 27.613 kg

Net weight of Fine Aggregate = (Weight of measure and Aggregate) – Weight of measure

Net weight of Aggregate = 27.613 kg – 4.85 kg = 22.763 kg

Volume of measure (v) = $\frac{\pi d^2}{4}$ *h d = 0.255m h = 0.27 m

Volume of measure (v) = $\frac{\pi * 0.255^2}{4}$*0.27 = 0.0138 m^3

Unit weight of Coarse Aggregate = $\frac{\text{Net Weight of Aggregate}}{\text{Volume of measure}} = \frac{22.763\ \text{kg}}{0.0138\ \text{m3}}$ = 1649.49 kg/m^3

- **Specific Gravity and Absorption of Coarse Aggregate**

A=Weight of Oven-dry Sample in air = 4984 g

B=Weight of Saturated Surface dry Sample in air = 5010 g

C= Weight of Saturated Sample in water = 3179.4 g

Bulk Specific Gravity = $\frac{A}{B-C} = \frac{4984\ g}{5010\ g - 3179.4\ g} = \frac{4984}{1830.6}$ = 2.72

Bulk Specific Gravity (SSD) = $\frac{B}{B-C} = \frac{5010\ g}{5010\ g - 3179.4\ g} = \frac{5010}{1830.6}$ = 2.74

Apparent Specific Gravity = $\frac{A}{A-C} = \frac{4984\ g}{4984\ g - 3179.4\ g} = \frac{4984}{1804.6}$ = 2.76

Absorption Capacity = $\frac{B-A}{A} * 100 = \frac{5010\ g - 4984\ g}{4984\ g} * 100 = \frac{26}{4984} * 100$ = 0.522 %

- **Aggregate Impact Value for Coarse Aggregate**

A=The initial mass of surface dry sample = 617.6 g

B= The mass of fractions passing the sieve 2.36 mm for separating the fines = 32.2 g

C= The mass of fractions retaining the sieve 2.36 mm for separating the fines = 584.4g

Percentage fines = $\frac{B}{A} * 100 = \frac{32.2\ g}{617.6\ g} * 100 = 5.21\%$

A-3: Tests for Crushed Marble Aggregate

- **Sieve Analysis of Marble Aggregate**

Seive Size (mm)	Weight of Seive (g)	Weight of sieve and retained (g)	Weight retained (g)	Percentage retained (%)	Cumulative Percent retained (%)	Cumulative passing (%)	ASTM C33 passing range (%)
25	1199.7	1199.7	0	0	0	100	95-100
19	1380.7	1826.2	445.5	22.28	22.28	77.73	-
12.5	1155.6	1989.3	833.7	41.69	63.96	36.04	25-60
9.5	1157.7	1556.2	398.5	19.93	83.89	16.12	-
4.75	1177.5	1490.8	313.3	15.67	99.55	0.45	0-10
Pan	1059.4	1068.4	9	0.45	100	0	0

Fineness modulus of marble aggregate is the total cumulative percent retained values of sieves (38.1,19,9.5,4.75,2.36,1.18,0.6,0.3 and 0.15mm) divided by 100

Sieve size (mm)	Cumulative % retained (mm)
38.1	0
19	22.28
9.5	83.89
4.75	99.55
2.36	100
1.18	100
0.6	100
0.3	100
0.15	100
Total $\sum$	705.72

Fineness Modulus (FM) = $\frac{\sum(Cumulative\ percent\ Retained)}{100} = \frac{705.72}{100} \approx 7.06$

❖ **Moisture Content of Marble Aggregate**

Weight of Original Sample = 2000 g

Weight of Oven dry Sample = 1999 g

Moisture Content = $\frac{\text{weight of Original Sample} - \text{Weight of Oven dry Sample}}{\text{Weight of Oven dry Sample}}$ *100

Moisture Content = $\frac{2000\ \text{g} - 1999\ \text{g}}{1999\ \text{g}}$ *100 = 0.05 %

❖ **Unit Weight of marble Aggregate**

Weight of measure = 4.85 kg

Weight of measure and Aggregate = 26.413 kg

Net weight of Fine Aggregate = (Weight of measure and Aggregate) – Weight of measure

Net weight of Aggregate = 26.413 kg – 4.85 kg = 21.563 kg

Volume of measure (v) = $\frac{\pi d^2}{4}$ *h d = 0.255m h = 0.27 m

Volume of measure (v) = $\frac{\pi * 0.255^2}{4}$*0.27 = 0.0138 m^3

Unit weight of Coarse Aggregate = $\frac{\text{Net Weight of Aggregate}}{\text{Volume of measure}}$ = $\frac{21.563\ \text{kg}}{0.0138\ \text{m3}}$ = 1562.54 kg/m^3

❖ **Specific Gravity and Absorption of Marble Aggregate**

A=Weight of Oven-dry Sample in air = 4989 g

B=Weight of Saturated Surface dry Sample in air = 5010 g

C= Weight of Saturated Sample in water = 3065 g

Bulk Specific Gravity = $\frac{A}{B-C} = \frac{4989\ g}{5010\ g-3065\ g} = \frac{4989}{1945} = 2.57$

Bulk Specific Gravity (SSD) = $\frac{B}{B-C} = \frac{5010\ g}{5010\ g-3065\ g} = \frac{5010}{1945} = 2.58$

Apparent Specific Gravity = $\frac{A}{A-C} = \frac{4989\ g}{4989\ g-3065\ g} = \frac{4989}{1924} = 2.59$

Absorption Capacity = $\frac{B-A}{A} * 100 = \frac{5010\ g-4989\ g}{4989\ g} * 100 = \frac{21}{4984} * 100 = 0.42\ \%$

❖ **Aggregate Impact Value for Marble Aggregate**

A=The initial mass of surface dry sample = 605 g

B= The mass of fractions passing the sieve 2.36 mm for separating the fines = 168.8 g

C= The mass of fractions retaining the sieve 2.36 mm for separating the fines = 436.2 g

Percentage fines = $\frac{B}{A} * 100 = \frac{168.8\ g}{605\ g} * 100 = 27.9\ \%$

Appendix B-Test Result for Mechanical Properties of Reinforcement Bars

Rebar Spec No.	Diameter		Av. Dia. (mm)	Area (mm^2)	Yield Load (kN)	Failure Load (kN)	Elongation (%)	Mass/ length (kg/m)	Length (cm)	Yield Strength (MPa)	Ultimate Strength (MPa)	Av.Yield Strength (MPa)	Av.Ultimate Strength (MPa)
	D1 (mm)	D2 (mm)											
12-1	11.49	12.7	12.1	114.9	62.8	73.7	7.9	861	100	546.59	641.45	549.2	643.49
12-2	11.47	12.72	12.1	114.9	63.4	73.9	7.8	869.5	100	551.81	643.2		
12-3	11.49	12.7	12.1	114.9	63.1	74.2	7.8	860.7	100	549.2	645.81		
14-1	13.55	14.7	14.13	156.7	87.9	103.7	8.7	1067	100	560.95	661.78	574.67	692.73
14-2	13.57	14.72	14.15	157.14	90.4	110.2	8.6	1075	100	575.27	701.27		
14-3	13.54	14.74	14.14	157.03	92.3	112.3	8.8	1162	100	587.78	715.14		
16-1	15.52	16.73	16.13	204.22	114.4	133.5	9.7	1555	100	560.19	653.72	567.28	655.95
16-2	15.49	16.74	16.12	203.96	116.3	133.9	10.0	1550	101	570.2	656.49		
16-3	15.55	16.7	16.13	204.22	116.7	134.3	9.7	1530	101	571.45	657.64		

Appendix C-Mix Design for C-30 Concrete

Material Physical Property Test Data

Test	Cement	Fine Aggregate	Coarse Aggregate	Marble Aggregate
Unit Weight (kg/m^3)	-	1531.52	1649.49	1562.54
Specific Gravity	3.15	2.45	2.72	2.57
Water Absorption (%)	-	2.33	0.522	0.42
Moisture Content (%)	-	1.71	0.376	0.05
Fineness Modulus	-	2.72	7.22	7.06

Step 1: - Choice of Slump

Addressing most common type of construction beams, col ums and reinforced walls ACI 211 Table: A1.5.3.1 recommends a slump ranging 25 to 100 mm. Minimum slump = 25 mm and Maximum Slump = 100 mm

Step 2: - Choice of nominal maximum size of aggregate

The maximum size of coarse aggregate size is 25 mm

Step 3: - Estimation of mixing water and air content

From Table A1.5.3.3 of ACI 211 standard the Approximate water content per unit volume of non-air entrained concrete for a nominal aggregate size of 25mm and slump range of 25 -50 mm is 179 kg/m^3, Air content = 1.5%

Step 4: - Selection of water-cement ratio (w-c)

Considering a mean 28th compressive strength of 38 MPa of non-air entrained concrete the water cement ratio linearly interpolated from ACI 211 Table A1.5.3.4(a) is 0.44

w-c = 0.44

Step 5: - Calculation of cement content

Water content = 179 kg/m^3

Water cement ratio = 0.44

Cement content = $\frac{\text{Water content}}{\text{Water cement ratio}} = \frac{179\ \text{kg/m3}}{0.44}$ = 406.82 kg/m^3

Step 6: - Estimation of coarse aggregate content

From ACI 211 Table A1.5.3.6 the volume of dry rodded coarse aggregate per unit volume of concrete for nominal maximum aggregate size 25 mm and fineness modulus of fine aggregate 2.72 is linearly interpolated and gives 0.678

The quantity of coarse aggregate per cubic meter of concrete is estimated as

CA = 0.678*1649.49 kg/m^3 = 1118.35 kg/m^3

Step 7: - Estimation of fine aggregate content

According to ACI 211 Table A1.5.3.7.1, the mass of a cubic meter of non-air-entrained concrete made with 25 mm nominal maximum aggregate size is 2380 kg/m^3

Fine Aggregate content (FA) = mass of fresh concrete – (water + cement + CA)

FA= 2380 - (179+406.82+1118.35) = 675.83 kg/m^3

Step 8: - Adjustment for moisture

Absorption capacity and moisture content of aggregate should be balanced. If the moisture content of the aggregate is lower than its absorption, we have to increase free water up to its absorption capacity.

FA water = 2.333 - 1.71 = 0.62 %

CA water = 0.522 – 0.376 = 0.146 %

Total water required = 179 + (0.0062*675.83+0.00146*1118.35) = 184.83 Kg/m^3

The quantity of ingredient per unit volume of concrete is summarized below for zero percent replacement of coarse aggregate.

Ingredients	Weight per unit volume of concrete (kg/m^3)
Water	184.83
Cement	406.82
Coarse Aggregate	1118.35
Fine Aggregate	675.83

Replacement of Waste marble is done by percent weight of natural coarse aggregate.

Ingredients	Quantity of ingredients per unit volume of concrete (kg/m^3)				
	MA 0	MA 25	MA 50	MA 75	MA 100
Water	184.83	184.83	184.83	184.83	184.83
Cement	406.82	406.82	406.82	406.82	406.82
Fine Aggregate	675.83	675.83	675.83	675.83	675.83
Coarse Aggregate	1118.35	838.76	559.17	279.59	0
Marble Aggregate	0	279.59	559.17	838.76	1118.35

Step 9: - Trial batch

There are nine cylindrical (150X300mm), six cubical (150X150X150mm) and three cylindrical (150X300mm) specimens for pullout bond strength test, compressive strength test and split tensile strength test respectively per mix giving a total volume of 0.083835 m^3.

Adding 15 % wastage = 0.01257525 m^3, the total volume per mix is 0.083835 m^3 + 0.01257525 m^3 = 0.09641025 m^3

Quantity of ingredients per mix

Ingredients	Mass of ingredients per mix (kg)				
	MA 0	MA 25	MA 50	MA 75	MA 100
Water	17.82	17.82	17.82	17.82	17.82
Cement	39.22	39.22	39.22	39.22	39.22
Fine Aggregate	65.16	65.16	65.16	65.16	65.16
Coarse Aggregate	107.82	80.87	53.91	26.96	0
Marble Aggregate	0	26.96	53.91	80.87	107.82

Appendix D- Compressive Strength Test Result

Mix Id	Test Age (Days)	Specimen No.	Weight (g)	Failure Load (kN)	Compressive Strength (MPa)	Average Compressive Strength (MPa)
MA 0	7	1	8286	674.5	29.97	30.3
		2	8243	677.8	30.13	
		3	8296	692.8	30.79	
	28	1	8231	1042.5	45.13	47.64
		2	8308	1102.8	49.01	
		3	8255	1097.4	48.77	
MA 25	7	1	8278	711.7	31.63	31.0
		2	8220	701.2	31.17	
		3	8241	679.5	30.2	
	28	1	8249	1082.8	48.13	48.1
		2	8236	1061.4	47.86	
		3	8340	1086.8	48.3	
MA 50	7	1	8251	761	33.82	33.81
		2	8246	731.9	32.53	
		3	8266	789.6	35.09	
	28	1	8196	1093.9	48.62	49.13
		2	8231	1109.8	49.51	
		3	8229	1108.3	49.26	
MA 75	7	1	8158	714.4	31.75	31.89
		2	8164	728.6	32.38	
		3	8148	713.2	31.53	
	28	1	7862	963.4	42.58	43.16
		2	7876	1012.9	45.02	
		3	7856	942.3	41.88	
MA 100	7	1	7658	245.9	10.93	12.35
		2	7769	307.5	13.63	
		3	7731	280.8	12.48	
	28	1	7818	592.2	26.32	27.24
		2	7874	613.0	27.24	
		3	7858	633.8	28.17	

Appendix E- Splitting Tensile Strength Test Result

Mix Id	Test Age (Days)	Specimen No.	Weight (g)	Failure Load (kN)	Split tensile Strength (MPa)	Average Split ensile Strength (MPa)
MA 0	28	1	13220	254.3	3.6	3.52
		2	13140	271.5	3.84	
		3	13157	220.1	3.11	
MA 25	28	1	13004	313.2	4.43	3.56
		2	13062	229.4	3.25	
		3	13090	212.8	3.01	
MA 50	28	1	13000	252.0	3.57	3.62
		2	13003	250.1	3.54	
		3	13059	265.4	3.75	
MA 75	28	1	12920	204.3	2.89	3.08
		2	12871	216.4	3.06	
		3	12760	231.4	3.27	
MA 100	28	1	12376	195.7	2.77	2.55
		2	12487	175.2	2.48	
		3	12490	170.0	2.41	

Appendix F- Pull-out Bond Strength Test Result

Specimen Id	Failure Load (kN)	Bond Stress (MPa)	Slip (mm)	Average failure load (kN)	Average bond stress (MPa)	Average slip (mm)	Failure Mode
MA0d12-1	49.5	21.88	0.025	48.28	21.34	0.97	Splitting
MA0d12-2	50.54	22.34	2.03				Pull-out
MA0d12-3	44.8	19.80	0.85				Pull-out
MA0d14-1	67.83	22.03	0.27	66.03	21.45	0.91	Pull-out
MA0d14-2	70.08	22.76	1.40				Pull-out
MA0d14-3	60.19	19.55	1.05				Pull-out
MA0d16-1	81.84	20.35	0.5	81.11	20.17	0.69	Pull-out
MA0d16-2	83.27	20.71	0.765				Pull-out
MA0d16-3	78.21	19.45	0.795				Pull-out
MA25d12-1	46.85	20.71	0.465	48.32	21.36	0.73	Pull-out
MA25d12-2	48.83	21.59	1.11				Pull-out
MA25d12-3	49.28	21.79	0.62				Pull-out
MA25d14-1	64.98	21.11	1.835	64.38	20.91	0.63	Pull-out
MA25d14-2	67.49	21.92	0.03				Pull-out
MA25d14-3	60.67	19.71	0.02				Pull-out
MA25d16-1	82.6	20.54	1.22	83.46	20.75	0.73	Pull-out
MA25d16-2	85.36	21.23	0.505				Splitting
MA25d16-3	82.41	20.49	0.465				Splitting
MA50d12-1	52.27	23.11	1.39	50.03	22.12	1.02	Pull-out
MA50d12-2	48.95	21.64	0.315				Pull-out
MA50d12-3	48.86	21.60	1.35				Pull-out
MA50d14-1	67.46	21.91	0.525	65.69	21.34	0.78	Pull-out
MA50d14-2	64.72	21.02	1.37				Pull-out
MA50d14-3	64.90	21.08	0.445				Pull-out
MA50d16-1	80.76	20.08	0.75	81.41	20.25	0.59	Splitting
MA50d16-2	83.80	20.84	0.47				Splitting
MA50d16-3	79.67	19.81	0.56				Splitting
MA75d12-1	52.35	23.14	0.85	48.79	21.57	0.98	Splitting
MA75d12-2	49.02	21.67	1.625				Splitting
MA75d12-3	44.99	19.89	0.475				Pull-out
MA75d14-1	60.57	19.67	0.81	66.39	21.56	1.31	Pull-out
MA75d14-2	71.13	23.10	1.125				Pull-out
MA75d14-3	67.46	21.91	1.995				Splitting
MA75d16-1	84.62	21.04	0.4	81.75	20.33	0.43	Splitting
MA75d16-2	83.00	20.64	0.645				Splitting
MA75d16-3	77.62	19.30	0.23				Pull-out
MA100d12-1	33.23	14.69	0.835				Pull-out

MA100d12-2	33.94	15.00	0.365	34.74	15.36	0.67	Pull-out
MA100d12-3	37.04	16.38	0.815				Pull-out
MA100d14-1	48.50	15.75	0.715	47.81	15.53	0.74	Pull-out
MA100d14-2	45.52	14.78	0.36				Pull-out
MA100d14-3	49.40	16.05	0.85				Pull-out
MA100d16-1	64.87	16.13	1.37	58.82	14.63	1.18	Pull-out
MA100d16-2	46.99	11.68	1.0				Pull-out
MA100d16-3	64.60	16.06	1.16				Pull-out

Appendix G- Chemical Composition Test Result of Marble Aggregate

	GEOLOGICAL INSTITUTE OF ETHIOPIA	Doc. Number: GLD/F5.10.2	Version No: 1
	Geochemical Laboratory Desk		Page 1of 1
Document Title:-	Complete Silicate Analysis Report	Effective date:	Nov. 2022

Customer Name:- Dereje Hirpha Lemma

Issue Date:-30/12/2022

Sample type :- Rock

Request No:- GLD/RQ/306/22

Sample Preparation: -200 Mesh

Report No:- GLD/RN/1195/22

Date Submitted:- 07/10/2022

Number of Sample:-One (01)

Analytical Result: In percent (%) Element to be determined Major Oxides & Minor Oxides.

Analytical Method: $LiBO_2$ FUSION, HF attack, GRAVIMETERIC, COLORIMETRIC and AAS

Collector's code	SiO_2	Al_2O_3	Fe_2O_3	CaO	MgO	Na_2O	K_2O	MnO	P_2O_5	TiO_2	H_2O	LOI	Weight of Sample
D-H-L-01	4.86	<0.01	0.12	51.22	0.80	0.24	<0.01	<0.01	0.15	<0.01	0.24	41.35	2.00Kg

Note: - This result represent only for the sample submitted to the laboratory.

Analysts
Haimanot Bayeh
Gadisa Wakuma

Checked By
Lidet Endeshaw

Approved By
Yohannes Getachew

Quality Control
Negash Worku

Appendix H- Sample Experimental Photo Gallery

Washing, drying and sieving of fine aggregate

Sieving of coarse aggregate using 25mm sieve

Collecting, crushing, sieving and packing of marble aggregate

Laboratory test for fine and coarse aggregates (Sampling, specific gravity and water absorption, gradation, dry rodded unit weight, weighing)

Laboratory test for marble aggregate (dry rodded unit weight, specific gravity and water absorption, gradation, oven drying, aggregate impact test)

Concrete specimens casted, cured and ready for test

Compressive and splitting tensile strength test setup and failure of specimen

Pull-out bond strength test setup and failure of specimen